MAP kinase-dependent opioid receptor expression in sensory neurons and PC2-dependent opioid peptide processing and release from immune cells

vorgelegt von
M.Sc. Biochemikerin
Reine Solange Sauer, geb. Yamdeu,
geboren in Kamerun

Von der Fakultät II - Mathematik und Naturwissenschaften
der Technischen Universität Berlin
zur Erlangung des akademischen Grades
Doktor der Naturwissenschaften
Dr. rer. nat.

genehmigte**:** Dissertation

Promotionsausschuss:

Vorsitzender: Prof. Dr. Thomas Friedrich
Berichter/Gutachter: Prof. Dr. Roderich Süssmuth
Berichter/Gutachter: Prof. Dr. Michael Schäfer

Tag der wissenschaftlichen Aussprache: 09.09.2011

Berlin 2011

D83

Abbreviations

ABC	Avidin-biotin peroxidase complex
ACTH	Adrenocorticotrope hormone
ANOVA	Analysis Of Variance
BAPTA	1,2-bis (o-aminophenoxy)ethane-N,N,N’,N’-tetraacetic acid
BCA	Bicinchoninic acid
BL	Baseline
Bp	Base pairs
BSA	Bovine serum albumin
CFA	Complete Freund's adjuvant
CGRP	Calcitonin gene-related peptide
CLIP	Corticotropin-like intermediate lobe peptide
CPE	Carboxypeptidase E
Cpm	Counts per minute
CREB	Cyclic adenosine monophosphate responsive element-binding protein
CRH	Corticotropin releasing factor/hormone
DAB	3',3'-Diaminobenzidine tetrahydrochloride
DAMGO	[D-Ala2, N-Me-Phe4, Gly-ol5]-enkephalin
DAPI	4’,6-DiAmino-2-phenylindole
DMSO	Dimethylsulfoxide
DNA	Deoxyribonucleic acid
DNTP	Deoxyribonucleoside triphosphate
DOR	Delta opioid receptor
DRG	Dorsal root ganglia
DTT	Dithio-1,4-threitol
DYN	Dynorphin A1-17
ECL	Enhanced chemiluminescence
EDTA	Ethylenediamine tetraacetic acid
EMSA	Electrophoretic mobility shift assays
END	Beta-endorphin1-31
ENK	Met-enkephalin
ER	Endoplasmic reticulum

ERK	Extracellular signal-regulated kinase
FITC	Fluorescein isothiocyanate
fMLP	formyl-Methionyl-Leucyl-Phenylalanine
FPR	formyl-Methionyl-Leucyl-Phenylalanine receptor
Grb2	Growth factor receptor-bound protein 2
H_2O_2	Hydrogen peroxide
HBSS	Hank's buffered salt solution
HRP	Horseradish peroxidase
IF	Immunofluorescence
Ig	Immunoglobulin
IHC	Immunohistochemistry
i.p	Intraperitoneal
i.pl.	Intraplantar
i.t.	Intrathecal
IL	Interleukin
IR	Immunoreactive
JNK/SAPK	C-Jun kinase/stress activated protein kinase
KCl	Potassium chloride
KH_2PO_4	Potassium phosphate
KOR	Kappa opioid receptor
LPH	Lipotropin
LSM	Laser scanning microscopy
MAPK	Mitogen-activated protein kinases
MAPKAP	Mitogen-activated protein kinase-activated protein kinase-2
MgCl	Magnesium chloride
MIP-2	Macrophage inflammatory protein-2
MOR	Mu opioid receptor
MPE	Maximal possible effect
mRNA	messenger ribonucleic acid
MSH	Melanocyte–stimulating hormone
N/OFQ	Nociceptin/orphanin FQ
Na_2HPO_4	Sodium phosphate
NaCl	Sodium chloride
NF-kB	Nuclear factor "kappa-light-chain-enhancer"of activated B-cells

NGF	Nerve growth factor
NLX	Naloxon
ORL	Orphan receptor
PBS	Phosphate buffered saline
PC	Prohormone convertase
PC12	Pheochromocytoma cells
PCR	Polymerase chain reaction
PD 98059	2´-amino-3´-methoxyflavone
PDYN	Prodynorphin
PENK	Proenkephalin
PFA	Paraformaldehyde
pg	Picogramm
PMN	Polymorphonuclear cells
PMSF	Phenylmethylsulfonylfluoride
POMC	Proopiomelanocortin
PPT	Paw pressure threshold
RIA	Radioimmunoassay
RNase	Ribonuclease
Rpm	Rotations per minute
SB203580	4-(4’-fluorophenyl)-2-(4’methylsulfinylphenyl))-5-(4’-pyridyl)imidazole
SD	Standard deviation
SDS	Sodium dodecylsulfate
SDS-PAGE	Sodium dodecyl sulphate-polyacrylamide gel electropheresis
SEM	Standard error of mean
Shc	Src homology containing
SIG	Signal peptide
SP	Substance P
STAT	Signal transducers and activators of transcription
TBE	Tris borate EDTA
TBS	Tris buffered saline
TEMED	N,N,N′,N′-tetramethylethan-1,2-diamin
TrkA	Tyrosine kinase A
UV	Ultraviolet
WB	Western blot

1 Summary

Opioids are well known for their central analgesic effects. However, growing evidence shows that opioids also elicit analgesic effects following activation of their receptors on peripheral sensory neurons. During local inflammatory pain opioid receptors increasingly accumulate on peripheral sensory nerve endings and opioid peptides are delivered by immigrating immune cells into subcutaneous inflamed tissue. To finally result in potent antinociception upon their release they have to penetrate the perineural barrier of peripheral sensory nerves. The work of this thesis examined i) whether nerve growth factor (NGF) dependent signaling pathways are responsible for the increased sensory neuron mu-opioid receptor expression during inflammatory pain; ii) whether the immune cell derived endogenous opioid peptides endorphine (END), enkephaline (ENK) and dynorphin (DYN) result from the correct processing of their precursors by specific prohormone convertases and a subsequent release; iii) whether exogenously applied or endogenously released opioid peptides penetrate the perineural barrier of sensory neurons and subsequently are able to elicit antinociception under normal and pathological conditions.

In an animal model of unilateral hindpaw inflammation following Freund's complete adjuvant (FCA) inoculation, i.pl. administration of the full opioid agonist fentanyl led to enhanced antinociceptive efficacy. Local immunoneutralization of NGF in FCA treated animals by a specific antiserum or i.pl. NGF treatment of naive animals resulted in a decrease or increase of antinociception, respectively. Radiolabeled ligand binding with [^{3}H]DAMGO, Western blot and immunohistochemistry using a mu-opioid receptor (MOR) specific antibody identified significant increases in the number of MOR binding sites, MOR protein as well as MOR-immunorreactive (MOR-IR) neuronal cells within dorsal root ganglia (DRG). In parallel, phosphorylated p38-MAPK (p-p38-MAPK) protein and the number of p-p38-MAPK-IR neurons expressing MOR in DRG as well as the peripherally directed axonal transport of MOR significantly increased. Finally, NGF-induced effects occurring in DRG, on

axonal transport and on the potentiation or enhanced efficacy of opioid antinociception were abrogated by the intrathecal inhibition of p38- but not ERK-1/2- MAPK suggesting a crucial role for NGF dependent signal pathways such as p38 MAP kinase.

Endogenous opioid peptides (END, ENK and DYN) are the ligands of such opioid receptors on sensory neurons. They are released during stressful stimuli and interact with peripheral opioid receptors to inhibit pain. However, the subcellular pathways of POMC, PENK and PDYN processing into END, ENK and DYN have not yet been delineated in inflammatory cells. Double immunofluorescence confocal microscopy showed colocalization of the opioid precursors POMC, PENK or PDYN with their key processing enzyme (PC2) within subcutaneous inflamed paw tissue. Immunohistochemistry and Western blot detected accumulation of the precursor proteins POMC, PENK or PDYN within circulating and resident immunocytes of PC2 knockout mice. Consistently, radioimmunoassay measured significant decreases in the total content and formyl-methionyl-leucyl-phenylalanine (fMLP)-induced release of opioid peptide endproducts END, ENK and DYN from immune cells. Inflammatory pain can be controlled by intraplantar opioid injection or by secretion of endogenous opioid peptides from leukocytes in inflamed rat paws. Antinociception requires binding of opioid peptides to opioid receptors on peripheral sensory nerve terminals. In the absence of inflammation, hydrophilic opioid peptides do not penetrate the perineurial barrier easily and, thus, do not elicit antinociception. Therefore, the aim was to examine the conditions under which endogenous, neutrophil-derived hydrophilic opioid peptides (i.e. Met-Enkephalin and β-endorphin) can raise nociceptive thresholds in noninflamed tissue in rats. Following intraplantar treatment with hypertonic saline, the perineurial barrier was reversibly permeable for hours and intraplantar injection of opioid peptides increased mechanical nociceptive thresholds. In addition, MIP2-induced recruitment of opioid peptide containing leukocytes into subcutaneous tissue without affecting the integrity of the perineural barrier resulted in the establishment of formyl-Met-Leu-Phe (fMLP)-triggered opioid peptide release

and subsequent pain inhibition. Taken together, in addition to the opioid system within the central nervous system increasing evidence suggests a role for the opioid system in the peripheral nervous system. Under conditions of inflammatory pain the number of opioid receptors on peripheral sensory nerves is up-regulated in an NGF p38 MAPK kinase pathway. In parallel opioid peptide expressing immune cells migrate from the circulation into direct vicinity of these nerves to release opioid peptides upon correct processing from their precursors to biologically active end products. In PC2 knockout mice this opioid processing was hindered leading to an accumulation of precursors and a lack of opioid peptide endproducts to be released. The perineural barrier which normally prevents opioid peptides from their access to peripheral opioid receptors is destroyed under inflamed conditions. Under non-inflammatory conditions the access of opioid peptides can be facilitated by hypertonic solutions. Antinociception mediated by endogenously released opioid peptides has, therefore, three important requirements: 1) a critical number of opioid receptors at the peripheral sensory neurons; 2) opioid peptide expression, correct processing and release from leukocytes and 3) opening of the perineurial barrier for opioid peptide access to sensory neuron opioid receptors. This may be important for intrinsic mechanisms of pain control as has been shown in the context of stress-induced analgesia.

2 Introduction

Opioids are the most effective and widely used drugs for pain treatment. They bind to opioid receptors on central as well as peripheral sensory neurons and induce potent analgesia both in humans and in experimental animal models of inflammatory pain. [1, 2] Opioid receptors were first identified as binding sites in certain brain areas by use of the radiolabeled ligands [^{3}H]naloxone, [^{3}H]dihydromorphine, and [^{3}H]etorphine. [3-5] As a consequence the opioid analgesics were classified as typical centrally acting analgesics. However, as early as 1976, Yaksh and colleagues showed that opioids elicited analgesic effects also at the level of the spinal cord, when given intrathecally. This effect was dose-dependent and reversible by naloxone, thus specific for an opioid receptor-mediated mechanism.[6] Consistently, opioid binding sites were identified in the dorsal horn of the spinal cord. [7] Initial reports in the early 1980s suggested the peripheral analgesic effects of opioids and subsequently opioid binding sites were identified on peripheral sensory neurons.[8-11]

Soon after the cloning of opioid receptors antibodies for their detection became available. [12, 13] Subsequent immunohistochemical experiments confirmed their distribution throughout the central and peripheral nervous system. [14, 15] Opioid receptors on peripheral sensory neurons are predominantly localized on small-sized DRG neurons (unmyelinated C-fibers) [15] and to a lesser degree on medium-sized thinly myelinated neurons (Aδ fibers). [15, 16] A recent study has postulated that the expression of MOR and delta-opioid receptor (DOR) occurs in different subsets of sensory neurons, i.e. unmyelinated calcitonin gene related peptide ($CGRP^+$) peptidergic neurons and myelinated $CGRP^-$ nonpeptidergic neurons, respectively.[17] As a consequence it was argued that they modulate either heat or mechanical pain, respectively. Wang et al., however, demonstrated that both DOR and MOR are expressed in both sensory neuron populations and upon activation reduce depolarization-induced Ca^{2+} currents in both populations of DRG neurons. [18]

The endogenous ligands of the peripheral opioid receptors, the opioid peptides, have been identified in resident immune cells which migrate from the circulation into subcutaneous tissue following local inflammatory pain. [19, 20] These cells are in direct vicinity of peripheral nerve terminals that innervate the skin. [21] Opioid peptides are known to derive from precursor peptides which are cleaved by specific processing enzymes to give the endproducts ß-endorphin (END), Met-enkephalin (ENK) and dynorphin (DYN). [22, 23] These endproducts are stored in dense-core vesicles and released upon certain stimuli, such as catecholamines and corticotrophin-releasing hormone.[24-26] Immmunosuppression, e.g. following total body irradiation, cyclosporine, or cyclophosphamid treatment significantly diminish the number of opioid expressing immune cells. [26, 27] The released opioid peptides activate their corresponding receptors on peripheral sensory nerve endings, resulting in the inhibition of painful stimuli. [28, 29] (See Fig. 1)

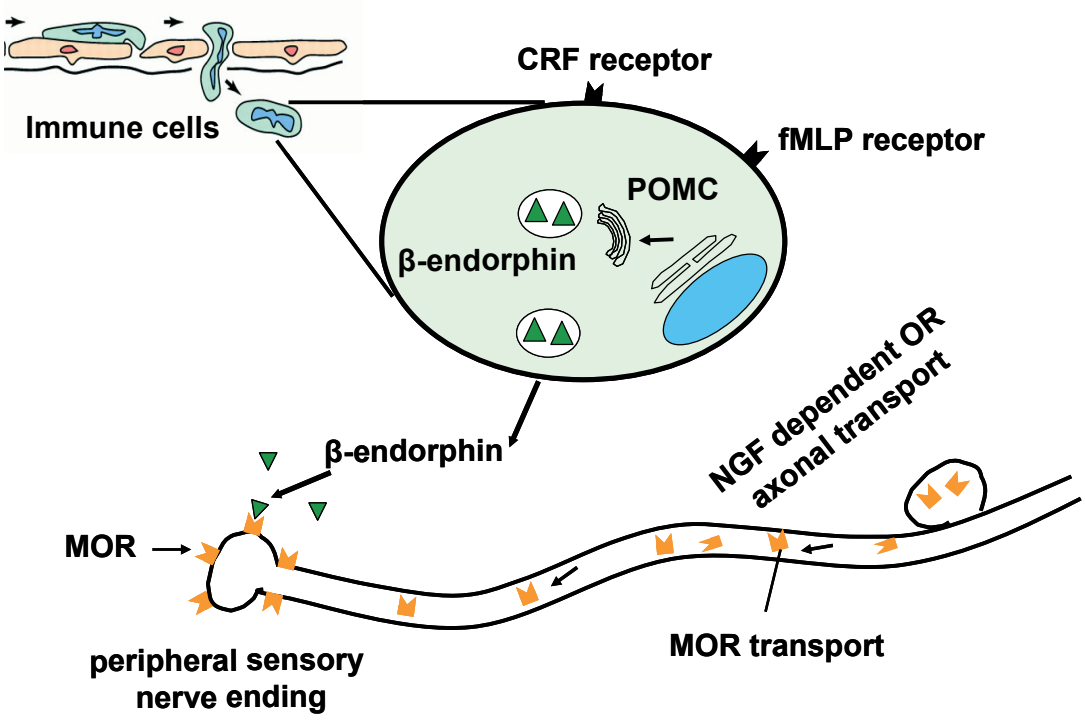

Figure 1: Upon localized tissue inflammation, there is enhanced NGF dependent synthesis and axonal transport of MOR to the peripheral sensory nerve endings. In parallel, various types of immune cells containing opioid peptides migrate from the circulation to the site of inflammation. Then, fMLP or CRF may activate their respective receptors on immune cells resulting in a release of opioid peptides e.g.β -endorphin. The liberated opioid peptides bind to the MOR of peripheral terminals of sensory neurons to inhibit pain (modified figure provided by Dr. Shaaban Mousa).

Analgesic effects following the peripheral administration of opioids are enhanced under conditions of inflammation which is in part due to an increased number (up-regulation) of opioid receptors on peripheral sensory nerve terminals. [30, 31] This has been confirmed by mRNA, Western blot, immunohistochemistry [30-34] and ligand binding studies. [35, 36] More recently, nerve growth factor (NGF) has been identified as one potential candidate that contributes to the inflammation-induced up-regulation of sensory neuron opioid receptors during inflammatory pain.[31] Consistently, NGF is also known to increase enkephalin-binding sites in cell culture,[37] to raise diprenorphine binding sites in isolated DRG, [38] and to increase MOR immunoreactivity in DRG of NGF-overexpressing transgenic mice. [39, 40] NGF has been shown to be increased in inflamed subcutaneous tissue and is described as a principal regulator of altered neuronal gene expression following inflammation. [41] NGF is implicated in elevated neuropeptide expression, [42, 43] and up-regulation of ion channels as well as G-protein-coupled receptors such as MOR [31] in nociceptive neurons.

During inflammation, mast cells, macrophages, keratinocytes, and T cells release NGF that binds to it receptor on the peripheral sensory neuron and activates the MAPK pathway [44, 45]. The NGF-receptor-MAPK complex is retrogradely transported to the DRG where it initiates gene transcription. Whether NGF alone is able to trigger the MOR up-regulation in peripheral sensory neurons and by which signaling pathway has not been examined yet and is a topic of the present thesis.

2.1 Nerve growth factor receptors and signaling pathways

NGF is a member of the neurotrophin family that promotes the survival and differentiation of sensory and sympathetic neurons**.** NGF binds to two distinct receptor subunits, the p75 (with low affinity) and/or the TrkA (with high affinity) subunits.[44] The extracellular domain of TrkA (Fig. 2) contains two cysteine-rich motifs that are separated by three leucine-rich motifs; these are followed by two Ig-like motifs. The catalytic domain includes the conserved

tyrosine residues which phosphorylation is necessary for the binding of different adaptor molecules as well as effectors of TrkA signaling. A majority of the actions of NGF are attributed to the activation of both TrkA and p75. Growing evidence suggests a significant cross-talk between these two receptors, e.g. p75 can augment the binding affinity of TrkA for NGF. Homologous or heterologous dimerization of these subunits activates a cascade of autophosphorylation events. [46]

Upon dimerization, the binding of adapter proteins such as Shc, Grb2 and the guanine-nucleotide exchange factor SOS to TrkA leads to the activation of Ras with a subsequent increase in the activity of the MAPK pathway and altered gene expression. [45] The MAPK family includes extracellular ERK, p38 MAPK, c-Jun N-terminal kinase/stress-activated protein kinase (JNK/SAPK), and ERK5. p38 MAPK operates through a separate intracellular cascade and serves as a mediator of cellular stress, such as inflammation. [47] It is involved in the regulation of several transcription factors that may bind to the corresponding binding sites on the DNA promoter and increased or decreased gene transcription. Indeed, Xing et al. showed that NGF activates p38 MAPK and its downstream effector MAPKAP kinase 2, which then catalyzes CREB phosphorylation at Ser-133. [48] In NGF-treated PC12 cells, inhibition of the p38/MAPKAP kinase 2 pathway abolished CREB Ser-133 phosphorylation indicating that this pathway contributes to CREB phosphorylation. Phosphorylated CREB then binds to its binding site or response element on the DNA within the nucleus and initiates transcription.

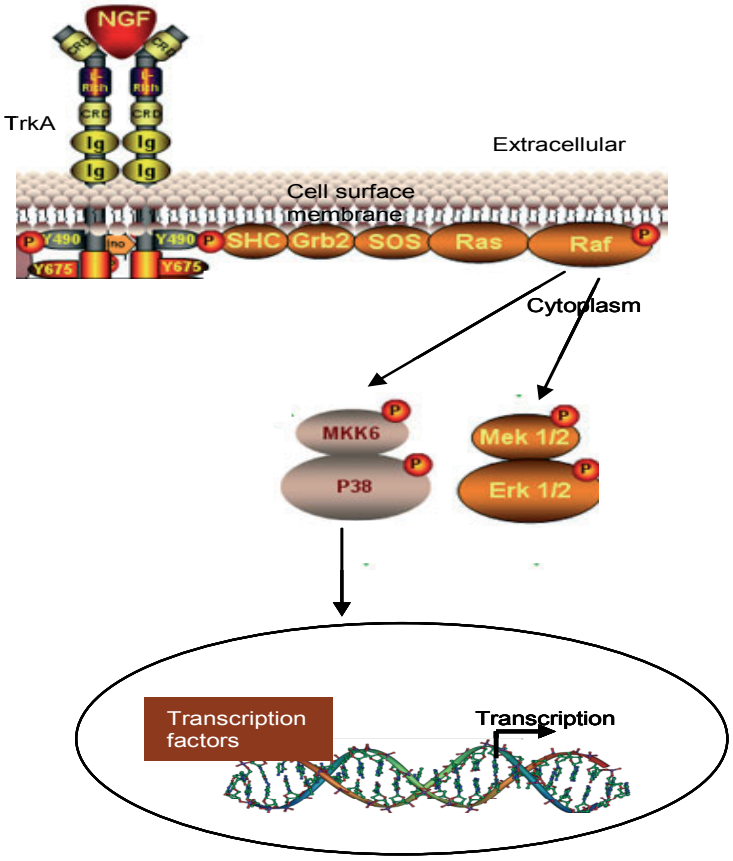

Figure 2: TrkA receptor signaling. TrkA is the high affinity receptor for NGF. It is located at the cellular membrane and is activated by binding of NGF to its extracellular domains. The extracellular region of TrkA is characterized by a number of distinct structural motifs. The amino-terminal sequence consists of three tandem leucine repeats flanked by two cysteine clusters and two immunoglobulin-like domains that are required for specific ligand binding. Phosphorylation at Tyr^{490} is required for SHC association and subsequent activation of the Ras-MAP kinase signaling cascade. MAPK activation results in activation of transcription factors (e.g. CREB) that bind on responsive elements on DNA in the nucleus and initiate gene transcription. (Modified from www.scienceslides.com/Ljd/trka-signaling access on 15.02.2011).

2.2 MOR-molecular structure and function

Opioid receptors are a group of Gi/Go protein-coupled receptors with opioids as ligands. [49] There are four major subtypes of opioid receptors: μ (*mu*), κ (*kappa*), and δ (*delta*) and the orphan (ORL1) receptor. [50] Mu opioid receptor (MOR) has an extracellular N-terminal domain, seven transmembrane helical domains connected by three extracellular and three intracellular loops and an intracellular C-terminal tail. [51] The extracellular N-terminal end is important for directing the binding of specific ligands to interact with the binding pocket. [52]

The transmembrane residues within the lipophilic environment of the cell membrane are key elements in ligand recognition and/or signal transduction, [53] whereas the C-terminal end, the second and third intracellular loop of the opioid receptor are important for the coupling of second messengers and the desensitization and internalization of the receptor. Opioid receptors demonstrate high sequence identity in their transmembrane domain (73%-76%) and in intracellular loops (63%-66%) and large divergence in the N- and C-terminal domains as well as extracellular loops (34%-40% identity). [54] In addition to exogenously applied opioids such as morphine, endogenous opioid peptides such as END, ENK, and DYN also bind to opioid receptors. Their binding characteristics reveal some preferences for certain opioid receptor subtypes, such as that END binds to MOR and DOR but much less to the kappa-opioid receptor (KOR), whereas ENK binds preferentially to MOR compared to DOR but not to KOR, and DYN binds mainly to KOR (Table 1).

Table 1**:** Binding characteristics as Ki (nM) of opioid peptides for the cloned MOR, DOR, and KOR. [55]

	KOR	DOR	MOR
Endorphin	52	1.0	1.0
Met-Enkephalin	>1000	1.7	0.65
DynorphinA	0.5	>1000	32

The MOR gene spans about 250 kb based on the mouse genome data bank. It contains 19 exons. [56, 57] The MOR promoter region is reported to have transcription factor binding sites for NF-κB, [58] CREB, [59] STAT1/3 [60] and STAT6. [61] A previous study by Kraus et al., (2001) demonstrated that MOR transcription in neuronal cell cultures is up-regulated by IL-4 through the binding of STAT6 transcription factor.

2.3 Endogenous opioid peptide processing

The endogenous opioids are endorphins (ENDs), enkephalins (ENKs), dynorphins (DYNs), and nociceptin. The endogenous opioid peptides are mainly derived from precursors, pro-opiomelanocortin (POMC), proenkephalin (PENK), prodynorphin (PDYN), and pronociceptin/orphanin FQ (N/OFQ). [51] All peptides derived from these precursors consist of the same pentapeptide sequence TyrGlyGlyPheMet/Leu (YGGFM/L), except for N/OFQ. The latter contains a phenylalanine (F) instead of the N-terminal tyrosine, a residue necessary for high-affinity binding to the classic opioid receptors, and is, therefore, not considered to be a ‘‘classical” opioid. [62, 63] Recently, Zadina et al. discovered two other opioid peptides, endomorphin-1 and 2, which bind with high selectivity to the MOR; however, they have no known precursor. [64] The most extensively characterized source of opioid peptides is the pituitary gland. [65, 66] Nevertheless, in inflamed tissue opioid peptides were found in immigrated immune cells. [27, 67] Moreover, these immune cells were found to express POMC, PENK and PDYN mRNA as detected by specific oligonucleotide probes against the respective precursors POMC, PENK, and PDYN using *in situ* hybridization. [68] These findings suggest that immune cells produce opioid peptides at the site of inflammation. Furthermore, previous studies demonstrated that END is located in secretory granules of various types of immune cells. [24] These cells also produce and release ENK. [69] Opioid precursor processing involves the prohormone convertases (PCs). [70] The PC1/3, PC2 and CPE are part of a family of enzymes known to participate in the processing of biologically active products through their endoproteolytic cleavage. Examination of the primary sequences of many secretory proteins had shown that conversion of a precursor to the active peptide by cleavage at basic motifs (usually R/K-R or R-X-X-R, where R is arginine, K is lysine and X can be any amino acid) is a common feature in nature. [71] The PC family of enzymes consists of seven distinct members named, furin, PC2, PC1/3, PC4, PACE4, PC5/6 and PC7. [72] Some of these enzymes, such as furin [73], PC5/6 [74] and PC7 [75] have an ubiquitous or widespread

tissue distribution. It is well established that PC2 is expressed in neuroendocrine cells and process precursors (mainly hormones and neuropeptides) that enter the regulated secretory pathway within pituitary and neuroendocrine cells. [76] The expression of neuropeptide processing enzyme PC2 was thought to be restricted only to the neuroendocrine system, however, PC2 expression has been found elsewhere such as immune cells. [24, 68, 77] All PCs are first synthesized as zymogens (proPCs) which undergo autocatalytic processing of their pro-segment within the endoplasmic reticulum, with the exception of proPC2, which is processed to PC2 within the *trans* Golgi network or the immature secretory granule. [78, 79] The intracellular localization of PCs and their isoforms and the study of intracellular precursor processing show that PC2 is a major enzyme processing precursors whose products are directed towards the dense core secretory vesicles [80] (calcium channel regulated).

2.3.1 POMC processing into END

The POMC gene maps to chromosome 2 in humans, to chromosome 12 in mice, and to chromosome 6 in rats. The gene contains three exons and two introns. Exon 2 encodes a signal peptide essential for classical protein processing and secretion. [81] Exon 3 encodes various bioactive peptides, such as ACTH, LPH, MSH, and END. There have been several reports of POMC mRNA in immune cells, but some studies report a lack of full-length transcripts. [82-84] A lack of exon 2 encoding the signal sequence necessary for endoplasmic reticulum membrane translocation suggests that the propeptide products are neither processed nor secreted and, therefore, are nonfunctional. [85] Recently, Lyons and Blalock (1997) and Sitte et al., (2007) identified the full-length POMC mRNA in immune cells. [86, 87] They found that in nonstimulated mononuclear cells the level of full-length POMC mRNA is low, but that mitogenic stimulation enhanced the abundance of this mRNA. This gene encodes a polypeptide hormone precursor POMC that undergoes extensive, tissue-specific, post-translational processing via cleavage by PCs. POMC is a 28–32 kDa molecule composed of

three main regions: an N-terminal α-MSH-containing sequence, the central ACTH (1–39) sequence (with the α-MSH precursor as its N terminus), and the C-terminal ß-lipotropin (LPH) sequence, which can be processed into γ-LPH and END (reviewed by (88). There are eight potential cleavage sites within the polypeptide precursor POMC and, depending on tissue type and the available convertases, processing may yield many biologically active peptides involved in diverse cellular functions. In the anterior pituitary, PC1 cleaves POMC to yield ACTH and ß-LPH. In the neurointermediate lobe and in the central nervous system, PC2 generates α-MSH, corticotropin-like intermediate lobe peptide (CLIP), ß-LPH, and END (reviewed by Mains RE, Eipper BA: Handbuch of physiology. The endocrine system. 2000;4:85-101) (see Fig. 3). END derives from the precursor POMC after proteolytic processing at pairs of basic amino acid sites.

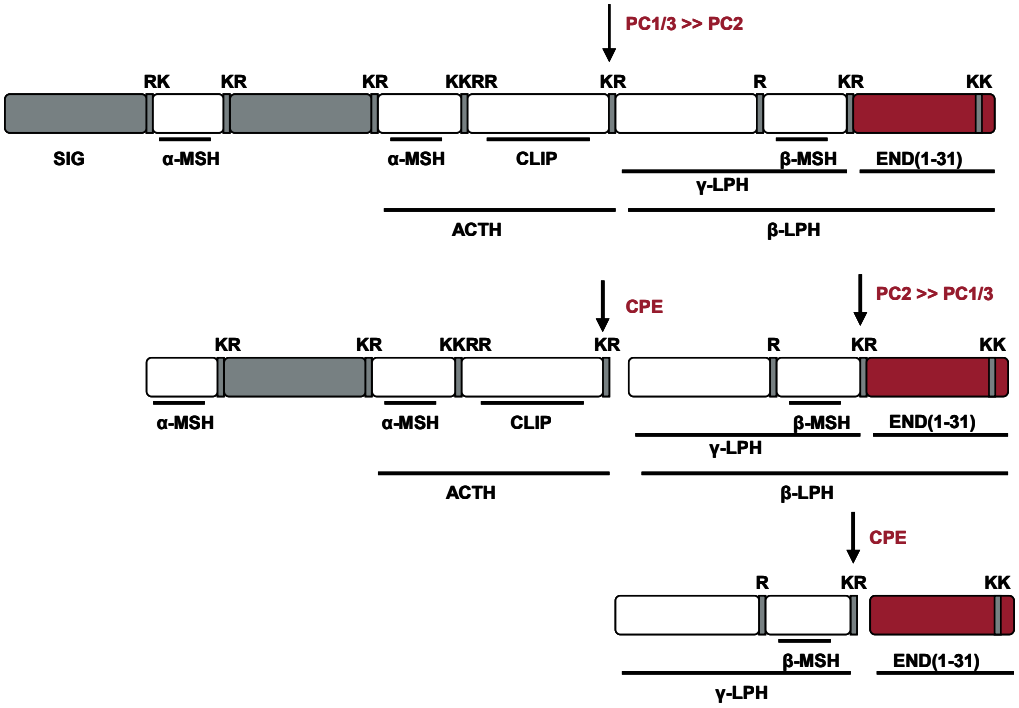

Figure 3: Schematic representation of rat proopiomelanocortin precursor and its processing in the pituitary at paired and single basic cleavage sites by PC1/3, PC2 and CPE. POMC is composed of 235 amino acid residues. Its posttranslational processing begins as the nascent polypeptide chain (pre-POMC) enters the endoplasmic reticulum directed by the signal peptide (SIG). Within the endoplasmic reticulum the signal peptide is removed from the N-terminus revealing the mature POMC. This precursor contains pairs of basic amino acids predominantly of the Lys-Arg type that are potential cleavage sites. PC1/3 cleaves POMC to yield predominantly intermediates like ACTH and β-LPH. PC2 generates endorphin from β-LPH. Following the precursor cleavage at single or multiple basic residues by endoproteases, CPE removes the basic amino acids from the C termini of the resulting peptides. R: arginine; K: lysine (After (79)).

2.3.2 PENK processing into ENK

The PENK gene, containing 4 exons, maps to human chromosome 8 (http://www.ensembl.org). In mice, PENK is located on chromosome 4 and contains two exons, but in rats it maps to chromosome 5 and comprises three exons (http://www.ensembl.org). The PENK is a protein precursor for several neuropeptides, including various ENKs [89]. In brain and adrenal medulla, PENK precursor yields four copies of (Met)enkephalin (http://www.ensembl.org). (amino acids: 100–104; 107–111; 136–140, 210–214) and single copies of each of (Leu)enkephaline (230-234), (Met)enkephalin-Arg-Gly-Leu (octapeptide) (186-193) and (Met)enkephalin-Arg-Phe (heptapeptide) (261-267),

which arise by enzymatic cleavage of the gene product through cleavage by PC2 at paired basic amino acids (see Fig. 4).

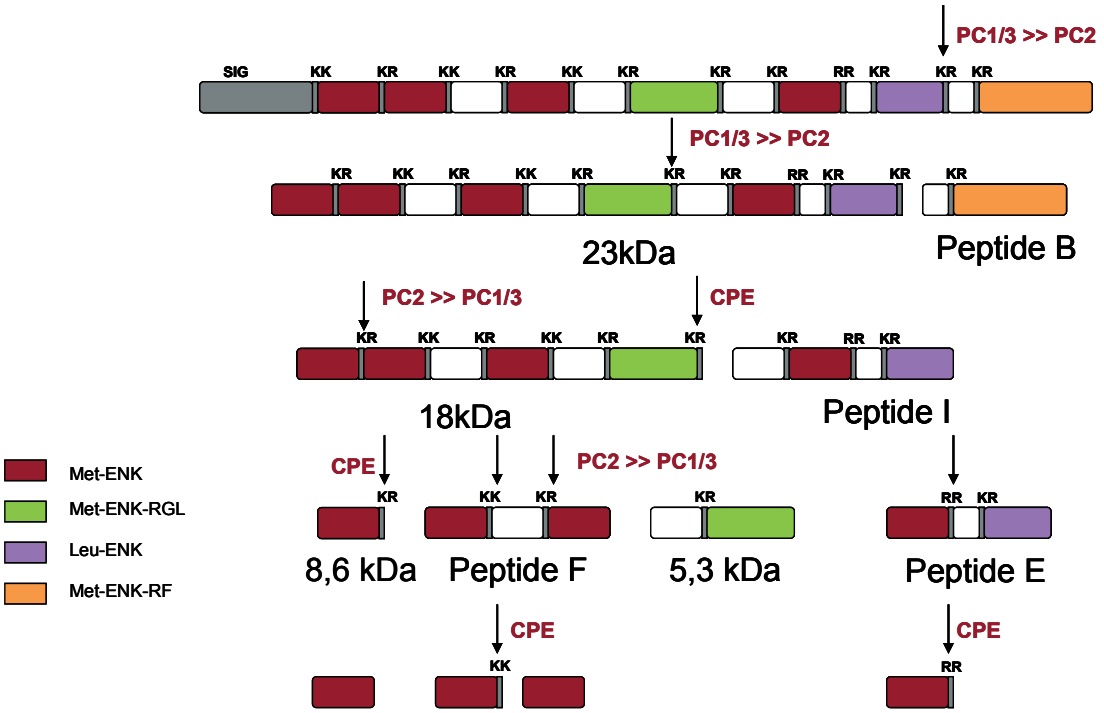

Figure 4: Schematic representation of rat PENK precursor and its processing at paired and single basic cleavage sites by PC1/3, PC2 and CPE. The nascent polypeptide chain (Pre-PENK) of 269 amino acid lengths comprises PENK and the N-terminal signal peptide. The signal peptide (SIG) is removed before the mature PENK polypeptide translocates towards the Golgi network. At the transgolgi network PC1/3 and PC2 cleave PENK into biologically active peptides. Carboxypeptidase E (CPE) is important for the sorting of the peptides to be packed into secretory granules and cleaves the paired amino acids that reside after PC1/3 and 2 cleavage. PENK-cleavage sites of PC1/3 and PC2 are indicated. PC1/3 cleaves PENK into intermediate sized processing products that are further cleaved by PC2 into small active peptides metENK. R: arginine; K: lysine (figure taken from (89)).

2.3.3 PDYN processing into DYN

The gene for prodynorphin maps to the human chromosome 20, to the mice chromosome 2, and to the rat chromosome 3 (http://www.ensembl.org). It consists of four exons. Prodynorphin, a multifunctional precursor of several important opioid peptides, is expressed widely in the brain and spinal cord [90]. It is processed at specific single and paired basic sites to generate various biologically active products. Limited proteolysis of the PDYN at dibasic and monobasic processing sites results in the generation of bioactive dynorphins. [90] In the brain and neurointermediate lobe of the pituitary, PDYN is processed to alpha- and beta- neo-END, dynorphins DYN A-17 and DYN A-8, DYN B-13, and leucine-ENK. The formation of DYN A-8 from Dyn A-17 requires a monobasic cleavage between Isoleucine and Arginine (see Fig. 5).

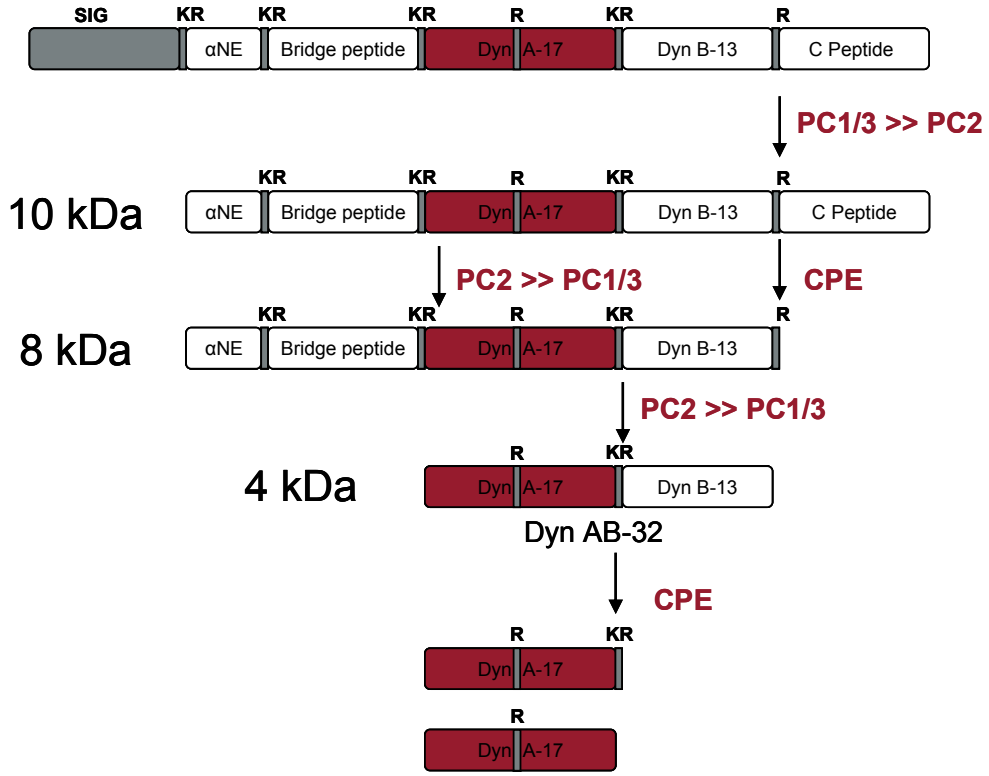

Figure 5: Schematic representation of rat prodynorphin precursor and its processing at paired and single basic cleavage sites by PC1/3, PC2 followed by C-terminal trimming by CPE to produce DYNA1-17. The nascent polypeptide chain (Pre-PDYN) of 248 amino acid lengths comprises PDYN and the N-terminal signal peptide. The signal peptide (SIG) is removed before the mature PDYN polypeptide translocates towards the Golgi network. At the transgolgi network PC1/3 and PC2 cleave PDYN into biologically active peptides. Carboxypeptidase E (CPE) is important for the sorting of the peptides to be packed into secretory granules and cleaves the paired amino acids that reside after PC1/3 and 2 cleavage. PDYN is processed primarily to higher-molecular weight DYN-containing intermediates peptides by the action of PC1/3, followed by the action of PC2 that cleaves intermediates into small active peptides DYNA1-17. R: arginine; K: lysine. (Modified from (90)).

In summary, while POMC, PENK and PDYN are expressed and correctly processed by PC1/3, PC2 and CPE within pituitary endocrine cells, so far there is no evidence whether this also occurs within cells of the immune system, although the entire mRNA of these precursors is transcribed. [86, 87] Therefore, one aim of this thesis was to investigate whether opioid peptide precursors are not only expressed but also processed to their endproducts within immune cells. In the next step the functional relevance of this processing for the release of the endproducts END, ENK, DYN was examined.

In earlier studies it was already shown that END and ENK are released from immune cells in a calcium-dependent manner consistent with a vesicular release. [26, 91] Using immunoelectron microscopy Mousa et al. demonstrated that END is localized within secretory granules packed in membranous structures of macrophages, monocytes, granulocytes, and lymphocytes and can be released by for instance noradrenaline from immune cells *in vitr*o. [24]

2.4 Perineurial barrier of peripheral nerve endings

A peripheral nerve structure consists of bundles of nerve fibers surrounded by connective tissue (Fig. 6). The outside layer is called the epineurium consisting of very dense irregular fibrous and adipose tissue that binds nerve fascicles together into a single nerve trunk. [92] Each bundle of nerve fiber (fascicle) is, in turn, enclosed in several concentric layers of flattened cells joined by so called "tight junctions", forming laminar structures called the perineurium (Benn E. Smith: Handbook of Clinical Neurophysiology. Anatomy and histology of peripheral nerve. 2006; 7: 3-22). The individual axon and their surrounding Schwann cells are surrounded by a small amount of loose connective tissue, which is called the endoneurium.

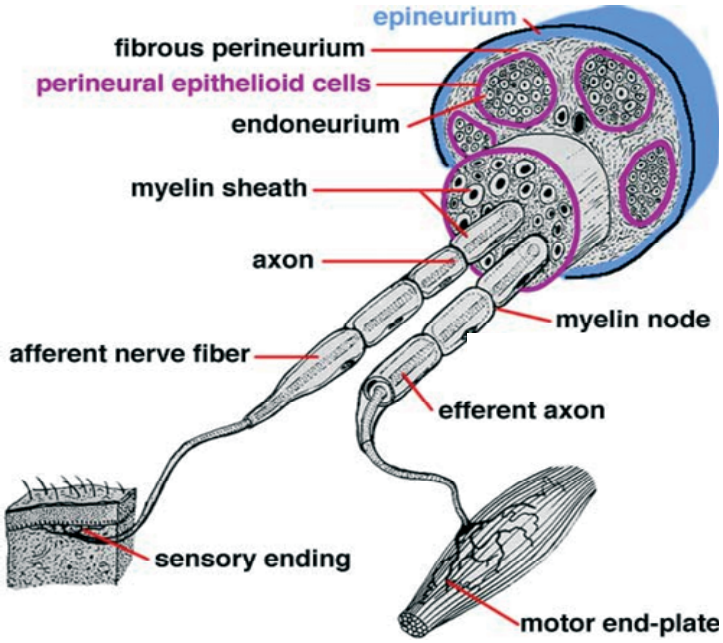

Figure 6: Anatomy of a peripheral nerve. The nerve usually consists of a variety of fascicles. Each fascicle is encased by perineurium. Inside the fascicle are a group of axons. Each axon has an insulating lining of myelin which is an outgrowth of a glia cell. Between the fascicles is a fatty tissue called the interfascicular epineurium. The nerve is then wrapped in the main epineurium (taken from the Atlas of vetenary Neurohistology).

Blood vessels usually are found in the epineurium and perineurium which give rise to a network of capillary vessels in the endoneurium. [92] Previous physiological and morphological studies have documented the epineurium and perineurium barrier function to a broad spectrum of macromolecules including proteins and its protective action against toxic and infectious agents. [93, 94] The tight junctions between the individual perineurial cells were identified as the morphological substrate of the barrier function. [95] Under pathological conditions like inflammation, the perineurium is permeable to macromolecules. Consistently, previous studies have shown that a modified hydrophilic opioid peptide such as DAMGO penetrates the perineural barrier of peripheral sensory nerves to elicit antinociception only when the integrity of this barrier is hampered, e.g. following inflammation or the use of hyperosmolar solutions. [96] There is a growing body of data suggesting that inflammatory conditions entail a deficiency of the perineurial barrier and/or an enhanced permeability of endoneurial capillaries, [97-100] that facilitates the access of molecules such as hydrophilic

opioid agonists to sensory neurons to inhibit inflammatory pain.[96, 101] Similar leakage of the perineurium could also be produced experimentally by the extraneural application of hyperosmolar solutions [96]. Hydrophilic opioids are ineffective, when injected into noninflamed tissue, both in behaviour and electrophysiological experiments. [96, 102, 103] Interestingly, intraplantar pretreatment of rats with hypertonic solutions followed by hydrophilic opioids elicits antinociceptive effects. [96, 103] Therefore, it is concluded that hypertonic solutions can facilitate the access of hydrophilic opioids like DAMGO to the receptor and increase their antinociceptive activity.

2.5 AIMS of the Thesis

This thesis aimed to investigate:

1. The up-regulation of sensory neuron MOR expression and efficacy by NGF in DRG neurons. NGF has been implicated in the up-regulation of the number and efficacy of sensory neuron MOR, resulting in enhanced analgesic effects of opioids applied to painful inflamed tissue. [31] For this reason, this part of the present study aimed to identify the sensory neuron NGF-dependent signaling pathways. In detail the experiments examined whether: a) exogenous as well as FCA-induced elevated endogenous NGF contribute to enhanced antinociception of a full (e.g. fentanyl) or partial (e.g. buprenorphine) opioid agonist; b) NGF-dependent increases in MOR binding, protein and immunoreactive cells in peripheral sensory neurons are abolished by p38-MAPK and/or Erk-1/2 inhibition; c) the number of MOR-IR neuronal cells colocalizing with activated p-p38-MAPK within DRG neurons is increased following i.pl. NGF; d) the number of MOR-IR neuronal cells returns to baseline levels following concomitant i.t. administration of the p38-and/or Erk-1/2 inhibitor MAPK inhibitor; e) local NGF enhances the anterograde axonal transport of MOR along the sciatic nerve via activation of p38-MAPK and/or Erk-1/2; f) NGF-induced enhanced antinociceptive effects of local opioids are abolished by i.t. application of a p38-MAPK and/or Erk-1/2 inhibitor.

2. The endogenous opioid peptide processing and subsequent release from immune cells in PC2 knockout mice versus wild type mice. Using transgenic mice, this study investigated whether the processing enzyme PC2 plays a crucial role in the processing of opioid peptides within circulating and resident immune cells and whether this interferes with their release. The experiments should investigate: (i) the colocalization of the opioid precursors POMC, PENK or PDYN with the key processing enzyme PC2 within subcutaneous inflamed paw tissue of wild type using double immunofluorescence confocal microscopy; (ii) the number of cells containing precursor proteins (POMC, PENK and PDYN) within inflamed paw tissue in wild type versus knockout mice by immunohistochemistry; (iii) the total content of opioid peptide precursor proteins in immune cells within circulation of wild type versus knockout mice by Western blot; (iv) the total content of opioid peptides in immune cells within circulation, inflamed paw tissue and PMN cells of wild type versus knockout mice by RIA; (v) the fMLP-induced release of active peptides such as END, ENK and DYN from PMN of wild type versus knockout mice.

3. The accessibility of opioid receptors by opioid peptides through the perineural barrier in noninflamed tissue. Inflammatory pain can be controlled by exogenous as well as endogenous opioid peptides released from leukocytes into inflamed rat paws. The present experiments sought to examine whether the peripheral application of exogenous as well as the release of endogenous opioid peptides leads to the passage of the perineural barrier of sensory neurons within normal tissue to elicit antinociceptive effects. The investigations should examine (i) the peripheral antinociceptive effects of exogenously applied opioid peptides such as END or ENK; (ii) the peripheral antinociceptive effects of endogenous opioid peptides released by fMLP from PMN whose recruitment was induced by MIP2 pretreatment; (iii) the perineurial permeability to the macromolecule horseradish peroxidase histochemically under normal and inflammatory conditions, and following the in vivo administration of different hypertonic solutions.

3 Materials and methods

3.1 Materials

3.1.1 Chemicals

Table 2: Chemicals and suppliers

Chemicals	Suppliers
Acetic acid	Sigma, Taufkirchen, Germany
Acrylamide 40:1	Carl Roth GmbH, Karlsruhe, Germany
Agarose	Sigma, Taufkirchen, Germany
Albumine from bovine serum	Sigma, Taufkirchen, Germany
Ammonium persulfate (APS)	Sigma, Taufkirchen, Germany
Aprotinin	Sigma, Taufkirchen, Germany
BAPTA/AM	Sigma, Taufkirchen, Germany
Bestatine	Sigma, Taufkirchen, Germany
Boric acid	Sigma, Taufkirchen, Germany
Bromophenol blue	Sigma, Taufkirchen, Germany
cacodylic acid-sodium salts	Sigma, Taufkirchen, Germany
Chaps	Cell Signaling Technology, Inc. Danvers, USA
DAB (3',3'-diaminobenzidine tetrahydrochloride)	Sigma, Taufkirchen, Germany
DAPI (4'-6-Diamidino-2-phenylindole)	Sigma, Taufkirchen, Germany
Dextran 500	GE Healthcare Europe GmbH, Freiburg, Germany
Dimethylsulfoxyde (DMSO)	Sigma, Taufkirchen, Germany
Dithiothreitol (DTT)	Cell Signaling Technology, Inc. Danvers, USA
DNA molecular weight marker	Roche Diagnostics Deutschland GmbH, Mannheim, German
Dibutylphtalate-polystyren-xylen (DPX)	Merck, Darmstadt, Germany
ECL detection reagent	GE Healthcare Europe GmbH, Freiburg, Germany
Ethidium Bromide	Sigma, Taufkirchen, Germany
Ethylendiaminetetraacetic acid (EDTA)	Sigma, Taufkirchen, Germany
Glutaraldehyd	Sigma, Taufkirchen, Germany
Glycerol	Sigma, Taufkirchen, Germany
Glycin	Sigma, Taufkirchen, Germany
Hank's balanced salts (HBSS)	Sigma, Taufkirchen, Germany

Heparin	Rotexmedica GmbH , Trittau, Germany
Horseradish peroxydase (HRP)	Sigma, Taufkirchen, Germany
Hydrogen peroxide (H_2O_2)	Sigma, Taufkirchen, Germany
Isoflurane curamed (1-Chlor-2,2,2-trifluoroethyl) difluoromethylether)	Rhodia Organique Fine Ltd. Bristol United Kingdom
Isopropanol	Sigma, Taufkirchen, Germany
Ponceau S	Sigma, Taufkirchen, Germany
Protein molecular marker	Invitrogen GmbH, Darmstadt, Germany
Metabisulfite	Sigma, Taufkirchen, Germany
Methanol	Carl Roth GmbH, Karlsruhe, Germany
Paraformaldehyde (PFA)	Sigma, Taufkirchen, Germany
Phenylmethanesulfonyl fluoride (PMSF)	Fluka Chemie AG, Buchs, Switzerland
Phosphate buffered saline (PBS, sterile, 0,1M pH 7.4)	Invitrogen GmbH, Darmstadt, Germany
Picric acid	Sigma, Taufkirchen, Germany
Potassium chloride (KCl)	Sigma, Taufkirchen, Germany
Potassium phosphate (KH_2PO_4)	Sigma, Taufkirchen, Germany
Precision plus protein standards	Bio-Rad Laboratories GmbH, München, Germany
Protein loading buffer	Fermentas GmbH, St. Leon-Rot, Germany
Proteinase K	Bio-Rad Laboratories GmbH, München, Germany
Ribonuclease A	Qiagen GmbH, Hilden, Germany
Sodium chloride (NaCl)	Carl Roth GmbH, Karlsruhe, Germany
Sodium dodecyl sulphate (SDS)	Sigma, Taufkirchen, Germany
Sodium phosphate (Na_2HPO_4)	Carl Roth GmbH, Karlsruhe, Germany
ß-Mercaptoethanol	Carl Roth GmbH, Karlsruhe, Germany
Sucrose	Carl Roth GmbH, Karlsruhe, Germany
Tetramethylethylenediamine (TEMED)	Carl Roth GmbH, Karlsruhe, Germany
Thiorphan	Sigma, Taufkirchen, Germany
Tissue-Tek compound	OCT, Miles, Elkhart, Indiana, USA
Trishydroxymethylaminomethane (Tris)	Sigma, Taufkirchen, Germany
Triton X-100	Sigma, Taufkirchen, Germany
Trypan blue Stain (0.4%)	Invitrogen GmbH, Darmstadt, Germany
Tween-20	Sigma, Taufkirchen, Germany
Xylenecyanol FF	Sigma, Taufkirchen, Germany

3.1.2 Kits

Table 3: Kits used for Immunostaining and Polymerase chain reaction

Kits	Company
Histogreen peroxydase kit	Linaris, Wertheim, Bettingen, Germany
Hotstar polymerase kit	Qiagen GmbH, Hilden, Germany
Vectastain avidin- biotin peroxydase complex (ABC) kit	Vector Laboratories, INC.Burlingame, CA, US
Taq Polymerase kit	Roche Diagnostics, Mannheim, Germany

3.1.3 Radiolabeled compounds

Rat **^{125}I- β-** Endorphin (^{125}I END) Peninsula, Belmont, CA, USA

Rat **^{125}I** –MetEnkephalin (^{125}I ENK**)** Peninsula, Belmont, CA, USA

Rat **^{125}I-** Dynorphin 1-17 (^{125}I DYN) Peninsula, Belmont, CA, USA

[^{3}**H**]-DAMGO Amersham, Buckinghamshire, England

3.1.4 Drugs

Table 4: Listing of drugs used and their doses

Drugs	Concentration	Company
β-NGF	4 µg/100 µl	R & D Systems, Minneapolis, USA
Freund's complete adjuvant (FCA)	150 µl	Calbiochem, San Diego, CA, USA
Fentanyl N-phenyl-N-[1-(2-phenylethyl)-4-piperidinyl]propanamide citrate salt	0.25-1 µg/µl	Sigma Aldrich, Taufkirchen, Germany
Buprenorphine hydrochloride (21-(Cyclopropyl-7α-[(S)-1-hydroxy-1,2,2-trimethylpropyl]-6,14-endo-ethano-6,7,8,14-tetrahydrooripavine hydrochloride	1-5 µg/µl	Sigma Aldrich, Taufkirchen, Germany
SB203580 (4-(4-fluorophenyl)-2-(4-methylsulfonylphenyl)-5-(4-pyridyl)-1H-imidazole)	1 µg/10 µl	Calbiochem, San Diego, CA, USA
PD98059 (2′-Amino-3′-methoxyflavone)	1 µg/10 µl	Calbiochem, San Diego, CA, USA
MIP-2 (macrophage inflammatory protein gamma)	3 µg/100 µl	PeproTech, London, Great Britain
Formyl-Methionyl-Leucyl-Phenylalanine (fMLP)	3 ng/100 µl	Sigma Aldrich, Taufkirchen, Germany
Naloxone	0.28 ng/100 µl	Sigma Aldrich, Taufkirchen, Germany
β-endorphin (END)	1 µg/100 µl	Bachem AG, Bubendorf, Switzerland
Met-enkephalin (ENK)	20 µg/100 µl	Bachem AG, Bubendorf, Switzerland
Oyster Glycogen	1 g/100 ml	Sigma Aldrich, Taufkirchen, Germany
Lidocaine	2% (v/v)	Sigma Aldrich, Taufkirchen, Germany

3.1.5 Standard buffers

Table 5: Buffers used for Western blots, polymerase chain reactions, radioimmunoassays and their preparations.

Buffer	Composition	Concentration
PBS	NaCl	140 mM
	KCl	30 mM
	Na_2HPO_4	6.5 mM
	KH_2PO_4	1.4 mM
TBE	Tris base	100 mM
	Boric acid	100 mM
	EDTA	2.5 mM
TBS-T	NaCl	0.15 mM
	Tris-HCl pH 8	10 mM
	Tween 20	0.05% (v/v)
HBSS	Calcium chloride (anhydrous)	0.1396 $g.L^{-1}$
	Magnesium sulfate (anhydrous)	0.09767 $g.L^{-1}$
	Potassium chloride	0.4 $g.L^{-1}$
	Potassium phosphate monobasic anhydrous	0.06 $g.L^{-1}$
	Sodium chloride	8 $g.L^{-1}$
	Sodium phosphate dibasic	0.04788 g. L^{-1}
Tail buffer	Tris pH 8.5	100 mM
	EDTA pH 8.0	5 mM
	SDS	2% (w/v)
	NaCl	200 mM
Tris-EDTA	Tris-HCl pH 7.4	10 mM
	EDTA pH 8.0	1 mM
Cacodylate buffer (stock 0.4 M)	cacodylic acid-sodium salt	85,6 $g.L^{-1}$
Stripping buffer	Tris pH 6.7	62,6 mM
	SDS	2% (w/v)
	ß-mercaptoethanol	100 mM
PBS 0.1 M (pH 7.4)	NaCl	1.37 M
	KCl	27 mM
	Na_2HPO_4	100 mM
	KH_2PO_4	20 mM

3.1.6 Technical Equipments

Table 6: Equipment used and the suppliers

Equipment	Suppliers
Algesiometer (Randall-Sellito)	Ugo Basile Srl, Comerio VA , Italy
Cryostat	Microm International GmbH, Walldorf, Germany
Fluorescence microscope	Carl Zeiss MicroImaging GmbH, Germany
Gamma counter, wallac wizard 1470	GMI, Inc. Minnesota, USA
Gel casting trays	Bio-Rad Laboratories GmbH, München, Germany
PHmeter MP220	Mettler-Toledo GmbH, Giessen, Germany
Power Pac300	Bio-Rad Laboratories GmbH, München, Germany
Spectrophotometer (UV 1601)	Shimadzu Europa GmbH, Duisburg, Germany
Thermocycler (Gene Amp 9700)	Applied Biosystems GmbH, Darmstadt, Germany
Thermomixer	Eppendorf AG, Hamburg, Germany
Transilluminator	Herolab GmbH, Wiesloch, Germany
Ultrapure water systems (Direct-QTM5)	Millipore GmbH, Schwalbach/Ts.,Germany
UV-light (Macro Vue UV25)	Hoefer, Inc. Holliston, MA, USA
Vacuum system (concentrator 5301)	Eppendorf AG, Hamburg, Germany
Sonicator 3000	Giltron, INC, Massachussetts, USA
Centrifuge Rotixa 50 RS	Hettich Zentrifugen, Tuttlingen, Germany

3.1.7 Oligonucleotide primers for PCR

Table 7: The primers used for polymerase chain reaction. They were purchased from TIB MOLBIOL GmbH, Berlin, and Germany.

Knock-out PC2	PC2-E33	5'-CGC TGC AAC AAG AAG GAT T-3'	19 mer	180 bp
	PKJ1-2	5'- CCA CTT GTG TAG CGC CAA GT-3'	20 mer	
Wild type PC2	PC2-E33	5'-CGC TGC AAC AAG AAG GAT T-3'	19 mer	117 bp
	PC2-PN	5'- TAG AGA AAC TTA CCA GGT ACC-3'	21 mer	

3.1.8 Antibodies and synthetic peptide antigens

Table 8a: Listing of primary antibodies used for the following applications: IHC = immunohistochemistry, RIA = radioimmunoassay, WB = Western blot

Primary Antibody	Dilution	Application	Immunogens	Company
Rabbit anti-POMC	1:1000	WB, IF	AA 27-52 of POMC precursor	Phönix Pharmaceuticals Inc. Burlingame, USA
Mouse monoclonal anti-POMC	1:1000	ICH	Beta endorphin 1-31	Biogenesis, Poole, UK
Mouse monoclonal anti-PENK	1:1000	WB, ICH, IF	Leu5-enkephalin conjugated to BSA	LifeSpan Biosciences, WA, USA
Rabbit anti-PDYN	1:1000	WB	AA 1-16 of human dynorphin A	Abcam, CSP, Cambridge, UK
Ginea pig anti-PDYN	1:200	ICH, IF	AA 235-248 of PDYN precursor	Neuromics, MN, USA
Rabbit anti-PC2	1:1000	WB, ICH, IF	AA 740-751 of human PC2	D. F. Steiner, University of Chicago, IL, USA
Rabbit anti-END	1:10	RIA	AA 6-31 of beta endorphine	Bachem AG, Bubendorf, Switzerland
Rabbit anti-ENK	1:10	RIA	Full length Met enkephaline (aa 1-5)	Bachem AG, Bubendorf, Switzerland
Rabbit anti-DYN	1:10	RIA	Full DYN A (AA 1-17)	Bachem AG, Bubendorf, Switzerland
Rabbit polyclonal anti-MOR	1:1000	WB	AA 389-400 of mu opioid receptor	Gramsch Laboratories, Schwabhausen, Germany
Mouse monoclonal anti-p38 MAPK	1:1000	WB	Full p38 MAPK	Cell Signaling Technology, Inc. Danvers, USA
Mouse monoclonal anti-pp38 MAPK	1:500	WB	Phosphorylated p38 MAPK at Thr 180 and Tyr 182	Cell Signaling Technology, Inc. Danvers, USA
Mouse monoclonal anti-beta-actin	1:10000	WB	N-terminal end of beta actin	Sigma Aldrich, Taufkirchen, Germany
Guinea pig polyclonal anti-CGRP	1:1000	IHC	Full length CGRP (AA 1-37)	Peninsula Laboratories, Belmont, CA, USA
Rabbit anti-NGF antiserum	1:12.5	Behavior	Raised against β- NGF	Cedarlane, Burlington, Ontario, Canada

Table 8b: Listing of secondary antibodies used for the following applications: IHC = immunohistochemistry, RIA = radioimmunoassay, WB = Western blot. IF = Immunofluorescence

Secondary antibodies	Dilution	Application	Company
Peroxidase-conjugated goat anti-rabbit	1:5000	WB	Amersham
Peroxydase rabbit anti-mouse	1:5000	WB	Abcam, CSP, Cambridge, UK
Biotinylated goat anti-rabbit	1:200	IHC	Vector Laboratories, Inc.)
Biotinylated goat anti-mouse	1:200	IHC	Vector Laboratories, Inc.)
Biotinylated goat anti-guinea pig	1:200	IHC	Vector Laboratories, Inc.)
Goat anti-rabbit (GARGG)	1:200	RIA	Bachem AG, Bubendorf, Switzerland
Goat anti-guinea pig (GAGGG)	1:200	RIA	Bachem AG, Bubendorf, Switzerland
Texas red conjugated goat anti-rabbit	1:200	IF	Vector Laboratories, Inc.)
FITC conjugated donkey anti-mouse	1:200	IF	Vector Laboratories, Inc.)
FITC conjugated donkey anti-guinea pig antibody	1:200	IF	Vector Laboratories, Inc.)

3.1.9 Consumable materials

Materials	Company
Hyper film ECL	GE Healthcare Europe GmbH, Freiburg, Germany
Filter (microcon YM10)	Millipore GmbH, Schwalbach/Ts.,Germany
Nitrocellulose membrane	Bio-Rad Laboratories GmbH, München, Germany
Mini-osmotic pump Model 2001	Alzet, Coopertino, CA, USA
PCR reaction tubes and caps	Applied Biosystems GmbH, Darmstadt, Germany
Pipettes (1-25 ml, one-way)	SARSTEDT AG & Co. Nümbrecht, Germany
Polyethylene PE10 catheter	Portex Ltd, Hythe, UK
Polysin microscope slides	Menzel GmbH & Co KG, Braunschweig, Germany
Reaction tubes 0.5, 1.5 and 2ml	Eppendorf AG, Hamburg, Germany
Sponge	Bio-Rad Laboratories GmbH, München, Germany
Syringes 1, 2,10 ml	Braun Melsungen AG,Melsungen, Germany
Transfer cassette	Bio-Rad Laboratories GmbH, München, Germany
Transfer Tank	Bio-Rad Laboratories GmbH, München, Germany
Tubes (15 and 50 ml)	Falkner Consulting für Messtechnologie GmbH, Gräfelfing-Lochham, Germany
Gelatine coated slides	Tekdon, INC, Florida, USA
Heparin-coated tubes	Becton Dickinson Franklin Lakes, NJ, USA

3.1.10 Softwares

Sigma stat and sigma plot softwares were used for statistical analysis and graphing, respectively. Image J software was used for quantification of Western blot signals.

Sigmaplot 10 software Systat Software Inc. Chicago, US

Sigmastat software Systat Software Inc. Chicago, US

ImageJ software Downloaded from http://rsb.info.nih.gov/ij/ (November 17, 2004)

3.2 Methods

3.2.1 Animals

Male Wistar rats (200-250 g, bred at the Charité Universitätsmedizin Berlin, Campus Benjamin Franklin, Germany) as well as male wild type and PC2 knockout mice of the genetic background C57BL/6j were housed in cages lined with ground corncob bedding. Animals were housed in cages and maintained on a 12 h light/dark schedule with food pellets and water ad libitum. Room temperature was maintained at 22±0.51ºC and a relative humidity between 60 and 65%. A 12/12 hr (8 a.m/8 p.m.) light/dark cycle was used. Experiments were performed in accordance with standard ethical guidelines and approved by the local animal care committee (Landesamt für Arbeitsschutz, Gesundheitsschutz und Technische Sicherheit, Berlin, Germany).

3.2.2 Surgical procedures in rats

3.2.2.1 Intrathecal catheter implantation

Intrathecal catheters were implanted in rats according to previously described protocols. [31] Animals were anesthetized with isoflurane in oxygen via the nose cone. A longitudinal skin incision was made in the lumbar region directly above the spinous processes of the vertebrae. The needle through which the catheter was set up was inserted in a 30º angle at the L5–L6 vertebra. The catheter (polyethylene PE10 catheter, 15 cm in length, 0.61 mm outer diameter) was carefully moved forward, while rotating it between the thumb and forefinger. This rotation facilitated the penetration through the intervertebral space and dura. The sign of dura penetration was observed by spontanous movement of the tail and hind limbs. The catheter was then carefully pushed upward 1-2 cm into the intrathecal space. The needle was carefully removed and the catheter was sealed with glue to the tissue. Another skin incision was made at the dorsal neck of the animal and the catheter was tunnelled under the skin and pulled out at the neck and the incisions were sutured. The intrathecal location of the catheter was

confirmed after surgery by administration of 10µl lidocain 2%. Lidocain caused bilateral hind limb paresis that lasted 10-20 minutes and no deficits occurred in animals injected with saline. The animals were finally allowed to recover for at least 2 days prior to experiments. Only animals exhibiting no motor deficits were used for further behavioural testing.

3.2.2.2 Drug delivery

The following substances were injected intraplantarly: 1) Freund's complete adjuvant (FCA), a water-in-oil emulsion with killed mycobacteria was injected in a volume of 150 µl. This treatment produced a localized inflammation of the inoculated paw characterized by redness, warming, swelling, and infiltration of various types of immune cells. 2) The beta subunit of NGF (β-NGF) (4 µg/100 µl) was dissolved in PBS and administered once per day. 3) Anti-NGF antiserum (8 µg/100 µl) dissolved in PBS was injected twice per day, the first injection administered 30 min before FCA injection. Fentanyl (0.25-1 µg/100 µl), buprenorphine (1-3 µg/100 µl), ß-endorphine (1 µg/100 µl), Met-enkephaline (20 µg/100 µl), MIP-2 (3 µg/100 µl) were dissolved in saline. MIP-2 was dissolved in normal saline and was administered 1 h before NaCl 10 %. fMLP (3 ng/100 µl) dissolved in normal saline was injected following 1 h NaCl 10%. Naloxone (0, 28 ng/100 µl) was dissolved in saline and co-injected with endorphine, enkephaline or fMLP. 3) Glycogen (1 %) was dissolved in water and injected intraperitonealy.

The following substances were given intrathecally: 1) the p38 MAPK inhibitor 4-(4-fluorophenyl)-2-(4-methylsulfonylphenyl)-5-(4-pyridyl)-1H-imidazole (SB203580) (1 µg/10 µl) was applied twice per day, 2) The ERK MAPK inhibitor 2′-amino-3′-methoxyflavone (PD98059) (1 µg/10 µl) or vehicle (DMSO, 2 %) was injected twice per day, with the first injection administered 30 min before the i.pl. NGF injection. The dose of p38 MAPK inhibitor or the ERK MAPK inhibitor was selected based on previously published experimental protocols. [104, 105] Inhibitors SB203580 or PD98059 were dissolved in dimethyl

sulfoxide (DMSO) diluted with sterile distilled water (final concentration 2 %), and injected intrathecally. 2 % DMSO solution was used as vehicle. For a 96 h experiments, after anchoring the intrathecal catheter, osmotic mini-pumps (Alzet, model 2001, 0.5 µl/h) were primed and attached to the catheter and the pumps were filled with solution of above mentioned inhibitors and implanted subcutaneously.

3.2.3 Nerve ligation

Rats were anesthetized with isoflurane. The right hind legs were shaved and the skin was sterilized with 70% ethanol. In rats anesthetized with isoflurane a tight ligation of the sciatic nerve was performed. The right sciatic nerve was surgically exposed and ligated with a 4.0 non-absorbable silk at the mid-femoral position. [31] The muscle and the adjacent fascia were closed with sutures, and the skin was closed with clips.

3.2.4 Experimental groups

Rats were divided into different treatment groups: 6-8 rats per group were used for behavioural experiments and 3 rats per group for Western blot and immunohistochemistry.

1) In one part of the experiments, 4 days after i.pl. treatment with vehicle, FCA, FCA with anti-NGF, NGF, FCA or NGF with i.t. inhibitors SB203580 or PD98059, nociceptive thresholds were assessed before (baseline) and after acute i.pl. injection of the full opioid agonist fentanyl or the partial opioid agonist buprenorphine using the paw pressure algesiometer. 2) The other part of the experiments rats pre-treated intraplantarly with FCA or MIP2 were used. In rats with FCA inflammation, nociceptive thresholds were assessed before (baseline) and after acute i.pl. injection of either END, ENK or fMLP alone or with NLX. In these experiments, rats without inflammation were treated intraplantarly with 100 µl 0.9 % or 10 % saline for disruption of the perineurial barrier 60 min after intraplantar administration of

MIP2 to recruite immune cells. Then 60 min later nociceptive thresholds were assessed before (baseline) and after acute i.pl. injection of either END, ENK or fMLP alone or with NLX.

3.2.5 Assessment of nociceptive thresholds

Mechanical thresholds were determined using the paw pressure algesiometer. Rats were handled once per day over four days before testing. On the day of testing to adjust the animals to the testing conditions, rats were held under paper wadding and incremental pressure was applied via a wedge-shaped, blunt piston onto the dorsal surface of the hind paw by means of an automated gauge. The pressure required to elicit paw withdrawal, the paw pressure threshold (PPT), was determined before and 5 min after i.pl. drug administration. The pressure required to elicit paw withdrawal, the paw pressure threshold (PPT) (cutoff at 250 g), was determined by averaging three consecutive trials separated by 10 s time intervals. The sequence of left and right paws was alternated between animals to avoid bias. The experimenter was blind to the experimental protocol.

3.2.6 Immunological and immunohistochemical methods

3.2.6.1 Western blot

The protein concentration was measured from cell extracts using a bicinchoninic acid (BCA) assay (Pierce). BSA at different concentrations was used as standard protein. Alinear standard curve was made and the concentration of unknown sample was read across the graph to the intersection with the curve. Samples were homogenized in boiling SDS sample buffer (100 mM Tris, 2% SDS, 20% glycerol) as previously described by Ji and Rupp in 1997. [106] Proteins separated by SDS-PAGE were immobilised onto nitrocellulose membranes by electrophoretic transfers. The extracts were separated using 10 % or 12 % SDS-PAGE. 60 µg proteins were loaded per lane and transferred onto nitrocellulose filters. To determine the

transfer efficiency, the membranes were reversibly stained in Ponceau S dye (0.1 % Ponceau S, 1 % acetic acid in distilled water). After complete washing of the Ponceau stain, unbound sites of the membranes were blocked by incubation for 1 h in 5 % skimmed milk powder in TBS-Tween (TBS-T). For immunodetection of protein bands, nitrocellulose membranes with immobilised proteins from rat's DRG or circulating immune cells of mice with hind paw inflammation were incubated with the following primary antibodies (table 8) a) Rabbit polyclonal MOR antiserum, mouse monoclonal antip38-MAPK, or anti-phospho-p38 MAPK (p-p38-MAPK) antibodies overnight at 4ºC for DRG proteins. b) Rabbit polyclonal anti-POMC, Rabbit polyclonal anti-PDYN, Rabbit polyclonal anti-PC2; mouse monoclonal anti-PENK antibodies overnight at 4ºC for circulating immune cells proteins. After incubation with the respective secondary antibodies (1:5000) (peroxidase-conjugated goat anti-rabbit, Amersham or peroxidase-conjugated rabbit anti-mouse, Abcam) for 2 h at room temperature, reactive bands were visualized in Enhanced ChemiLuminescence (ECL) solutions for 1 min and immediately exposed to autoradiographic film for 5–20 min. Finally, the blots were incubated for 30 min at 56 °C in stripping buffer (62.6 mM Tris-HCl, pH 6.7, 2 % SDS, 100 mM mercaptoethanol) and reprobed with monoclonal mouse anti-beta-actin antibody as a loading control.

3.2.6.2 Quantification of immunoblotting

Western blots were scanned and the Java Image processing and analysis software (ImageJ) was used to quantify differences in immunodensities. The upper and lower threshold density ranges were adjusted to provide an image with immunoreactive material (ECL reaction product) appearing in black pixels and nonimmunoreactive material appears in white pixels. A standardized box was positioned over each band. The area and density of pixels within the threshold values representing immunoreactivity were measured, and the integrated density (the product of the area and density) was calculated. Integrated densities of controls and

treated groups were compared and statistically analyzed. A percent change from control (treated/control) was then calculated to demonstrate differences compared to the control group. As Western blot ECL reactions can vary despite a standard protocol, comparison of both groups was performed within the same blot.

3.2.6.3 Immunohistochemistry

Animals were deeply anesthetized with isoflurane and perfused transcardially with 20 ml 0.1 M PBS (pH 7.4) and 50 ml cold PBS containing 4 % paraformaldehyde and 0.2 % picric acid (pH 7.4; fixative solution). Tissue of the inflamed paw was removed, postfixed for 45 min at 4 °C in the fixative solution and cryoprotected overnight at 4 ºC in PBS containing 10 % sucrose. The tissues were then embedded in Tissue-Tek compound (OCT, Miles, Inc., Elkhart, IN) and frozen. Consecutive sections (8 μm thick) prepared on cryostat were mounted onto gelatin-coated slides.

3.2.6.3.1 Single immunohistochemical staining procedures

Immunohistochemical staining of the sections was performed with a Vectastain avidin-biotin peroxidase complex (ABC) kit. Incubations were performed at room temperature, and PBS was used for washing (three times for 10 min each time) after each step. The sections were incubated with PBS, 0.3 % H_2O_2, and 10 % methanol for 45 min to block endogenous peroxidase. To prevent nonspecific binding, the sections were incubated for 60 min in PBS containing 0.3 % Triton X-100, 1 % BSA, 4 % goat serum, and 4 % horse serum (block solution). The sections were then incubated overnight at 4 ºC with the following primary antibodies: mouse monoclonal antibody against POMC, PENK or guinea pig polyclonal antibody against PDYN. Thereafter, the sections were incubated for 1 h with the appropriate secondary antibodies: a biotinylated goat anti-rabbit, goat anti-mouse or goat anti-guinea pig secondary antibody and then with ABC for 45 minutes. Finally, the sections were washed and

stained with 3',3'-diaminobenzidine tetrahydrochloride (DAB) containing 0.01 % H_2O_2 in 0.05 M Tris-buffered saline (pH 7.6) for 3–5 min. After the enzymatic reaction, the sections were washed in tap water, counterstained with thionin, then dehydrated in alcohol, cleared in xylene, and mounted in DPX.

3.2.6.3.2 Histochemistry of horseradish peroxidase (HRP)

In order to assess the perineurial permeability, rats received intraplantar injections of 10 % NaCl and subsequently 8 mg horseradish peroxidase (HRP). Then 5, 60 or 120 min later, rats were perfused with 1.25 % glutaraldehyde, 1 % paraformaldehyde in PBS containing 5% sucrose. Skin and adjacent subcutaneous tissue were dissected from the plantar surface of the hindpaws. To visualize HRP, transverse sections (30 μm) of subcutaneous tissue were mounted on slides and incubated in the dark with 200 mg of diaminobenzidine tetrahydrochloride in 100 ml of cacodylate buffer (0.1 M, pH 5.1) and 1 % hydrogen peroxide for 30 min at room temperature. The sections were then washed in cacodylate buffer, left in air to dry at room temperature, and finally coverslipped with entelan.

3.2.6.4 Double Immunofluorescence

Double immunofluorescence staining was performed for DRG and sciatic nerve from rats or inflamed subcutaneous tissue of mice as followed: 1) Rat DRG or sciatic nerve mounted tissue sections were incubated with the following primary antibodies: rabbit polyclonal MOR antibody alone or in combination with mouse monoclonal pp38-MAPK antibody or guinea pig polyclonal antibody against CGRP (Table 8). The tissue sections were washed with PBS and then incubated with the appropriate secondary antibodies: Texas red conjugated goat anti-rabbit antibody alone or in combination with FITC conjugated donkey anti-mouse or anti-guinea pig antibody. 2) Inflamed paw mounted tissue sections of mice were incubated with the following primary antibodies: rabbit polyclonal PC2 in combination with mouse

monoclonal POMC, PENK or Guinea pig PDYN antibody (Table 8). The tissue sections were washed with PBS and then incubated with the appropriate secondary antibodies. Texas red conjugated goat anti-rabbit antibody alone or in combination with FITC conjugated donkey anti-mouse or anti-guinea pig antibody. Finally, the tissues were washed in PBS, mounted on vectashield and viewed under a Zeiss LSM 510 laser scanning microscope.

3.2.6.4.1 Quantification of immunoreactive cells

Following single immunostaining, the total number of immunoreactive cells was counted by a blinded experimenter in three tissue sections per animal. Five squares (38.4 mm^2 each) per section were analyzed using a Zeiss microscope (objective, 40 x 10 Carl Zeiss, Oberkochen, Germany). This number was divided by the total number of cells per square in each section. The percentage of immunostained cells was determined by the formula: immunostained cells/total number of immune cells x 100. The proportion was calculated as percentage of the total number of immunoreactive cells in each section. For quantification of immunoreactivity images of red (Texas red) immunofluorescence were obtained using a Zeiss LSM 510 laser scanning microscope and the Image-Analysis software package 2.5 SP2 from Zeiss was applied to quantify changes in immunodensities. [31, 107] Images were threshold to exclude background fluorescence and gated to include intensity measurements only from positively stained cells. For images analysis, a standardized box was positioned over the proximal part of the ligated sciatic nerve of all groups to determine the mean product of the area (μm^2) and mean intensity of pixels within the threshold value and to calculate the integrated optical intensity (product of area and mean intensity).

3.2.6.5 Specificity controls

To demonstrate specificity of staining, the following controls were included: 1) Preabsorption of antibody against MOR, POMC, PENK, PDYN or PC2 with a synthetic peptide for MOR

(Gramsch Laboratories, Schwabhausen, Germany), POMC (Phoenix Pharmaceuticals), or recombinant PC2 (provided by D. F. Steiner) for 24 h at 4 ºC; 2) omission of either the primary antisera, the secondary antibodies or the avidin–biotin complex; 3) omission of either the first or second primary antibody and either the first or second secondary antibody.

3.2.7 Genotyping of mice

3.2.7.1 Tail DNA preparation

Tails (2 mm) from mice were excised. To prepare templates for genotyping, a quick protocol for tail lysis with proteinase K was used. [108] 90 µl of tail buffer and 9 µl proteinase K (10 mg/ml) were added to the tails and incubated overnight at 55 ºC. Tail preparations were further heated at 95 ºC for 10 minutes for proteinase K inactivation and 750 µl of Tris-EDTA + RNase A (100 mg/ml) were added, mixed and stored at 4 °C for short term or -20 °C for long term.

3.2.7.2 Genotyping of mice by polymerase chain reaction (PCR)

PCR reaction without DNA was carried out as a negative control (to confirm the absence of contamination). PCR reaction with DNA from wild type mice was carried out as a positive control and compared with knockout mice. PCR was carried out as described by Furuta et al. [109] All three primers were mixed together (Table 7) and one PCR was performed. 117 bp products were amplified corresponding to the wild type mice and 180 bp products corresponding to knockout mice. Heterozygote mice presented both bands. The amplification consisted of an initial denaturation step of 5 min at 94 ºC, followed by a 35 cycles of 30 s at 94 °C , 30 s at 55 °C and 1 min at 72 ºC. The final extension step was 5 min at 72 ºC. DNA products were mixed with loading buffer loaded in a 2.5 % agarose gel together with Marker IX and after electrophoretic migration the bands were detected using UV trans-illumination.

Table 10: Pipetting scheme for standard PCR: PC2

Reagent	Volume (µl)	Final concentration
Forward primer (10 µM)	2	0.4 µM
Reverse primer (10 µM)	2	0.4 µM
dNTP mix (0.125 mM)	1	2.5 µM
MgCl2 (25 mM)	4	2.0 µM
10x reaction buffer	5	
Taq polymerase (1 U/µl)	0.4	0.008 U/µl
RNAse free water	33.6	
Tail preparation	2	

3.2.8 Isolation of leukocytes from circulating blood and peritoneal cavity

FCA was injected in all mice at a volume of 20 µl intraplantarly. 48 h after induction of inflammation blood samples (1-1.5 ml/mice) were collected by cardiac puncture and kept in heparin-coated tubes (Becton Dickinson Franklin Lakes, NJ, USA). White blood cells were separated from red blood cells by dextran gradient sedimentation. Dextran solution (3 % Dextran 500 in 0.9 % NaCl) was overlaid by an equal volume of blood and left for 20 min at room temperature for sedimentation. Erythrocytes were removed from the supernatant by hypotonic lysis using 0.2 % NaCl for 30 s and the reaction was stopped by adding an equal volume of 1.6 % NaCl. After 10 min centrifugation at 1200 rpm, 4 ºC, the pellets were resuspended in 1ml HBSS buffer. Cells were counted, centrifuged at 1200 rpm at 4 ºC for 20 min and the supernatants were stored at -80 ºC for further experiments. Mice peritoneal PMN were harvested by lavage of the peritoneal cavity with 2 ml PBS/2 mM EDTA, 4 h after i.p. injection of 2 ml 1 % oyster glycogen in PBS [(110)] and cells were isolated as indicated above.

3.2.9 Peptide extraction from inflamed paw tissue and circulating immune cells

Mice were killed and tissues from inflamed paws were dissected and frozen in liquid nitrogen. Tissues were then ground into a fine powder using a mortar and pestle. 200 µl of metabisulfite were added to $3x10^6$ isolated circulating immune cells and 1 ml for 1g of paw powder and these samples were boiled for 10 min, cool down on ice and quick spin. The samples were then sonicated on ice (30 s/cycle for 20 cycles). Acetic acid 1 M (1:4) was added to each tube. All tubes were vortexed and incubated on ice with gentle shaking for 1 h. Samples were centrifuged at 13000 rpm for 20 to 30 min at 4°C and the supernatant was filtered through a Microcon YM-10 unit (in order to rule out high molecular weight peptides that includes precursors) and centrifuged again at 11300 rpm for 24 min at 4 °C. The supernatant were concentrated with a vacuum centrifuge (Speed Vac) and dissolved in RIA buffer for RIA experiments.

3.2.10 Opioid peptide release from PMN

PMN cells were purified by hypotonic lysis of erythrocytes using 0.2 % NaCl for 30 s and the reaction was stopped by adding an equal volume of 1.6 % NaCl. For determination of opioid peptide release, cells were preincubated with cytochalasin B (5 mg/ml) for 5 min in Hank's balanced salt solution containing the proteinase inhibitors bestatin (5 mg/ml), aprotinin (40 mg/ml) and thiorphan (100 mM) [70] and were stimulated with fMLP (1000 nM). Cells were concomitantly incubated with fMLP and calcium chelating agent BAPTA/AM (100 µM), fMLP alone or buffer (for basal release). Release was terminated after 7 min of incubation by rapid cooling, centrifugation, and harvesting of the supernatant. Supernatants were stored at -20 ºC until further analysis by radioimmunoassay using commercially available kits for met-enkephalin, beta-endorphin, or dynorphin.

3.2.11 Opioid peptide immune cell content by Radioimmunassay (RIA)

Radioimmunoassay was performed for END, ENK and DYN using the same protocol. Samples (circulating immune cells, inflamed paw and PMN cells) were reconstituted in RIA buffer (containing 0.1 M Sodium Phosphate, 0.05 M NaCl, 0.01 % NaN_3, 0.1 % bovine serum albumin and 0.1 % Triton X-100) and assays were performed using RIA kits. Tubes were prepared in duplicate containing 100 µl of standard concentrations of END or ENK or DYN or unknown samples (except total count, non-specific binding and total binding tubes dissolved in RIA buffer. Samples and standards and total binding tubes were sealed and incubated with rabbit anti-END or anti-ENK or anti-DYN (100 µl) overnight at 4 °C. On day 2, rabbit ^{125}I END or ^{125}I ENK or ^{125}I DYN (100 µl, 12000–15000 cpm) were added and tubes were incubated overnight at 4 °C. On day 3, 100 µl each of the the secondary antibody goat anti-rabbit IgG and normal rabbit serum (Bachem) were added to all samples to precipitate primary antibody-protein complexes. After 90 min at room temperature the reaction was stopped by adding 500 µl of RIA buffer in all tubes. Tubes were finally spun at 1700 g for 20 min at 4 ºC. Except the total count tubes, the supernatant was aspirated and bound radioactivity in the pellets was counted as count per min (cpm) in a Gamma counter (GMI, Inc. Minnesota, USA). To determine specific binding, the mean cpm of non-specific binding samples was subtracted from all other samples. Calculations were made automatically as follows: Bmax: Total binding - Non-specific binding and to determine B/B_{max} for the standards and unknown samples the following calculation was used: B/B_{max} = (cpm-value – non-specific binding) * 100 $\%/B_{max}$. A standard curve was generated on a semilog graph paper where $\%B/B_{max}$ = f (log of the standard concentrations of the peptide). Using $\%B/B_{max}$ calculated for each sample, the point of intersection with the best fit curve and the X-axis coordinate is equivalent to the concentration of peptide (pg /100 µl) assayed sample.

3.2.12 Statistics

Paw pressure threholds (PPT) obtained from behavioral experiments are expressed either in gram or in percent of maximal possible effect according to the formula (% MPE) = 100 x (PPT post injection – PPT basal)/ (250 cut-off –PPT basal). [111] Values are expressed as means ± standard deviation (SD) or standard error of mean (SEM). For two group comparisons normally distributed data were analyzed by Student t-test (Sigma stat; Jerrold H. Zar: Biostatistical analysis, 2nd Ed.) not normally distributed data were analyzed by the Mann-Whitney rank sum test. Multiple group comparisons were analyzed by one way ANOVA or by ANOVA on ranks in case of not normally distributed data (Sigma stat; Jerrold H. Zar: Biostatistical analysis, 2nd Ed.). Dose response curves were analyzed by linear regression ANOVA and compared using two-way ANOVA (Sigma stat; Jerrold H. Zar: Biostatistical analysis, 2nd Ed.). The post hoc tests chosen were the Student Newman Keul's test or Dunn's test (Sigma stat; Jerrold H. Zar: Biostatistical analysis, 2nd Ed.). Differences were considered significant if $p<0.05$.

4 Results

4.1 NGF-dependent enhancement of antinociceptive effects of peripheral full and partial opioid agonists

A significant and dose-dependent increase in PPT was observed in control rats, when the full MOR agonist fentanyl was intraplantarly injected at doses of 0.5–1.0 µg (Fig. 7 A, B). This is consistent with the development of dose-dependent antinociception. In rats with FCA hindpaw inflammation, the dose-response curve elicited by i.pl. injection of the same doses of fentanyl significantly shifted to the left towards enhanced potency (Fig. 7 A). Immunoneutralization of endogenous NGF by anti-NGF antiserum in FCA inflamed hindpaws reversed this left-ward shift in potency (Fig. 7 A). In contrast, pretreatment of naive rats with i.pl. NGF (4 µg/100 µl) resulted in a similar left-ward shift towards enhanced potency of i.pl. fentanyl (Fig. 7 B). In control rats, i.pl. injection of the partial opioid agonist buprenorphine (1-5 µg) did not increase PPT consistent with a lack of peripheral efficacy (Fig. 7 C, D). In rats with FCA hindpaw inflammation, administration of the same doses of buprenorphine significantly and dose-dependently increased PPT (Fig. 7 C, D). However, the maximum peripheral antinociceptive effects of i.pl. buprenorphine were lower than those elicited by i.pl. fentanyl. Immunoneutralization of NGF by anti-NGF antiserum in FCA-treated rat hindpaws significantly abolished the antinociceptive efficacy elicited by i.pl. buprenorphine (Fig. 7 C). In contrast, pretreatment of naive rats with i.pl. NGF (4 µg/100 µl) resulted in a similar degree of enhanced efficacy of i.pl. buprenorphine (Fig. 7 D).

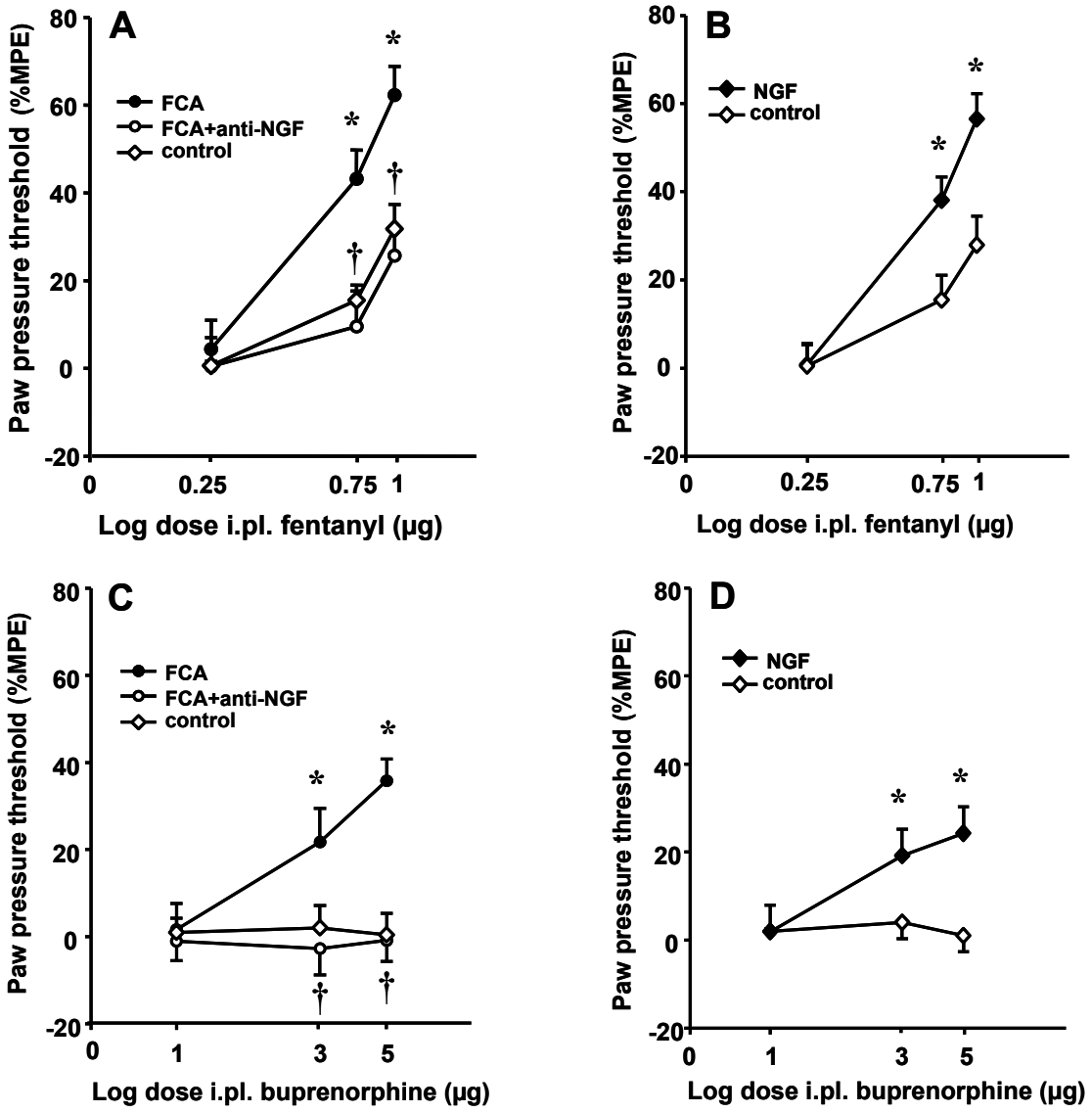

Figure 7: Antinociceptive effects of i.pl. fentanyl or buprenorphine following pretreatment with i.pl. vehicle, FCA, NGF or NGF plus anti-NGF-Ab. Pretreatment of Wistar rats (6-8 per group) were performed by intraplantar vehicle, FCA (150µl), NGF (4µg/100µl), or NGF plus anti-NGF-Ab (8µg/100µl) four days before experiments. Paw pressure thresholds were determined by a modified Randall-Selitto algesiometer measuring the threshold to increasing mechanical pressure at which the animal withdrew its hindpaw. Increased PPT represents increased antinociception. (A, B) Intraplantar injection of the full opioid agonist fentanyl produced a significant and dose dependent increase in PPT of control animals. Pretreament with i.pl. FCA (A) or NGF (B) shifted the dose-response curve to the left towards higher antinociceptive potency. Immunoneutralization of endogenous NGF in FCA-inflamed hind paws by i.pl. anti-NGF-Ab (A) reversed this left-ward shift in potency. (C, D) Intraplantar injection of the partial opioid agonist buprenorphine did not alter PPT of control animals. Pretreament with i.pl. FCA (C) or NGF (D) resulted in significant PPT increases towards higher antinociceptive efficacy. Immunoneutralization of endogenous NGF in FCA-inflamed hind paws by i.pl. anti-NGF-Ab (C) reversed this increase in antinociceptive efficacy. Data represent means ± SD. $P<0.05$, two-way ANOVA and Student-Newman-Keuls test, *denotes significant differences of FCA or NGF versus Control; †denotes significant differences of FCA versus FCA plus anti-NGF.

4.2 The involvement of p38 MAPK in NGF-dependent increases of MOR binding sites, immunoreactive cells and protein in DRG

In DRG of rats treated with i.pl. NGF with or without the i.t. p38 MAPK inhibitor SB203580 or i.t. ERK1/2 MAPK inhibitor PD98059, MOR-specific [3H]DAMGO binding sites were evaluated and compared to vehicle (Fig. 8). The number of [3H]DAMGO binding sites in DRG was significantly increased 24 h after NGF treatment compared to that of control rats (Fig. 8 A). This increase in MOR specific [3H]DAMGO binding sites induced by NGF was significantly reversed following i.t. p38 MAPK inhibitor SB203580, but not following i.t. ERK1/2 inhibitor PD98059 (Fig.8 A). Analysis of MOR immunofluorescence staining of DRG showed a significant up-regulation in the percentage of MOR-IR cells in DRG (40.2 ± 7.3 %) at 24 h following locally administered NGF in comparison to vehicle-treated animals (32.1 ± 6.2%). Intrathecal application of the p38 MAPK inhibitor SB203580 (27.7 ± 4.6 %) significantly reduced the percentage of MOR-IR cells in comparison to NGF-treated animals (Fig.8 B). Protein bands at the expected molecular weight of 50 kDa were detected by Western blot analysis of DRG tissue extracts of control animals, corresponding to MOR-IR, (Fig. 8 C). Following 24 h after i.pl. NGF treatment, the integrated optical density of MOR-IR protein bands was significantly increased by 67% compared to that of vehicle-treated animals. This increase was prevented following the i.t. administration of the p38 MAPK inhibitor SB203580. In parallel, at 24 h after NGF treatment the integrated optical density of phosphorylated pp38 MAPK-IR protein bands at the expected molecular weight of 43 kDa was significantly increased 8-fold compared to that of vehicle-treated animals (Fig.8D). This increase was significantly reduced from 8 to 5.6-fold by i.t. administration of the p38 MAPK inhibitor SB203580 (Fig. 8 D). In contrast, the integrated optical density of total p38 MAPK-IR protein bands at the expected molecular weight of 38 kDa increased only slightly by 0.4-fold in NGF treated compared to vehicle treated animals and did not significantly change following i.t. treatment of the p38 MAPK inhibitor SB203580 (Fig. 8 E).

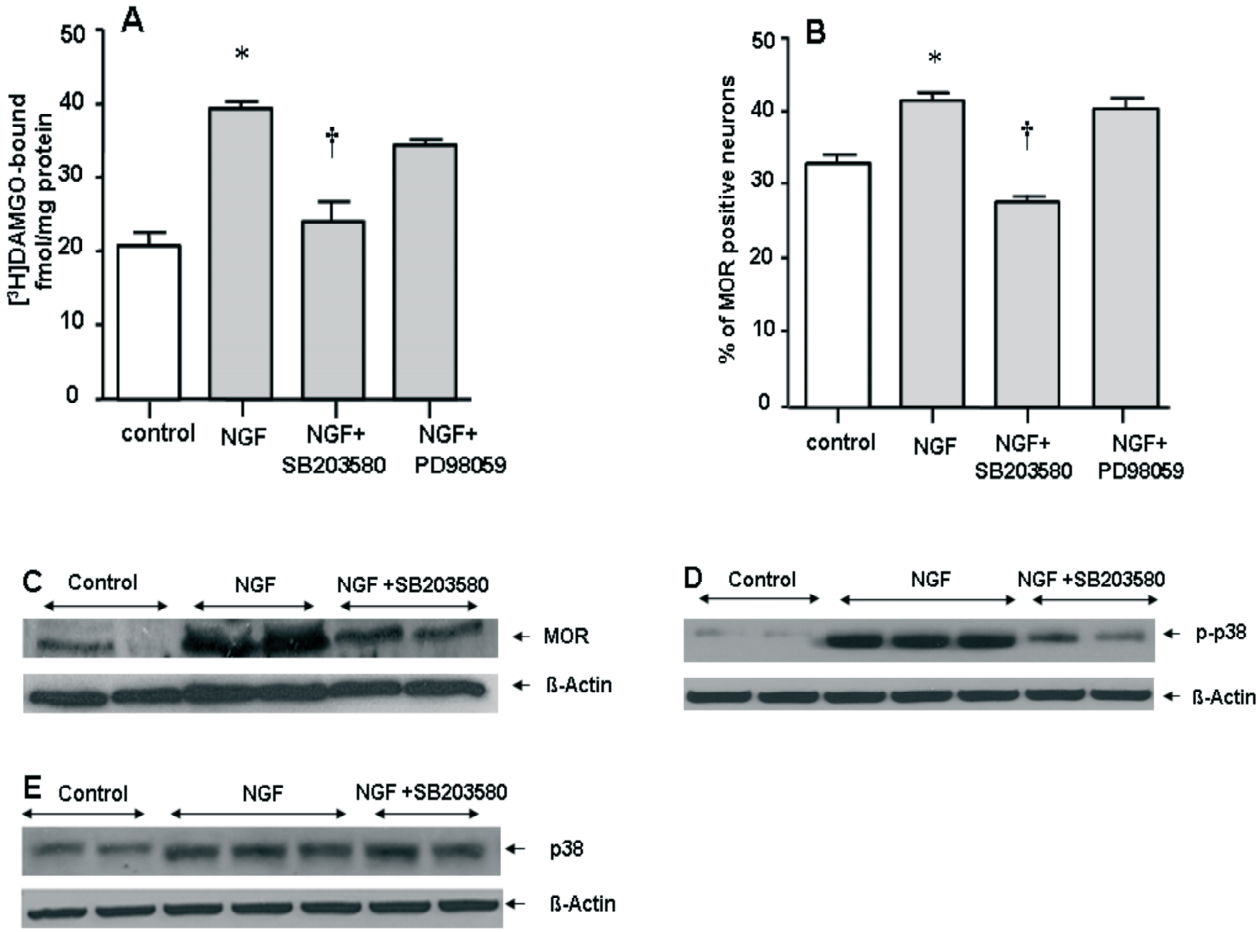

Figure 8: Determination of MOR binding sites (A), MOR-ir neurons (B), MOR protein (C) and p-p38 (D) or p38 (E) MAPK protein in DRG neurons. Animals were treated with i.pl. vehicle (control), NGF (4 µg/100 µl), NGF plus the i.t. p38 MAPK inhibitor SB203580 (1 µg) or the i.t. ERK MAPK inhibitor PD98059 (1 µg), DRG removed and examined for: (A) differences in MOR specific binding sites by the MOR selective radiolabeled ligand [^{3}H]DAMGO (0.01–1 nM); (B) differences in the number of MOR labelled neurons immunohistochemically stained by a specific anti-MOR-Ab; (C-E) differences in the intensity of the MOR- (50 kDa), pp38 (43 kDa), p38 (38 kDa) and β-actin (42 kDa) specific protein bands. Differences indicate that NGF pretreament resulted in an increase in MOR binding sites, MOR-ir neurons, and MOR protein paralleled by an increase in activated pp38 which was inhibited by i.t. application of the p38 MAPK inhibitor SB203580, but not the ERK MAPK inhibitor PD98059. Data are expressed as means ± SEM. $P<0.05$, ANOVA and Student-Newman-Keuls test, *denotes significant differences of NGF versus control; † denotes significant differences of NGF versus NGF plus SB203580.

4.3 NGF-dependent increase in phosphorylated p-p38-MAPK of MOR expressing neurons is prevented by i.t. p38 MAPK inhibitor SB203580

MOR and p-p38-MAPK in DRG of control animals were examined by double immunofluorescence confocal microscopy. The results showed MOR-IR neurons (51.1 ± 2.2 %) colocalizing with p-p38 MAPK, whereas some neurons expressed MOR (48.9 ± 2.2 %) alone (Fig.9A-C). Following 24 h after i.pl. NGF treatment, the percentage of MOR-IR neurons colocalizing with p-p38- MAPK was significantly increased (83.2 ± 3.5 %) compared to that of vehicle-treated animals (Fig. 9 D-F). This NGF-induced elevation in the percentage of MOR colocalization with p-p38-MAPK in DRG neurons was significantly attenuated following i.t p38 MAPK inhibitor SB203580 (55 ± 2.9 %) (Fig. 9 G-I).

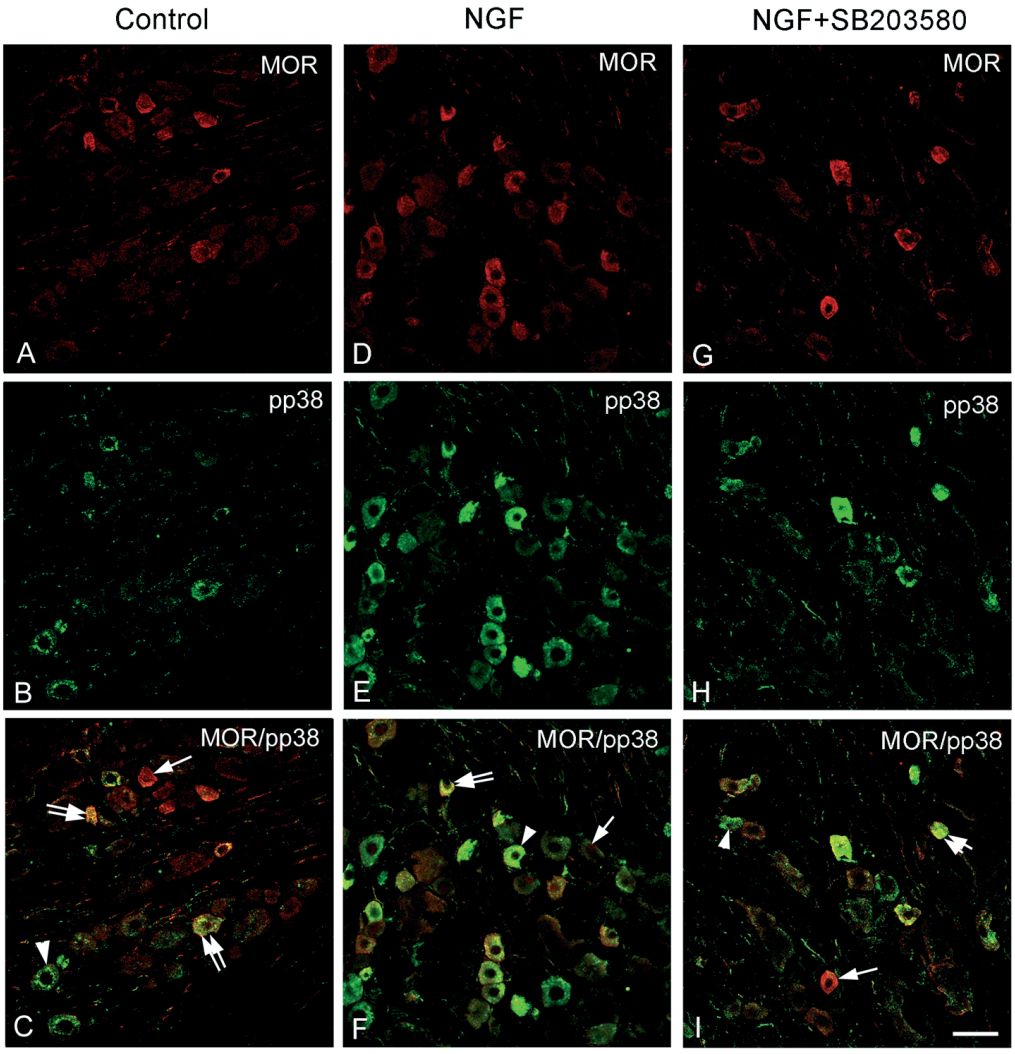

Figure 9: Double immunofluorescence confocal microscopy of MOR and p-p38 colocalization in DRG neurons. Double-immunofluorescence staining of representative DRG sections from control, NGF, or NGF plus i.t. SB203580 treated rats with MOR- (Texas red fluorescence) and p-p38 (FITC green fluorescence) specific antisera. (A, D, G) MOR-ir neurons and p-p38-ir (B, E, H) clearly colocalized as observed with yellow cells (arrows) (C, F, I), however, few cells contained only MOR or p-p38. Following NGF treatment the number of MOR-ir neurons colocalizing with p-p38 was higher than in control animals and this increase was prevented by the i.t. p38 inhibitor SB203580. Merging Texas red and FITC green fluorescence resulted in yellow colour representing a high degree of colocalization of MOR with p-p38. Scale bar, 20 µm.

4.4 Phosphorylation of p38 MAPK mediates NGF-dependent increases in the axonal transport of sciatic nerve MOR

The axonal MOR immunoreactivity proximal to a sciatic nerve ligature was examined using double immunofluorescence confocal microscopy in rats treated with i.pl. NGF (Fig. 10 D-F), NGF with i.t p38 MAPK inhibitor SB203580 (Fig. 10 G-I) or vehicle (Fig. 10 A-C). MOR immunoreactivity expressed in CGRP-IR nerve fibers accumulated mainly proximal to the ligature of the sciatic nerve. Compared to vehicle treated animals (Fig. 10 A-C), intraplantar NGF treatment induced a significant increase in axonally transported MOR immunoreactivity by 44 % on CGRP-IR nerve fibers proximal to the ligature (Fig. 10 D-F). Intrathecal pretreatment with the p38 MAPK inhibitor SB203580 significantly prevented this increase in axonally transported MOR of CGRP-IR nerve fibres (Fig. 10 G-I).

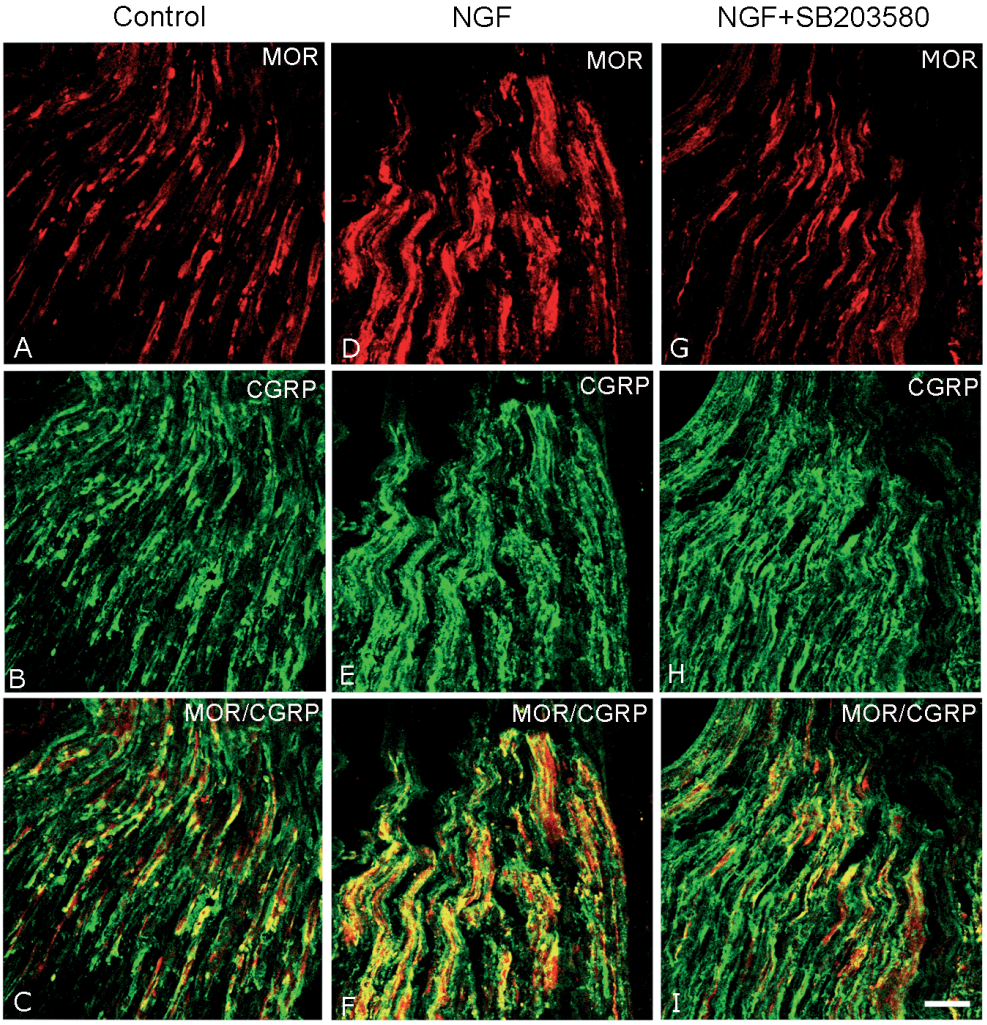

Figure 10: Double immunofluorescence confocal microscopy of axonally transported MOR colocalizing with CGRP in sciatic nerves. Double immunofluorescence staining of longitudinal sciatic nerve sections of control, NGF, or NGF plus i.t. SB203580 treated rats with MOR- (Texas red fluorescence) and CGRP (sensory neuron marker) (FITC green fluorescence) specific antisera. To better visualize axonally transported MOR the sciatic nerve was ligated for 24 h. MOR immunoreactivity colocalized with the sensory neuron marker CGRP, accumulated proximal to the ligature (upper end of each picture) and can be seen in longitudinally directed orientation along the axons of the sciatic nerve. Following NGF treatment MOR-immunoreactivity increased which was prevented by the i.t. p38 MAPK inhibitor SB203580. Merging Texas red and FITC green fluorescence resulted in yellow colour representing colocalization of MOR with CGRP. Scale Bar = 20 µm.

4.5 NGF-induced potentiation of i.pl. fentanyl or buprenorphine antinociception is reversed by i.t. p38 MAPK inhibitor SB203580, but not by the ERK1/2 MAPK inhibitor PD98059

In rats pretreated with i.t. administration of the p38 MAPK inhibitor SB203580, NGF dependent potentiation of i.pl. fentanyl antinociception was significantly reversed (Fig. 11 A). However the NGF-induced fentanyl potentiation did not change, when rats were pretreated with the ERK1/2 MAPK inhibitor PD98059 (Fig. 11 B). NGF dependent enhanced efficacy of i.pl. buprenorphine antinociception was significantly abolished following i.t. administration of the p38 MAPK inhibitor SB203580 but not the ERK1/2 MAPK inhibitor PD98059 (Fig. 11 C, D).

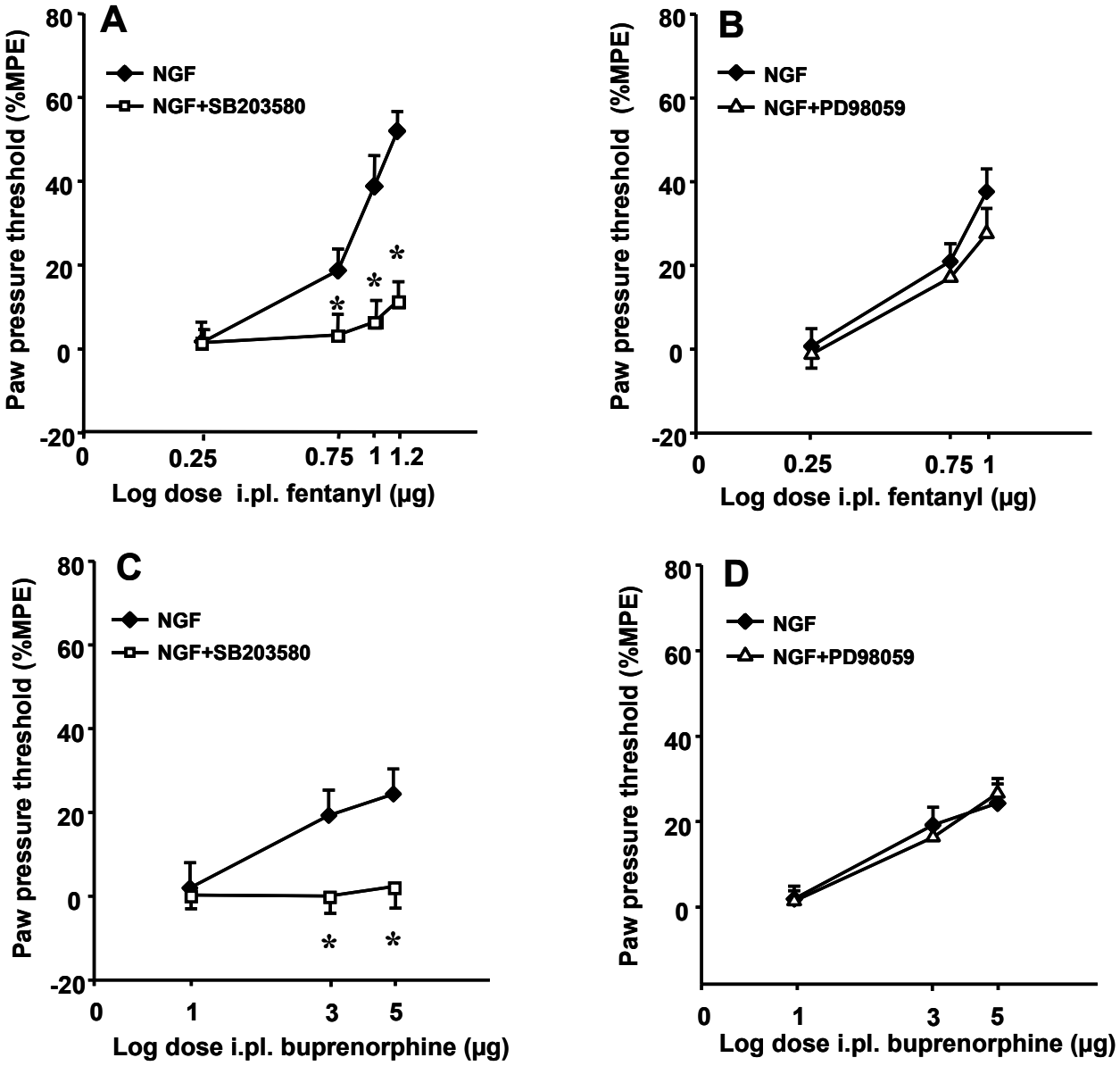

Figure 11: Antinociceptive effects of i.pl fentanyl or buprenorphine following pretreatment with i.pl. NGF, NGF plus i.t. p38 MAPK inhibitor SB203580, or NGF plus i.t. ERK1/2 MAPK inhibitor PD98059. Paw pressure thresholds were determined by a modified Randall-Selitto algesiometer measuring the threshold to increasing mechanical pressure at which the animal withdraws its hindpaw. Increased PPT represents increased antinociception. (A, B) Intraplantar injection of the full opioid agonist fentanyl produced a significant and dose dependent increase in PPT of NGF treated rat hindpaws. Pretreatment with i.t. p38 MAPK inhibitor SB203580 produced a right-ward shift towards lower antinociceptive potency. In contrast, i.t. ERK1/2 MAPK inhibitor PD98059 did not show any significant alterations in PPT. (C, D) Intraplantar injection of the partial opioid agonist buprenorphine produced a dose dependent, however somewhat lower increase in PPT of NGF treated rat hindpaws. Pretreatment with the i.t. p38 MAPK inhibitor SB203580 abolished PPT increases towards a lack of antinociceptive efficacy. In contrast, i.t. ERK1/2 MAPK inhibitor PD98059 did not show a reduction in PPT increases. Data represent mean ± SD. $P<0.05$, two-way ANOVA and Student-Newman-Keuls test, * denotes significant differences of NGF versus NGF plus SB203580.

4.6 FCA-induced potentiation of i.pl. fentanyl or buprenorphine antinociception is reversed by i.t. p38 MAPK inhibitor SB203580, but not by the ERK1/2 MAPK inhibitor PD98059

Intraplantar fentanyl elicited a dose dependent increase in PPT in control rats at doses of 0, 5-1 μg (Fig. 12 A, D). The antinociceptive effect of fentanyl is indicated by an increase in PPT. In vehicle treated rats, i.pl. injection of the full MOR agonist fentanyl (0.5–1.0 μg) elicited a significant and dose-dependent increase in PPT, consistent with the development of dose-dependent antinociception (Fig. 12 A, B). Following FCA–induced inflammation into rats' hindpaws, the dose-response curve elicited by i.pl. fentanyl significantly shifted to the left towards enhanced potency (Fig. 12 A, B). Buprenorphine did not increase PPT in control rats (Fig. 12 C, D), indicating the lack of efficacy. The antinociceptive effects of buprenorphine were increased following i.pl. FCA treatment (Fig. 12 C, D). However, the maximum peripheral antinociceptive effects observed were smaller compared to those elicited by fentanyl. Inflamed rats pretreated with intrathecal administration of p38 MAPK inhibitor SB203580 showed a significant reduction of the PPT elevations after fentanyl or buprenorphine injections (Fig. 12 A, C) but treatment of the animals with the ERK1/2 MAPK inhibitor did not change the antinociception compared with control animals (Fig. 12 B, D).

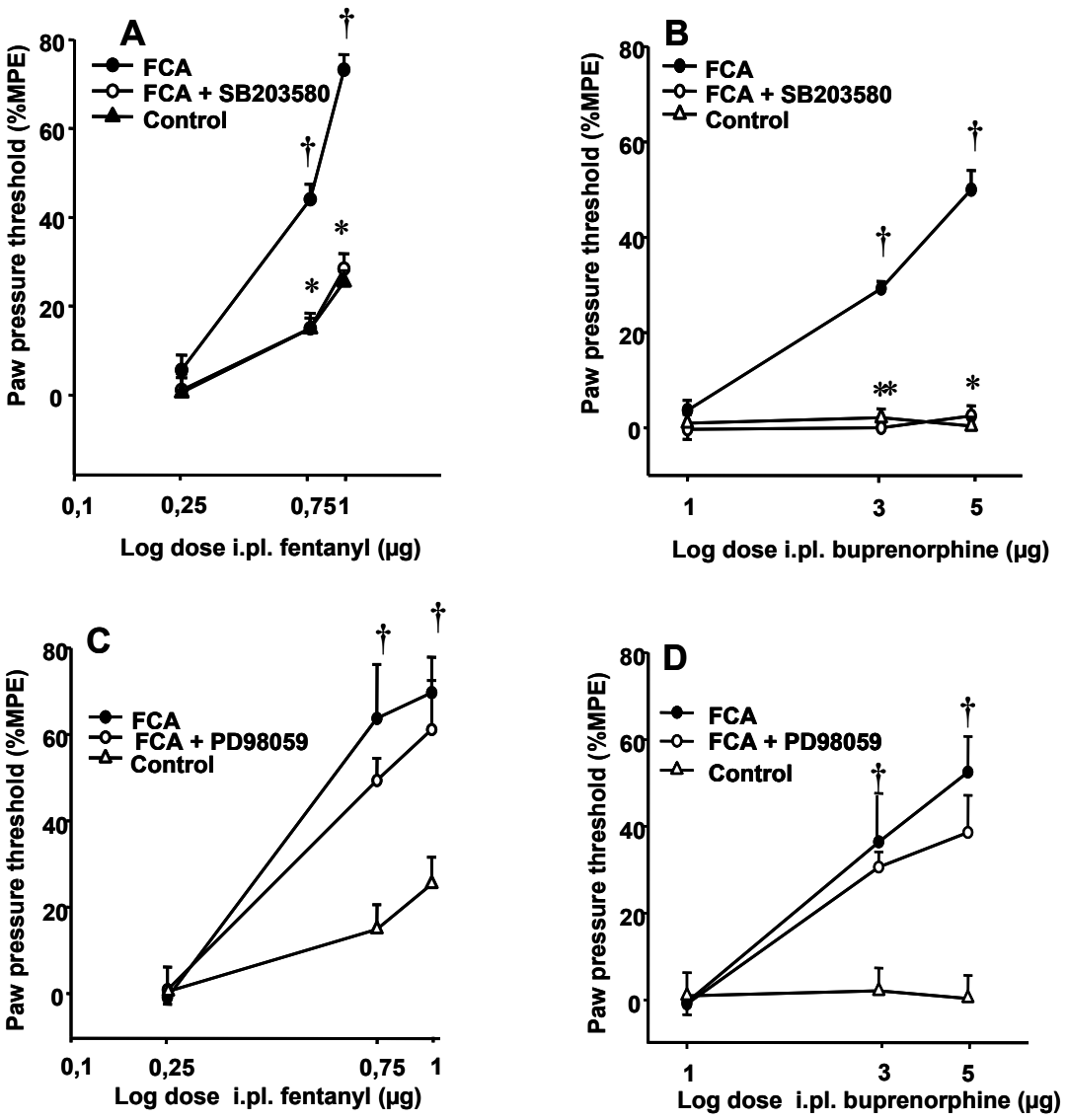

Figure 12: Antinociceptive effects of i.pl. fentanyl or buprenorphine following pretreatment with i.pl. vehicle, FCA, FCA plus i.t. p38 inhibitor SB203580, or FCA plus i.t. ERK inhibitor PD98059. (A, B) Paw pressure thresholds were determined by a modified Randall-Selitto algesiometer measuring the threshold to increasing mechanical pressure at which the animal withdraws its hindpaw. Increased PPT represents increased antinociception. Intraplantar injection of the full opioid agonist fentanyl produced a significant and dose dependent increase in PPT of control and FCA treated rat hindpaws. FCA treatment shifted this dose-response curve to the left towards higher antinociceptive potency. Pretreatment with i.t. p38 MAPK inhibitor SB203580 reversed this left-ward shift towards lower antinociceptive potency. In contrast, i.t. ERK1/2 MAPK inhibitor PD98059 did not show any significant alterations in PPT. (C, D) Intraplantar injection of the partial opioid agonist buprenorphine did not alter PPT of control, but produced a dose dependent, however somewhat lower, increase in PPT of FCA treated rat hindpaws. Pretreatment with the i.t. p38 MAPK inhibitor SB203580 abolished PPT increases towards a lack of antinociceptive efficacy. In contrast, i.t. ERK1/2 MAPK inhibitor PD98059 did not show a reduction in PPT increases. Data represent mean ± SD. $P<0.05$, two-way ANOVA and Student-Newman-Keuls test, * denotes significant differences of FCA vs FCA + SB203580.

4.7 Colocalization of POMC, PENK and PDYN with the processing enzymes PC2 in immune cells of inflamed subcutaneous tissue

Resident immune cells of the inflamed subcutaneous tissue from the hindpaws of untreated wild type mice stained positive for POMC, PENK and PDYN when respective POMC, PENK and PDYN antibodies were used (Fig. 13 A, D, and G). Furthermore, these cells also stained positive for PC2. Their merged images displayed a high degree of colocalization which appeared as yellow fluorescence, implying that both the opioid peptide precursors and the processing enzymes colocalize, as illustrated in Fig. 13 C, F, I. Few cells contained either each opioid precursor or enzyme alone.

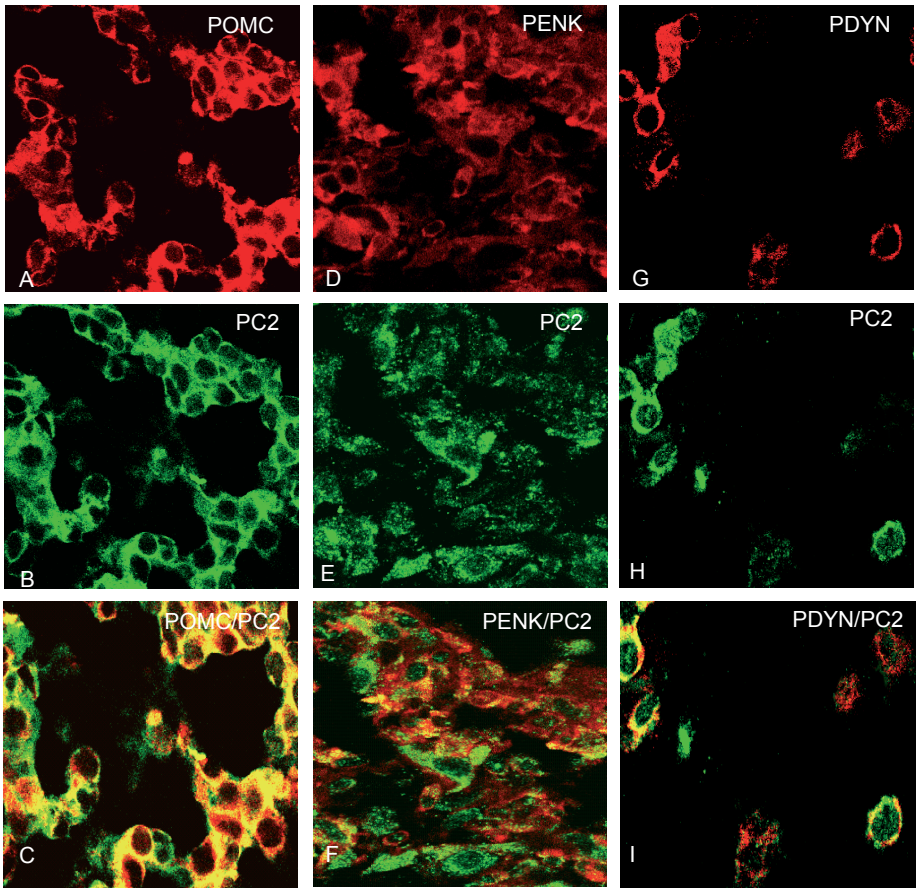

Figure 13: Double immunofluorescence confocal microscopy of POMC, PENK and PDYN colocalizing with the processing enzyme PC2 in immune cells of inflamed subcutaneous tissue. Double immunofluorescence staining of inflamed subcutaneous paw tissue shows colocalization of POMC, PENK and PDYN (A, D, G) (Texas red fluorescence) with the processing enzymes PC2 (B, E, H) (FITC green fluorescence) using a monoclonal mouse anti-POMC, -PENK and -PDYN antibody in combination with a polyclonal rabbit anti-PC2 antibody. Cells double stained for POMC/PC2 (A–C), PENK/PC2 (D–F), and PDYN/PC2 (G–I). Most POMC, PENK and PDYN-immunoreactive cells contained PC2. Merging Texas red and FITC green fluorescence resulted in yellow colour representing colocalization of each opioid precursor with PC2. Scale bar, 20 µm.

4.8 Genotyping and Western blot analysis of PC2 knockout mice

Homozygous PC2 knockout offspring were obtained by mating heterozygous males and females. Elimination of expression of PC2 in all of the homozygous mice was determined by standard PCR and Western blot analysis.

PC2 knockout mice, generated in the C57BL/6J mouse strain were phenotypically normal at birth and showed no gross disturbances in body proportions such as growth and weight. The genotypes showed that genomic DNA from tails revealed amplification of the PC2 gene at the

appropriate size bands of 117 bp for WT. In PC2 knockout mice a 180 bp product was amplified corresponding to the allele at the junction between exon 3 and Neomycin cassette. Both 117 and 180 bp products were observed in PC2 heterozygotes mice (+/-). To confirm the absence of PC2 gene expression in PC2 knockout mice, Western blot analysis detected a 68 kDa protein in wild-type (+/+) mice, consistent with the mature protein which was absent in PC2 knockout mice.

4.9 Defective POMC, PENK and PDYN processing in circulating and resident immune cells of PC2 knockout mice

Circulating leukocytes were isolated from FCA-treated wild type, PC2 knockout mice and analyzed by Western blot displaying POMC immunoreactive bands with an expected molecular weight of 32 kDa. Moreover, optical density analysis of blots from three independent experiments showed an approximately 5-fold accumulation of POMC in PC2 knockout mice compared to wild type (Fig. 14 A). Consistently, semiquantitative analysis of the immunohistochemistry demonstrated that the number of POMC- IR cells in inflamed subcutaneous paw tissue from PC2 knockout was significantly increased compared to that of wild type mice (Fig. 14 B).

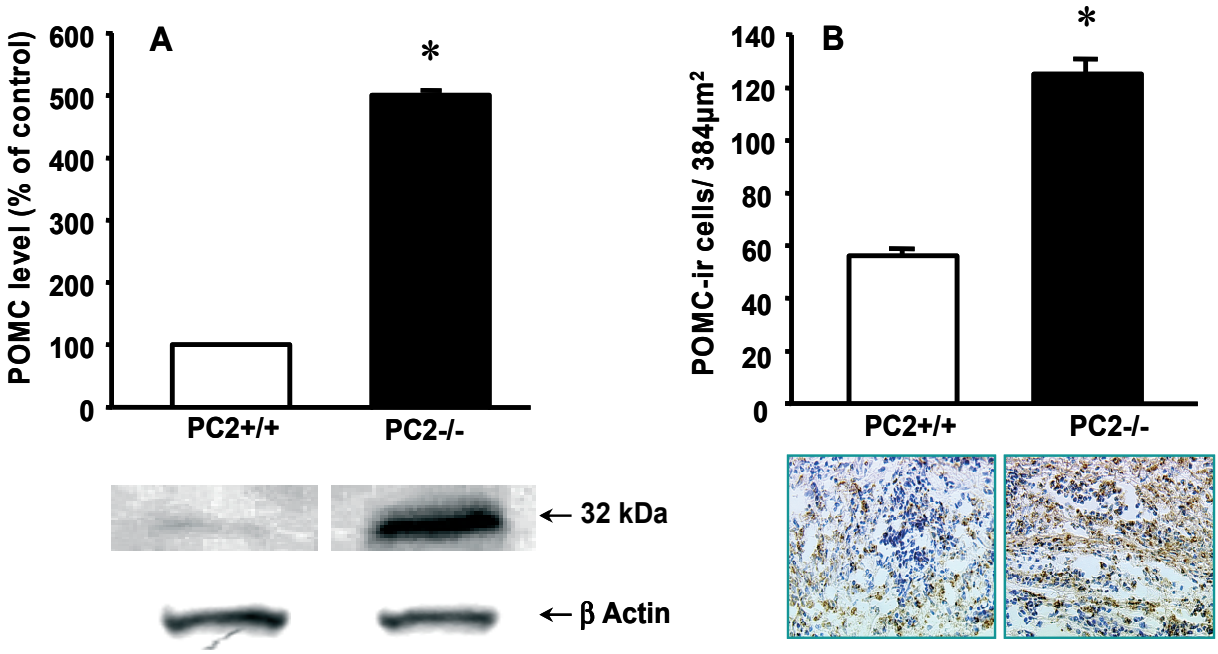

Figure 14: POMC accumulation in circulating and resident immune cells of mice lacking prohormone convertase 2. (A) Optical density analysis of Western blots detecting POMC specific protein bands in circulating leukocytes from homozygous PC2 -/- (PC2 knockout mice) mice and their wild type littermates (+/+) with FCA hindpaw inflammation. Anti-POMC-antibody detected an expected protein band of 32 kDa in circulating immune cells which intensity increased significantly in PC2 knockout compared to wild type mice. Data represent values from three independent experiments in duplicate. (B) Immunohistochemical identification of POMC in sections of inflamed subcutaneous tissue POMC-IR is shown as brown extranuclear staining in immigrated immune cells. Counted POMC-IR cells per square (384 μm^2) were significantly higher in PC2 knockout compared to wild type mice. $P<0.05$, Mann-Whitney U test; "*" denotes significant differences of wild type versus knockout animals.

PENK and PDYN were also well expressed in circulating immune cells of PC2 knockout mice and migrated on SDS/PAGE with the expected molecular size of 30 and 28 kDa, respectively (Fig. 15 A; Fig. 16 A). The optical density analysis of Western blot bands revealed a significant increase in the level of unprocessed PENK- and PDYN-immunoreactivity in circulating immune cells compared to wild type, consistent with PENK and PDYN accumulation in these cells of PC2 knockout mice. In Fig. 15 B and in Fig. 16 B, immunohistochemical analysis showed significant increases in PENK- and PDYN-IR cells in resident immune cells of FCA inflamed subcutaneous tissue of PC2 knockout mice compared to wild type, suggesting that PENK and PDYN had accumulated in these cells in PC2

knockout mice. Therefore, PC2 knockout mice with hindpaw inflammation showed accumulation of POMC, PENK and PDYN in circulating as well as in resident immune cells in comparison to wild type controls.

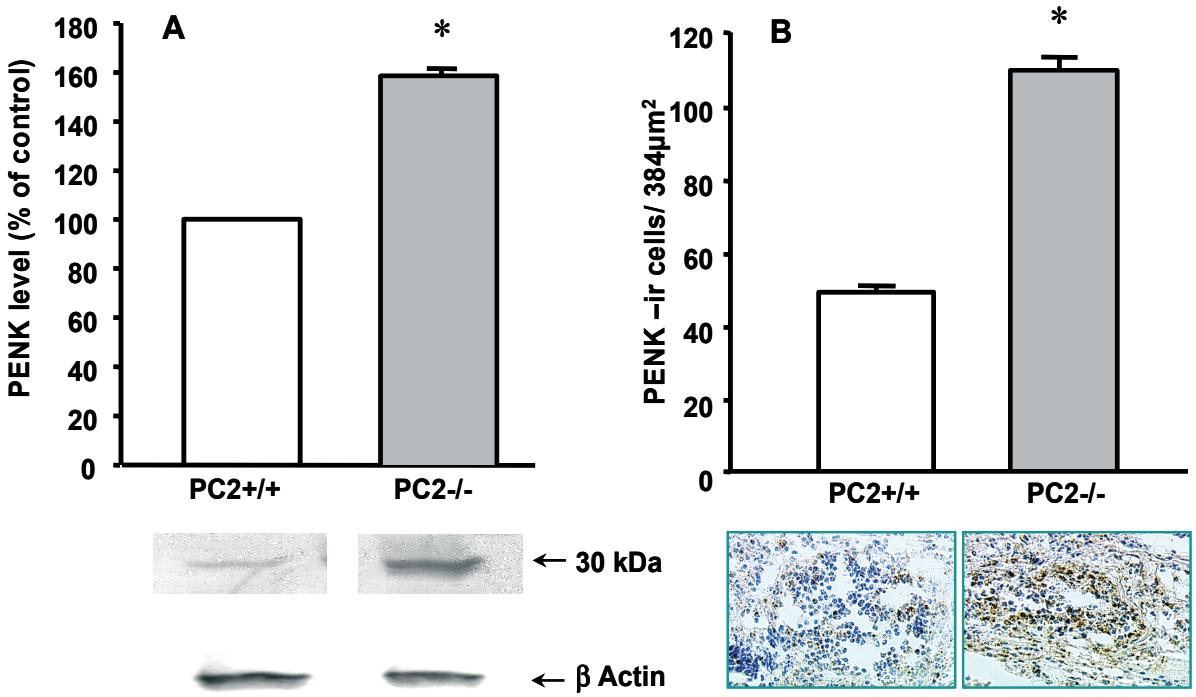

Figure 15: PENK accumulation in circulating and resident immune cells of mice lacking prohormone convertase 2. (A) Optical density analysis of Western blots detecting PENK specific protein bands in circulating leukocytes from homozygous PC2 -/- (PC2 knockout) mice and their wild type littermates (+/+) following FCA hindpaw inflammation. Anti-PENK antibody detected an expected protein band of 30 kDa in circulating leukocytes which intensity increased significantly in PC2 knockout compared to wild type mice. Data represent values from three independent experiments in duplicate (B) Immunohistochemical identification of PENK in sections of inflamed subcutaneous tissue PENK-IR is shown as brown extranuclear staining in immigrated immune cells. Counted PENK-IR cells per square (384 μm^2) were significantly higher in PC2 knockout compared to wild type mice. $P<0.05$, Mann-Whitney U test; "*" denotes significant differences of wild type versus knockout animals.

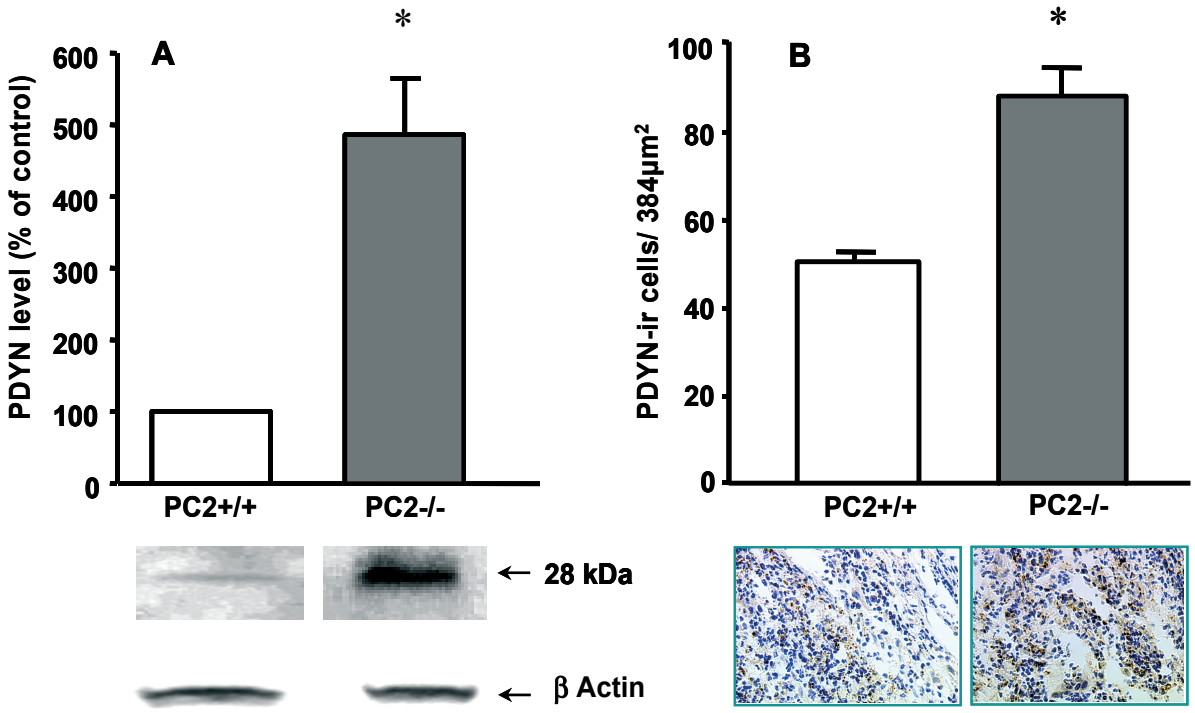

Figure 16: PDYN accumulation in circulating and resident immune cells of mice lacking prohormone convertase 2. (A) Optical density analysis of Western blots detecting PDYN specific protein bands in circulating leukocytes from homozygous PC2 -/- (PC2 knockout) mice and their wild type littermates (+/+) with FCA hindpaw inflammation. Anti-PDYN antibody detected an expected protein band of 28 kDa in circulating immune cells which intensity increased significantly in PC2 knockout compared to wild type mice. Data represent values from three independent experiments in duplicate. (B) Immunohistochemical identification of PDYN in sections of inflamed subcutaneous tissue PDYN-IR is shown as brown extranuclear staining in immigrated immune cells. Counted PDYN-IR cells per square (384 μm^2) were significantly higher in PC2 knockout compared to wild type mice. $P<0.05$, Mann-Whitney U test; "*" denotes significant differences of wild type versus knockout animals.

4.10 Reduction of END, ENK and DYN in circulating and resident immune cells of PC2 knockout mice with FCA hindpaw inflammation

In circulating immune cells END (Fig. 17 A), ENK (Fig. 17 B) and DYN (Fig. 17 C) were expressed in wild type mice. However, the content of all these opioid peptides significantly decreased in circulating immune cells of PC2 knockout mice. In addition, immune cells that immigrated into inflamed subcutaneous tissue revealed a significant decrease in END (Fig. 17

D), ENK (Fig. 17 E) and DYN (Fig. 17 F) content in PC2 knockout mice compared to wild type.

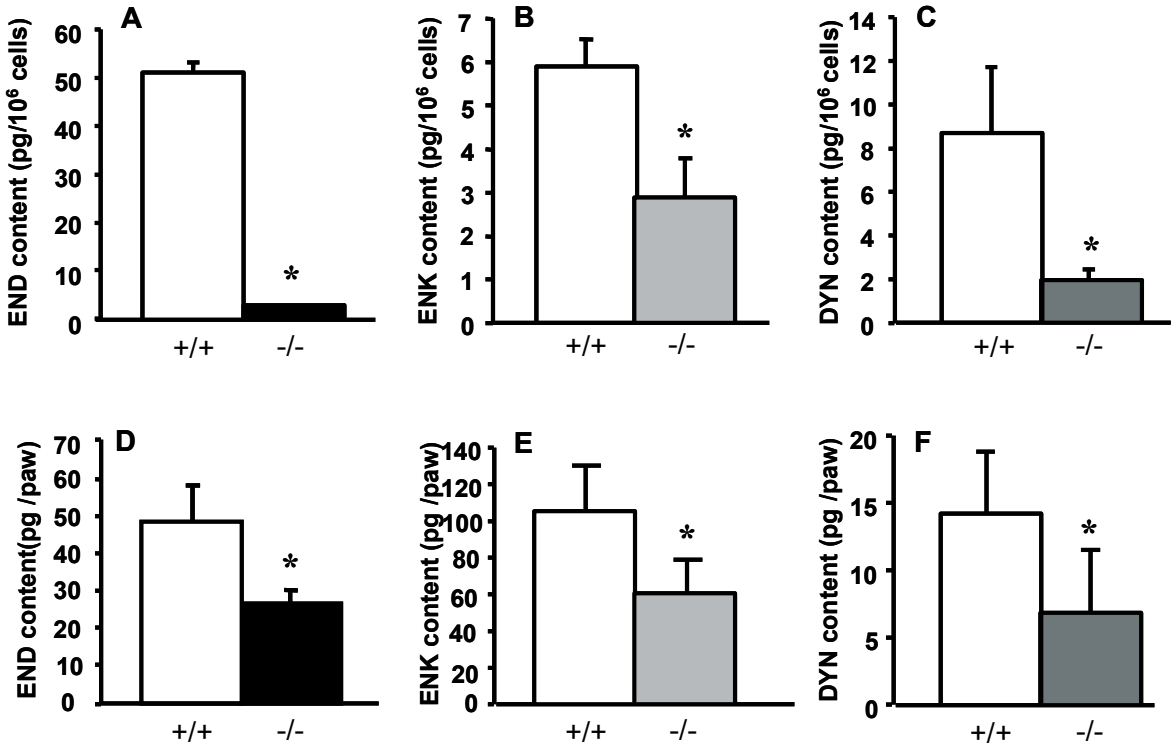

Figure 17: Quantification of END, ENK, and DYN in circulating and resident immune cells of wild type and PC2 knockout mice by radioimmunoassay. Circulating and resident immune cells of wild-type and PC2 knockout mice were analyzed using radioimmunoassay to measure the END (A and D), ENK (B and E), and DYN (C and F) content. In circulating and resident immune cells of PC2 knockout mice ir-END, -ENK and -DYN were significantly decreased compared to wild type. $P<0.05$, Student t-test."*" denotes significant differences of wild type versus knockout animals.

To demonstrate that differences in opioid peptide content of immune cells were relevant for their release subsequent experiments were performed in polymorphonuclear cells (PMN) recruited from the peritoneal cavity of mice following i.p. glycogen (1 % for 4 h) challenge as described by Rittner et al. in 2006. With this an easier availability of large quantities of leukocytes needed for the release experiments was achieved. Results of the radioimmunoassay revealed a significant decrease in the content of END (Fig. 18 A), ENK (Fig. 18 B) and DYN (Fig. 18 C) in PMN cells of PC2 knockout mice compared to wild type.

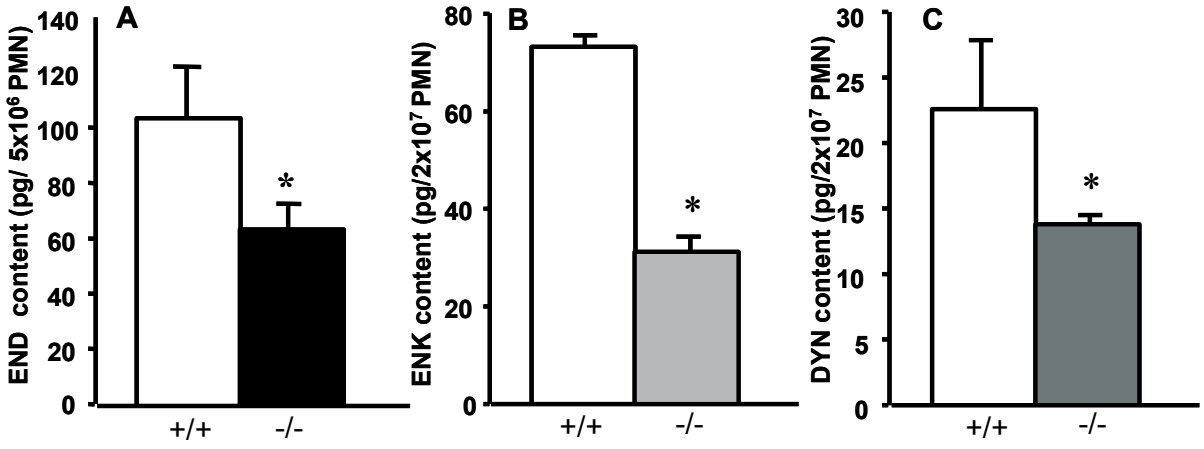

Figure 18: Quantification of ir-END (A), ir-ENK (B) and ir-DYN (C) in PMN cells of wild type and PC2 knockout mice recruited from the peritoneal cavity following glycogen challenge. PMN cells were recruited from the peritoneal cavity of mice after 4 h of an i.p. glycogen (1 %) challenge. PMN cells of WT and PC2 KO mice were analyzed using radioimmunoassay. Ir-END (A), ir-ENK (B) and ir-DYN content in PMN cells was significantly lower in PC2 knockout mice than in wild type mice. Data from three independent experiments in duplicate represent means ± SD. $P<0.05$, Student t-test. * denotes significant differences of wild type versus knockout animals.

4.11 FMLP-induced END, ENK and DYN release from PMN cells in vitro is reduced in PC2 knockout mice

PMN cells, recruited after 4 h of i.p. 1 % glycogen challenge were viable according to trypan blue cell viability. An analysis gate was set on PMN cells that were stained for the fMLP receptor FPR. The FPR was identified by specific binding of FITC-labeled fMLP in the presence of 1 μM unlabeled fMLP (to detect and subsequently subtract nonspecific binding) (grey histogram) and illustrated graphically (Fig. 19 A). The FPR staining using FITC-conjugated fMLP (1 μM) reveals a high intensity of the fluorescence (Black line histogram). Following incubation of PMN cells with fMLP the release of END in the supernatant significantly increased over basal release (supernatant from cells incubated only with the buffer HBSS) (Fig. 19 B). However, this release was significantly attenuated in PC2 knockout mutant compared to wild type. The basal release of END did not change in PMN cells from PC2 knockout in comparison to wild type. Elevation of intracellular calcium is required for

opioid peptide release. ([110, 112]) Chelating intracellular calcium by 1,2-bis (2-amino-phenoxyl)-ethane-N,N,N,N-tetra-acetic acid tetrakis (acetometyl ester) (BAPTA/AM) prevented fMLP-induced END release from PMN cells of both PC2 knockout and wild type mice, confirming calcium dependency.

The incubation of PMN cells of wild type and PC2 knockout mice with HBSS buffer resulted in the basal release of ENK and DYN in the supernatant. The basal release of ENK and DYN did not change in PMN cells of PC2 knockout in comparison to wild type. When these cells were incubated with fMLP, an opioid peptide releasing agent, the release of ENK and DYN observed was significantly increased over basal release (Fig. 20 A, B). This release was significantly attenuated in PC2 knockout compared to wild type mice.

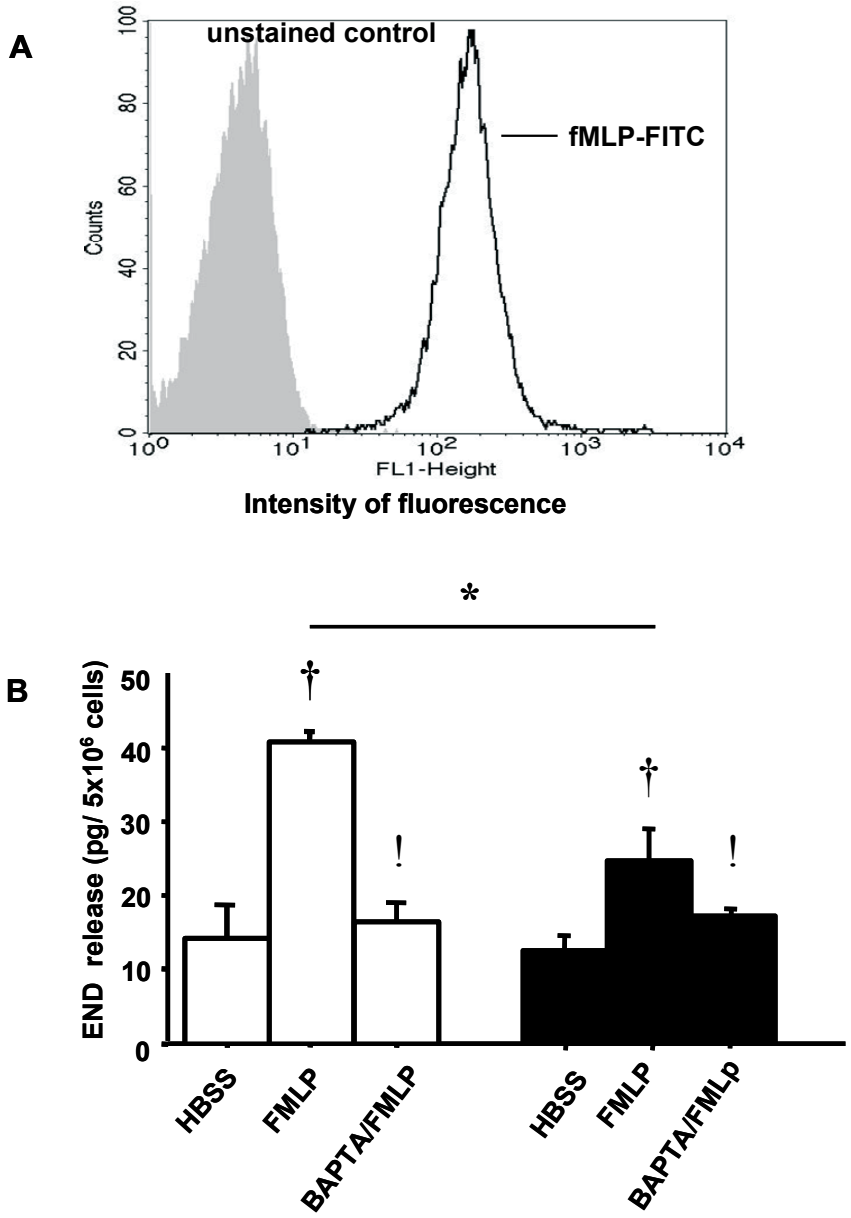

Figure 19: fMLP receptor (FPR) characterization and fMLP-induced END release from PMN cells of PC2 knockout mice. PMN cells were recruited from the peritoneal cavity following intraperitoneal injection of 1% glycogen. (A): Expression of FPR was determined on rat PMN cells by flow cytometry. Grey histogram: control conditions, black histogram: incubation with fMLP-FITC. The FPR-staining using FITC-conjugated fMLP (1 µM) indicates higher fluorescence intensity (B): Peritoneal neutrophils ($5x10^6$) were incubated with or without FPR agonist fMLP (1 µM) and END release was measured in the supernatant by radioimmunoassay. The fMLP-induced release was prevented by concomitant incubation with BAPTA (100 µM), an intracellular Calcium chelator. Data from three independent experiments in duplicate represent means ± SD. $P<0.05$, One way ANOVA, post-hoc Student-Newman-Keuls Method) "* " denotes significant differences of fMLP-induced END release in PMN cells of wildtype mice versus fMLP–induced END release in PMN cells of PC2 knockout mice. "†" denotes significant differences of HBSS (END release without fMLP) versus fMLP-enduced END release. "**!**" denotes significant differences of FMLP-induced END release versus FMLP-induced END release in the presence of BAPTA.

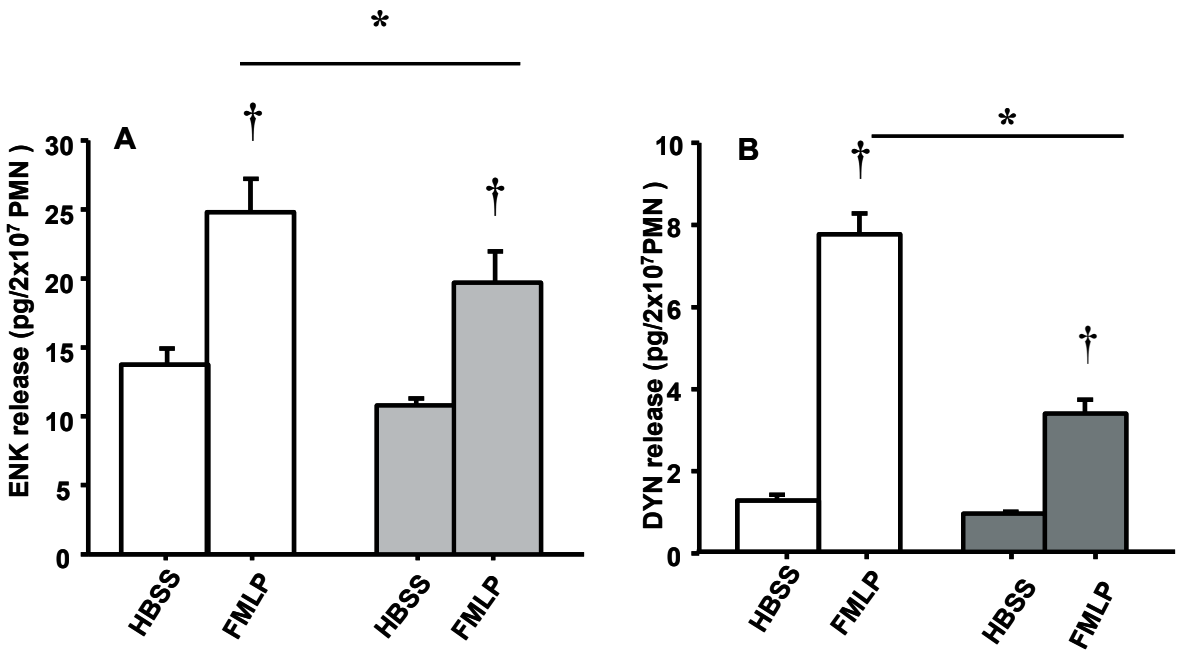

Figure 20: fMLP-induced ENK and DYN release from PMN cells of PC2 knockout mice. Peritoneal neutrophils ($2x10^7$) were incubated with or without fMLP (1 μM) and ENK and DYN in the supernatant were quantified by radioimmunoassay. Data from three independent experiments in duplicate represent mean ± SD. $P<0.05$, One way ANOVA, post-hoc Student-Newman-Keuls Method. "*" denotes significant differences of fMLP-induced ENK or DYN release in PMN cells of wild-type mice versus fMLP –induced ENK or DYN release in PMN cells of PC2 knockout mice. "†" denotes significant differences of HBSS (ENK or DYN release from PMN without fMLP stimulation) versus fMLP-enduced ENK or DYN release.

4.12 Antinociceptive effects of exogenously applied END and ENK as well as endogenously released opioid peptides in inflamed tissue

fMLP is a potent trigger of opioid peptide END and ENK release from mice PMN cells as seen in the results above. Therefore, local injection of fMLP was tested for its antinociceptive effect in vivo at early time points (2 h) of FCA-induced inflammation. Intraplantar injection of the opioid peptides END and ENK in animals with FCA hindpaw inflammation produced significant changes in paw pressure threshold (PPT), however, not in control animals without any inflammation (Fig. 21 A, B). In addition, the opioid peptide releasing agent fMLP injected into FCA inflamed hindpaws elicited similar PPT elevations (Fig. 21 C). These antinociceptive effects by intraplantar END, ENK and fMLP peptides were completely reversed by i.pl. administration of the opioid receptor antagonist naloxone.

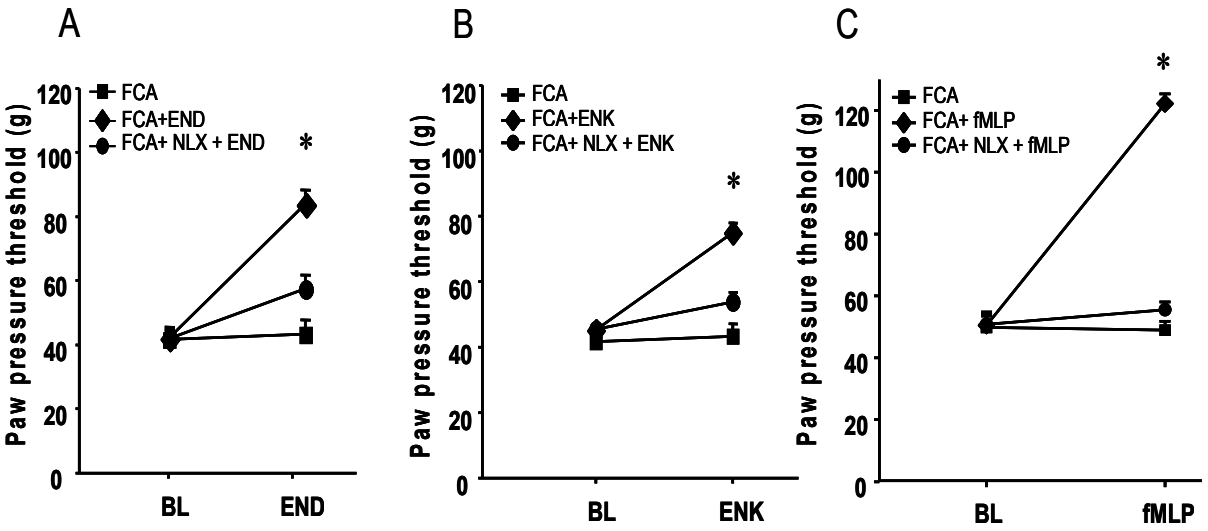

Figure 21: Antinociceptive effects of i.pl. END, ENK and the opioid peptide releasing agent fMLP in rats with and without FCA hindpaw inflammation. Paw pressure thresholds were determined by a modified Randall-Selitto algesiometer measuring the threshold to increasing mechanical pressure (PPT) at which the animal withdraws its hindpaw. Increased PPT represents increased antinociception. Baseline (BL) PPT was measure before opioid administration. Locally injected opioid peptides (END, ENK) or endogenous release of opioid peptides by fMLP induced antinociception in rats with FCA hindpaw inflammation. The opioid peptides END (1 µg) (A) and ENK (20 µg) (B) were administered i.pl. in untreated, FCA treated rats and rats receiving a concomitant administration of the opioid receptor antagonist naloxone (0.28 ng/100 µl) (C) The opioid peptide releasing agent fMLP (3 ng /100 µl) was administered i.pl. in untreated and FCA treated rats. Data represent means ± SEM. $P<0.05$, ANOVA on ranks, post hoc Dunn's method; "*" denotes significant differences of control versus FCA treated animals.

4.13 Antinociception by leukocyte-derived opioid peptides in noninflamed tissue - role of hypertonicity and the perineural barrier

Intraplantar injection of the opioids END and ENK produced no change in PPT of control rats compared to baseline PPT. Local pretreatment with hypertonic saline (to reversibly disrupt the integrity of the perineural barrier) 60 min before the i.pl. administration of the opioid peptides END and ENK lead to significant increases in nociceptive thresholds, while hypertonic saline alone did not affect PPT (Fig. 22 A, B). The antinociceptive effects produced by i.pl. END and ENK after hypertonic saline were reversible by i.pl. injection of the opioid antagonist naloxone. While fMLP triggered opioid peptide release from PMN cells in vitro, nociceptive thresholds were unchanged in rat hindpaws without inflammation (Fig. 22 C). Recruitment of PMNs by i.pl. treatment with the macrophage inflammatory protein-2

(MIP-2) induced no changes in PPT. Following MIP2 recruitment of PMNs and i.pl. administration of hypertonic saline (NaCl 10 %), fMLP injected into the noninflamed paw showed a significant increase in PPT, consistent with perineurium barrier opening. Intraplantar (i.pl.), but not subcutaneous (s.c) administration of naloxone blocked this antinociceptive effect of fMLP after hypertonic saline.

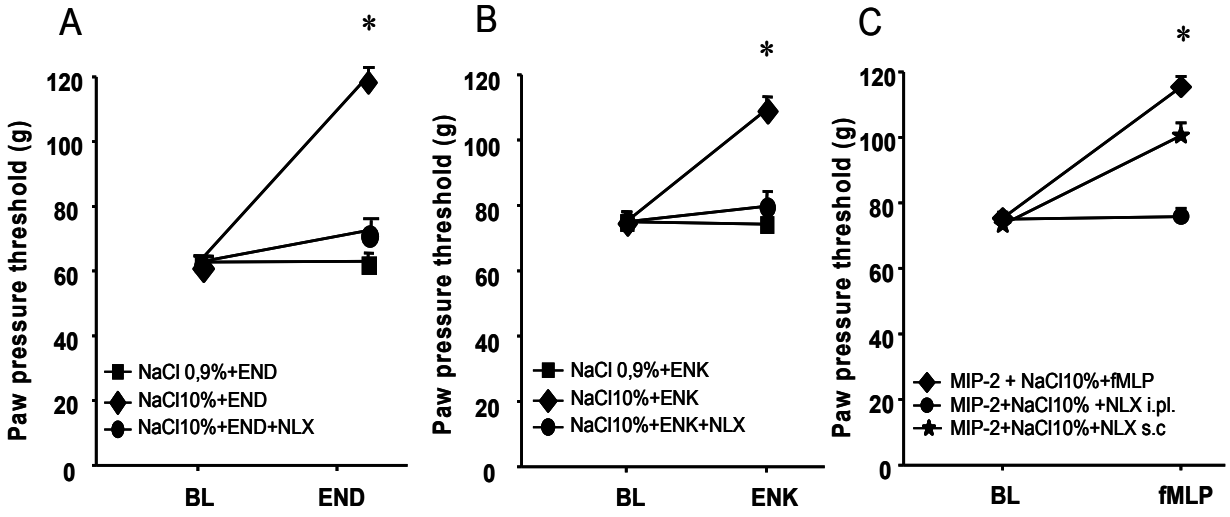

Figure 22: Antinociceptive effects of i.pl. END, ENK and the opioid peptide releasing agent fMLP following local treatment with 0.9 % or 10 % saline. Paw pressure thresholds were determined by a modified Randall-Selitto algesiometer measuring the threshold to increasing mechanical pressure at which the animal withdraws its hindpaw. Increased PPT represents increased antinociception. To determine the antinociceptive effects of exogenously applied opioid peptides in the presence of hypertonicity, rats were treated i.pl. with 100 µl saline (NaCl 0.9 % (black square) and 10 % (black diamonds) followed by an intraplantar injection of the opioid peptides ß-endorphin (A) and Met-enkephalin ENK (B). These rats received opioid peptides in the presence of 10 % NaCl or in combination with 0.28 ng/100 µl naloxone intraplantarly. Paw pressure thresholds were quantified before (baseline, BL) and after injection of opioids. (C) Rats were intraplantarly injected with 3 µg/100 µl MIP-2 for neutrophil recruitment followed by an intraplantar injection of hypertonic saline. One hour later paw pressure thresholds were measured before and 5 min after intraplantar inoculation of fMLP. To test for peripheral opioid receptor dependency fMLP was co-injected with the opioid receptor antagonist naloxone (intraplantarly) or subcutaneously as a control for systemic effects. Data represent mean ± SEM. $P<0.05$, ANOVA on ranks, Dunn's method. "* "denotes significant differences of control versus hypertonic saline treated animals.

4.14 Local hypertonicity with 10 % NaCl induced prolonged opening of the perineurial barrier

After intraplantar injection of the macromolecule horseradish peroxidase (HRP), cross-sections of plantar subcutaneous paw tissue, the HRP reaction products are seen in connective tissue and in perineurium following saline (Fig. 23 A) or hypertonic saline NaCl 10% treatment (Fig.23B-D). In control paws the perineurial barrier was impermeable as demonstrated by the lack of intraneurally stained horseradish peroxidase (Fig. 23 A). The reaction product was diffusely distributed in the connective tissue and in the outer parts of the perineurium with a difference in staining intensity at the level of the inner layer of the perineurium. This restriction could be overcome by intraplantar injection of hypertonic saline NaCl 10 % (Fig. 23 B-D) leading to a reversible disruption of the barrier as seen by the intraneural staining of horseradish peroxidise 5 min after injection of 10 % NaCl. This opening could be demonstrated for at least 120 min after injection of hypertonic saline (Fig.23 C and D) indicating a prolonged opening of the perineurial barrier.

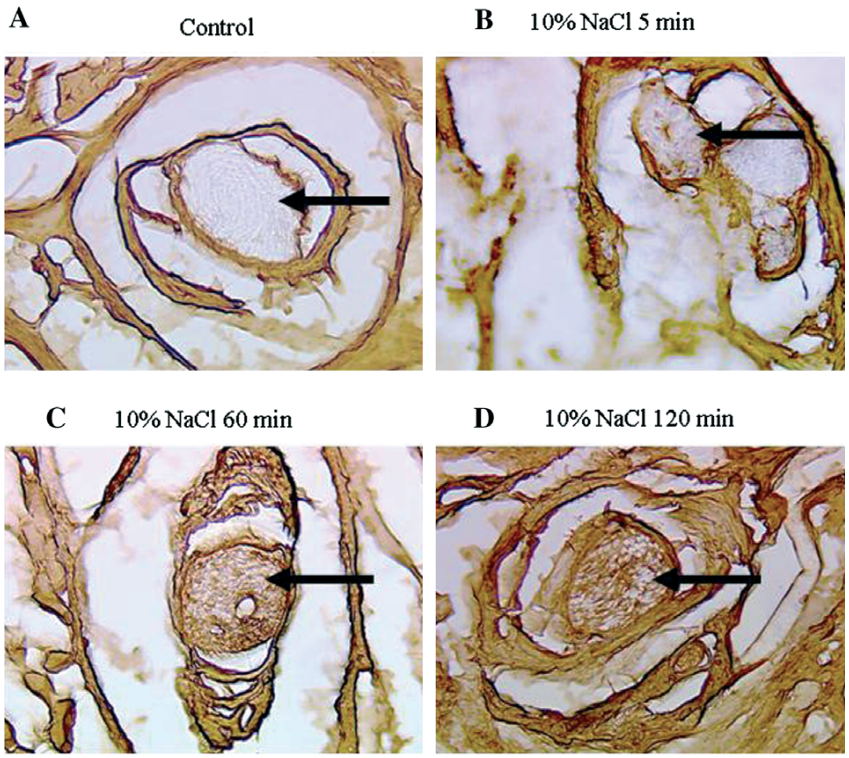

Figure 23: Time course of perineurial barrier permeability in the paw after hypertonic or isotonic saline. Peripheral nerve fibers are embedded in the endoneurium which is then surrounded by the perineurium functioning as a barrier for penetration of substances. (A–D) Male Wistar rats were intraplantarly injected with 100 µl 10 % NaCl (control 0.9 % NaCl) or horseradish peroxidase (8 mg) and were sacrified after intervals of time. Extra- or intraneural staining of peripheral nerve fibres within subcutaneous paw tissue was performed at 5, 60 and 120 min after injection of horseradish peroxidase and observed on light microscopy (magnification 40x; arrows are pointing at the nerve).

5 Discussion

The main findings of this thesis are that: (1) local NGF in rat hindpaws contributes to the up-regulation of sensory neuron MOR expression and subsequent enhanced efficacy of opioids through activation of the p38 MAPK pathway; (2) opioid peptide precursors proopiomelanocortin (POMC), proenkephalin (PENK) and prodynorphin (PDYN) are coexpressed with the processing enzyme prohormone convertase PC2 in circulating and resident immune cells of mice with FCA-induced paw inflammation; (3) in PC2 knockout mice the processing of POMC, PENK and PDYN into their respective end-products and their release is hindered in circulating and resident immune cells; 4) exogenous administration of opioid peptides as well as their fMLP-induced endogenous release from immune cells result in peripheral opioid receptor-mediated antinociception depending on the accessibility of these receptors through the perineural barrier.

5.1 NGF-dependent enhanced antinociceptive effects of i.pl. full and partial opioid agonists.

Intraplantar injection of low, systemically inactive doses of the full MOR agonist fentanyl produced a dose-dependent increase of PPT, i.e. an antinociceptive effect, in normal rats. Following unilateral FCA hindpaw inflammation this dose-dependent antinociception shifted to the left, consistent with an enhanced potentiation of fentanyl. In contrast, administration of buprenorphine, a partial MOR agonist, produced no antinociceptive effect in normal animals, but produced a significant and dose-dependent elevation of PPT in FCA treated animals, consistent with an increased buprenorphine efficacy during inflammatory conditions. The antinociceptive efficacy of i.pl. buprenorphine was smaller compared to those of i.pl. fentanyl. These results are supported by those of Hernández et al., in 2009 which have also shown antinociceptive effects following the i.pl. administration of fentanyl and buprenorphine with a higher efficacy of fentanyl than of buprenorphine. [113] Interestingly, the improved

antinociceptive effects of the full and partial opioid agonists were reversed following immunoneutralization of NGF by injections of a specific NGF antiserum into inflamed hindpaws, suggesting the contribution of endogenous NGF to the enhanced opioid efficacy. Since the NGF concentration is known to be highly increased in inflamed subcutaneous tissue, [114] the present study examined whether i.pl. administration of NGF in normal rat hindpaws would result in changes of peripheral opioid effects similar to those observed during inflammation. Indeed the results showed that local NGF treatment caused an enhanced antinociception of i.pl. fentanyl and buprenorphine. The higher efficacy of fentanyl compared to buprenorphine is consistent with a requirement of higher receptor occupancy for partial opioid agonists such as buprenorphine than with the full opioid agonist fentanyl as described previously by Yassen et al., in 2006. [115] These findings are in line with a previous study that reported a relatively low number of MOR binding sites in DRG of normal rats that was up-regulated following local inflammation. [35] Also, in 2003, Silbert et al. quantified single-cell MOR mRNA levels and measured opioid inhibition of Ca^{2+} channels on identified nociceptors and low-threshold mechanosensors (non-nociceptors) isolated from rats. [116] They found that negligibly few non-nociceptors express MOR mRNA, thereby rendering non-pain sensations insensitive to opioids. On the other side a close correlation was found between the increased opioid receptor efficacy in the inhibition of peak Ca^{2+} currents and the opioid receptor mRNA expression within neuronal DRG. Taken together, both endogenously raised NGF concentrations within inflamed subcutaneous tissue as well as local treatment with NGF led to increased potency of i.pl. full and enhanced efficacy of i.pl. partial opioid agonists presumably via an up-regulation in the number of MOR of peripheral sensory neurons.

5.2 NGF-dependent up-regulation of sensory neuron MOR through p38 MAPK activation.

The aim of the next experiments was to examine whether indeed NGF induces an up-regulation of sensory neuron MOR and whether this occurs via the MAPK pathway. MOR proteins were identified within DRG by Western blot analysis revealing a band with the expected molecular weight of 50 kDa, supporting previous reports. [117] In agreement with Western blot results, immunohistochemical experiments identified MOR immunoreactivity in small-to-medium size DRG neurons coexpressing the neuropeptides substance P (SP) and calcitonin gene-related peptide (CGRP). [14, 15, 18, 31, 118] Both MOR proteins and MOR-IR neurons showed a significant up-regulation following local NGF treatment. This was further supported by a rise in the number of MOR specific [^{3}H]DAMGO binding sites. In a similar way, NGF overexpression in transgenic mice exhibited an increase in MOR expression in DRG neurons. [40] In other studies, NGF treatment also increased MOR specific [^{3}H]DAMGO as well as enkephalin binding sites in cell culture [37, 119] and raised diprenorphine binding sites in isolated DRG. [38]

Intrathecal administration of the p38 MAPK inhibitor SB203580, but not the ERK-1/2 inhibitor PD98059, significantly reversed NGF-induced increases in MOR proteins, MOR specific [^{3}H]DAMGO binding sites as well as the number of MOR-IR neurons in DRG. In Western blot analysis the NGF-induced up-regulation of MOR proteins was concomitant with a 5.6-fold increase in phosphorylated, i.e. activated p-p38 MAPK in DRG, whereas the total p38 MAPK increased only slightly, but not statistically significant. Increased concentrations of endogenous NGF during inflammatory pain as well as exogenously applied NGF are known to bind to its receptors TrkA and p75 and then being retrogradely transported as early endosomes to the cell somata of sensory neurons within DRG. [120] These NGF/TrkA carrying early endosomes also colocalize with activated signaling proteins such as p38 MAPK which has been shown to be involved in different pain conditions. [121] The reversal of the NGF-

induced MOR up-regulation by the p38 MAPK inhibitor SB203580 suggests the involvement of the p38 MAPK signaling pathway. These findings are in line with the previous study by Ohmichi et al. (1992) which demonstrated that NGF dose dependently induced p38 MAPK phosphorylation in pheochromacytoma cells transfected with trkA receptor.[122] Similarly, Xing et al., (1998) showed that the phosphorylated forms of p38 MAPK were increased in extracts of NGF-treated PC12 cells compared to extracts of untreated PC12 cells after cell lysates separation by SDS-PAGE.[48] Colocalization of MOR and phosphorylated, i.e. activated p38 MAPK was confirmed by double immunofluorescence confocal microscopy demonstrating an increase in the number of MOR-IR neurons colocalizing with phosphorylated p38 MAPK. This was suppressed by the i.t. p38 MAPK inhibitor SB203580, but not with ERK 1/2 inhibitor PD98059. In line with other studies the NGF-induced increase in p38 MAPK activation was restricted to small to medium size DRG neurons, most of which are nociceptors. [123] This indicates that p38 MAPK activation in DRG neurons following NGF treatment is not a universal response of the neurons to stress, but is mainly restricted to nociceptive NGF-responsive/TrkA-expressing neurons. A possible mechanism that explains the up-regulation in the number of sensory neuron MOR in DRG following intraplantar injection of NGF is that p38 MAPK increases the expression of the MOR in DRG neurons. Many studies were performed in cell lines investigating possible transcription factors that regulate MOR expression. Activated p38 MAPK translocates from the cytoplasm to the nucleus and phosphorylates the transcription factors like cAMP-response element-binding protein CREB [47]and STAT1/3. [124] These transcription factors then bind to their response element sites on the promoter regions of the DNA and initiate the transcription of genes. These studies and others have identified the transcription factors mediating MOR by Western blot analysis, using reporter gene constructs to localize the promoter region of MOR. The investigators also used electrophoretic mobility shift assays (EMSAs) to further characterize the binding sites of transcription factors on this promoter. This led to the identification of

multiple transcription factor binding sites for MOR promoters, including CREB, [59, 125] STAT6, [61] NF-kB, [58] and STAT1/3 [60] binding sites. Interestingly, phosphorylation of STAT3 and CREB are increased in mouse DRGs after peripheral inflammation. [126]

Opioid receptors synthesized in DRG neurons undergo anterograde axonal transport towards peripheral nerve terminals which leads to enhanced density of opioid receptors on cutaneous nerve fibers. [31, 127] Therefore, the subsequent experiments examined whether the number of axonally transported MOR to the peripheral nerve terminals was altered by NGF treatment with or without i.t. p38 MAPK inhibition. Double immunofluorescence confocal microscopy of MOR with the sensory neuron marker CGRP-IR and their quantitative analysis in the ligated sciatic nerve showed a significant increase of MOR proximal to the ligature following NGF treatment. This increase in axonally transported MOR was attenuated by intrathecal injection of the p38 MAPK inhibitor SB203580 suggesting that subsequent to the NGF-induced up-regulation of MOR in DRG the axonal transport of sensory neuron MOR towards the peripheral subcutaneous tissue is increased and is dependent on the activation of the DRG p38 MAPK pathway.

5.3 NGF-induced enhanced opioid antinociception is dependent on p38 MAPK activation

Finally, the contribution of the p38 and ERK1/2 MAPK pathway to the NGF or FCA-induced enhanced antinociceptive effects of peripheral full and partial opioid agonists was examined. The results showed that the enhanced antinociception of the full and partial opioid agonists was attenuated by the intrathecal injection of the p38 MAPK inhibitor SB203580, but not of the ERK-1/2 MAPK inhibitor PD98059. These findings underscore the functional role of p38 MAPK in the mediation of an NGF-induced up-regulation of DRG MOR (reviewed in (128)). However, it does not fully exclude that ERK-1/2 MAPK may also be involved for example at an earlier time interval, since only one time point at a very late phase of FCA- or NGF-

treatment was investigated. Taken together, NGF through the activation of the p38 MAPK pathway contributes to the enhanced expression and efficacy of MOR within primary afferent neurons.

5.4 Defective POMC, PENK and PDYN processing of immunocytes in inflamed tissue of mice lacking prohormone convertase 2

The endogenous ligands of these MOR on peripheral sensory neurons were detected as opioid peptides within immigrated immune cells in close proximity to these neurons. Upon certain stimuli, e.g. releasing factors such as corticotrophin-releasing factor, the opioid peptides are released from immune cells and upon binding to their neighbouring opioid receptors result in the inhibition of pain. [2, 28] Opioid peptides derive from distinct precursor proteins, namely POMC, PENK and PDYN. In the pituitary gland, appropriate processing yields their respective end-products, the endogenous opioid peptides END, ENK and DYN. The relative contribution of the processing enzyme PC2 to POMC, PENK and PDYN processing and its functional relevance remain unknown in inflammatory cells. Therefore, the aim of these experiments was to elucidate in mice lacking PC2 the consequences of defective POMC, PENK and PDYN processing within circulating as well as immigrated immunocytes of inflamed tissue. Using immunohistochemistry, Western blot and radioimmunoassay techniques, it was shown that the precursor proteins as well as intermediate compounds greatly accumulated within immunocytes of mice lacking PC2. In parallel, there was a dramatic reduction in the cell content of the active peptides such as END, ENK and DYN within circulating and resident immune cells of PC2 knockout mice. Consistently, these mice exhibited a functional reduction in the fMLP-induced END, ENK or DYN release from circulating PMN during inflammatory pain. Taken together, these findings suggest that PC2 plays a crucial role for opioid peptide processing within immunocytes during inflammatory pain.

5.4.1 Colocalization of PC2 with opioid peptide precursors POMC, PENK and PDYN within immune cells of inflamed subcutaneous tissue

Using double immunofluorescence confocal microscopy the processing enzyme PC2 was colocalized with the opioid precursors POMC, PENK or PDYN within immunocytes of subcutaneous inflamed paw tissue. These results are in line with a previous study that showed co-expression of PC2 with POMC in the pituitary. [129] Also, the results of the present study support those of Nakashima et al. in 2001, who reported that POMC is colocalized with PC1 and PC2 in the immune cells of the red pulp of the rat spleen. [130] In addition, in the present study Western blot analysis of PC2, POMC, PENK and PDYN in circulating leukocytes demonstrating a band of approximately 68, 32, 30 and 28 kDa, respectively, correspond to those previously observed in circulating leukocytes. [24]

5.4.2 Accumulation of POMC, PENK and PDYN in circulating and resident immune cells of PC2 knockout mice

The genotype of knockout mice determined by PCR of genomic DNA and Western blot analysis confirmed the lack of PC2 in circulating immune cells of PC2 knockout mice. Using immunohistochemistry, accumulation of precursor proteins POMC, PENK and PDYN were detected within immunocytes of these knockout mice as reflected by the increased number of immune cells containing these precursors. To strengthen these results from immunohistochemistry experiments, Western blot analysis investigated the changes in the levels of opioid precursor proteins in circulating immune cells of PC2 knockout mice. The levels of precursor proteins POMC, PENK and PDYN were dramatically increased in PC2 knockout compared to wild type mice. These findings suggest that opioid precursor processing in immune cells was defected in PC2 knockout mice. These findings in immune cells are supported by studies showing that inactivation of the PC2 enzymatic activity with RNA antisense in the brain, pituitary gland or transfected neuronal cells severely affected the

processing of POMC, [131] PENK [132] and PDYN [90] as reflected by the increased protein levels of these precursors. Also, Allen et al. (2001), Miller et al., (2003) and Laurent et al., (2004), reported that the lack of PC2 activity greatly caused an accumulation of POMC as well as β-LPH within pituitary gland and brain in PC2-deficient mice. [131, 133, 134] Furthermore, the present study investigated the changes in the biologically active peptides in immune cells of PC2 knockout mice using RIA techniques. In parallel to the accumulation of opioid precursors, RIA analysis revealed that END, ENK as well as DYN content in circulating, resident (from inflamed paw) immune cells and PMN cells of PC2 knockout mice was significantly decreased compared to wild type. These findings in immune cells are in line with published data showing a dramatic reduction in the content of END [131] and DYN [90] in pituitary gland as well as ENK in the brain of PC2 knockout mice. [89, 134] Subsequently, the consequences of inadequate opioid peptide processing from its precursor to the end-products END, ENK and DYN in PC2 knockout mice on their release from immune cells was investigated. In the present study flowcytometry observations implied that fMLP receptor (FPR) is expressed on mice PMN cells. Moreover, it was shown that the incubation of PMN cells with fMLP resulted in a release of END, ENK and DYN in wild type mice. This is consistent with previous studies by Rittner et al., in 2006 demonstrating that fMLP induces opioid peptide release from PMN cells [110] through the activation of FPR that increases the intracellular calcium concentration. [135-137] Indeed, fMLP-induced END release from PMN cells is shown to be calcium dependent since BAPTA could block the observed release. This indicates a vesicular release of peptides as previously described in rat's neutrophils [69, 138] or potassium-stimulated release in neuronal and immune. [139, 140] A possible mechanism explaining the release of opioids from immune cells is the elevation of intracellular calcium that is required for release. [110, 112] In fact, FPR is known to signal through Gi proteins stimulating phospholipase C leading to mobilization of calcium from intracellular stores. [136] This is consistent with the observation that the chelation of intracellular calcium by

BAPTA/AM abolished fMLP-induced END release from PMN cells of both knockout and wild type mice. Interestingly, fMLP-induced END, ENK and DYN release was significantly decreased in PMN cells of PC2 knockout mice compared to wild type. These results are in agreement with a significant reduction in the contents of END, ENK and DYN in immune cells of PC2 knockout mice compared to wild type. Taken together, the results from these experiments confirm the functional relevance of PC2 in the processing of POMC, PENK and PDYN to functionally active peptides such as END, ENK and DYN and their release which is relevant for the control of pain under inflammatory conditions.

5.5 Accessibility of opioid receptors by opioid peptides through the sensory neuron perineural barrier and its consequence for pain inhibition

This part of the thesis aimed to provide further evidence that exogenous as well as endogenously synthesized and released opioid peptides have a functional relevance in animals with inflammatory pain. Indeed, locally applied END or ENK produced a dose-dependent elevation of PPT in FCA-induced inflamed but not in the contralateral saline-treated rat's paw. This is in line with a previous study showing that END and ENK released from immune cells after CRF stimulation in inflamed paw produced peripheral analgesia that could be blocked with antibodies to ENK and END. [140] These results indicate that locally applied exogenous opioids can reach the endoneurium to produce peripherally mediated antinociception under inflammatory conditions. These findings support previous studies showing that locally applied opioid peptides produced analgesic effects in several animal pain models such as FCA-induced inflammation, [141] in carrageenan-induced inflammation [142] as well as in pain after knee surgery and in chronic arthritis. [143]

It has been suggested that inflammatory pain can be controlled by secretion of endogenous opioid peptides from leukocytes in inflamed rat paws. Opioid peptide release from PMNs can be induced by various releasing agents like fMLP that is shown to stimulate the release of

ENK in vitro. [69] Since PMNs are the major opioid containing cell population during early inflammation, the present study examined whether they could be stimulated with fMLP to release endogenous opioid peptides and produce antinociceptive effects. fMLP was able to induce an increase paw pressure threshold in rats with early FCA induced inflammation compared to normal rats treated with saline and the effects were reversible with i.pl. naloxone, consistent with the opioid mediated antinociceptive effect of fMLP. These results are supported by previous studies showing that in FCA induced inflammation PMN are recruited by specific chemokines and these opioid containing PMN can secrete opioid peptides leading to the reversal of inflammatory pain. [110, 138, 144] To further confirm this notion, hypertonic saline (10 %) was given before i.pl. opioid agonists END or ENK in noninflamed paw. Indeed, this study demonstrates that hypertonic solution enables opioid agonists END or ENK to produce opioid receptor-specific antinociception in noninflamed paws. This is consistent with a previous study by Antonijevic et al., (1995), which showed that if the perineural barrier is made permeable by hypertonic solutions (i.e. mannitol), injection of opioids into the paws increase nociceptive thresholds in noninflamed tissue. [96] A presumable mechanism is explained by the study of Kajimura et al., 1997 that investigated the role of endothelial cell size and shape in the control of permeability properties of endothelial barriers. [145] Reported data show that perfusion with hypertonic solutions increased blood-brain barrier solute transport and postulated that this occurred by cell shrinkage-induced opening of the tight junction. [146] In the present study, histochemical experiments demonstrate that HRP, applied extraneurally *in vivo*, does not penetrate into the endoneurium of cutaneous nerves in noninflamed paw. In normal tissue, the perineural administration of hypertonic saline enhances the passage of HRP into the endoneurium. Thus, the present study demonstrated that a deliberate leakage of the perineurial and/or endoneurial capillary barrier can be produced *in vivo* by hypertonic solution. Early studies already demonstrated that hypertonic saline increases permeability for [^{14}C] sucrose [147] and speculated that conformational changes in

tight junctions induced by cell shrinkage could account for this longer lasting effect. Taken together, these findings support the contention that artificial disruption of the blood nerve barrier facilitates the access of macromolecules to sensory neurons.

In contrast to CFA-induced inflammation leading to the recruitment of diverse types of immune cells, in this study, intraplantar injection of the neutrophil specific chemokines MIP2 induces selective recruitment of neutrophils into noninflamed paw tissue without causing overt signs of inflammation or inflammatory pain. These findings are supported with data reported by Rittner et al. in 2006, [110] Piccolo et al., in 1999, [148] and Moore et al., in 2000. [149] In the present study exogenous as well as endogenous opioid peptide induced-peripheral analgesia and perineural disruption coincide during very early stages of an inflammatory reaction and that both can be mimicked by hypertonic solutions in normal tissue. These findings have interesting implications such as exogenous as well as endogenous opioid peptides induced-peripheral analgesia under inflammatory conditions can also be brought to normal tissue as well.

6 References

1. Trescot, A. M., S. E. Glaser, H. Hansen, R. Benyamin, S. Patel, and L. Manchikanti. 2008. Effectiveness of opioids in the treatment of chronic non-cancer pain. *Pain Physician* 11:S181-200.
2. Stein, C., M. Schafer, and H. Machelska. 2003. Attacking pain at its source: new perspectives on opioids. *Nat Med* 9:1003-1008.
3. Pert, C. B., G. Pasternak, and S. H. Snyder. 1973. Opiate agonists and antagonists discriminated by receptor binding in brain. *Science* 182:1359-1361.
4. Terenius, L. 1973. Characteristics of the "receptor" for narcotic analgesics in synaptic plasma membrane fraction from rat brain. *Acta Pharmacol Toxicol (Copenh)* 33:377-384.
5. Simon, E. J., J. M. Hiller, and I. Edelman. 1973. Stereospecific binding of the potent narcotic analgesic (3H) Etorphine to rat-brain homogenate. *Proc Natl Acad Sci U S A* 70:1947-1949.
6. Yaksh, T. L., and T. A. Rudy. 1976. Analgesia mediated by a direct spinal action of narcotics. *Science* 192:1357-1358.
7. Pert, C. B., and S. H. Snyder. 1976. Opiate receptor binding--enhancement by opiate administration in vivo. *Biochem Pharmacol* 25:847-853.
8. Bartho, L., and J. Szolcsanyi. 1981. Opiate agonists inhibit neurogenic plasma extravasation in the rat. *Eur J Pharmacol* 73:101-104.
9. Joris, J. L., R. Dubner, and K. M. Hargreaves. 1987. Opioid analgesia at peripheral sites: a target for opioids released during stress and inflammation? *Anesth Analg* 66:1277-1281.
10. Faull, R. L., and J. W. Villiger. 1987. Opiate receptors in the human spinal cord: a detailed anatomical study comparing the autoradiographic localization of [3H]diprenorphine binding sites with the laminar pattern of substance P, myelin and nissl staining. *Neuroscience* 20:395-407.
11. Besse, D., M. C. Lombard, J. M. Zajac, B. P. Roques, and J. M. Besson. 1990. Pre- and postsynaptic location of mu, delta and kappa opioid receptors in the superficial layers of the dorsal horn of the rat spinal cord. *Prog Clin Biol Res* 328:183-186.
12. Kieffer, B. L., K. Befort, C. Gaveriaux-Ruff, and C. G. Hirth. 1992. The delta-opioid receptor: isolation of a cDNA by expression cloning and pharmacological characterization. *Proc Natl Acad Sci U S A* 89:12048-12052.
13. Evans, C. J., D. E. Keith, Jr., H. Morrison, K. Magendzo, and R. H. Edwards. 1992. Cloning of a delta opioid receptor by functional expression. *Science* 258:1952-1955.
14. Arvidsson, U., M. Riedl, S. Chakrabarti, J. H. Lee, A. H. Nakano, R. J. Dado, H. H. Loh, P. Y. Law, M. W. Wessendorf, and R. Elde. 1995. Distribution and targeting of a mu-opioid receptor (MOR1) in brain and spinal cord. *J Neurosci* 15:3328-3341.
15. Ji, R. R., Q. Zhang, P. Y. Law, H. H. Low, R. Elde, and T. Hokfelt. 1995. Expression of mu-, delta-, and kappa-opioid receptor-like immunoreactivities in rat dorsal root ganglia after carrageenan-induced inflammation. *J Neurosci* 15:8156-8166.
16. Chen, Y., C. Geis, and C. Sommer. 2008. Activation of TRPV1 contributes to morphine tolerance: involvement of the mitogen-activated protein kinase signaling pathway. *J Neurosci* 28:5836-5845.
17. Scherrer, G., N. Imamachi, Y. Q. Cao, C. Contet, F. Mennicken, D. O'Donnell, B. L. Kieffer, and A. I. Basbaum. 2009. Dissociation of the opioid receptor mechanisms that control mechanical and heat pain. *Cell* 137:1148-1159.
18. Wang, H. B., B. Zhao, Y. Q. Zhong, K. C. Li, Z. Y. Li, Q. Wang, Y. J. Lu, Z. N. Zhang, S. Q. He, H. C. Zheng, S. X. Wu, T. G. Hokfelt, L. Bao, and X. Zhang.

Coexpression of delta- and mu-opioid receptors in nociceptive sensory neurons. *Proc Natl Acad Sci U S A* 107:13117-13122.

19. Mousa, S. A., H. Machelska, M. Schafer, and C. Stein. 2000. Co-expression of beta-endorphin with adhesion molecules in a model of inflammatory pain. *J Neuroimmunol* 108:160-170.
20. Machelska, H., S. A. Mousa, A. Brack, J. K. Schopohl, H. L. Rittner, M. Schafer, and C. Stein. 2002. Opioid control of inflammatory pain regulated by intercellular adhesion molecule-1. *J Neurosci* 22:5588-5596.
21. Stein, C., A. H. Hassan, R. Przewlocki, C. Gramsch, K. Peter, and A. Herz. 1990. Opioids from immunocytes interact with receptors on sensory nerves to inhibit nociception in inflammation. *Proc Natl Acad Sci U S A* 87:5935-5939.
22. Mains, R. E., and B. A. Eipper. 1984. Post-translational processing of neuropeptide precursors. *NIDA Res Monogr* 54:168-183.
23. Tanaka, S. 2003. Comparative aspects of intracellular proteolytic processing of peptide hormone precursors: studies of proopiomelanocortin processing. *Zoolog Sci* 20:1183-1198.
24. Mousa, S. A., M. Shakibaei, N. Sitte, M. Schafer, and C. Stein. 2004. Subcellular pathways of beta-endorphin synthesis, processing, and release from immunocytes in inflammatory pain. *Endocrinology* 145:1331-1341.
25. Binder, W., S. A. Mousa, N. Sitte, M. Kaiser, C. Stein, and M. Schafer. 2004. Sympathetic activation triggers endogenous opioid release and analgesia within peripheral inflamed tissue. *Eur J Neurosci* 20:92-100.
26. Schafer, M., L. Carter, and C. Stein. 1994. Interleukin 1 beta and corticotropin-releasing factor inhibit pain by releasing opioids from immune cells in inflamed tissue. *Proc Natl Acad Sci U S A* 91:4219-4223.
27. Czlonkowski, A., C. Stein, and A. Herz. 1993. Peripheral mechanisms of opioid antinociception in inflammation: involvement of cytokines. *Eur J Pharmacol* 242:229-235.
28. Schafer, M., S. A. Mousa, Q. Zhang, L. Carter, and C. Stein. 1996. Expression of corticotropin-releasing factor in inflamed tissue is required for intrinsic peripheral opioid analgesia. *Proc Natl Acad Sci U S A* 93:6096-6100.
29. Mousa, S. A., C. P. Bopaiah, C. Stein, and M. Schafer. 2003. Involvement of corticotropin-releasing hormone receptor subtypes 1 and 2 in peripheral opioid-mediated inhibition of inflammatory pain. *Pain* 106:297-307.
30. Puehler, W., C. Zollner, A. Brack, M. A. Shaqura, H. Krause, M. Schafer, and C. Stein. 2004. Rapid up-regulation of mu opioid receptor mRNA in dorsal root ganglia in response to peripheral inflammation depends on neuronal conduction. *Neuroscience* 129:473-479.
31. Mousa, S. A., B. P. Cheppudira, M. Shaqura, O. Fischer, J. Hofmann, R. Hellweg, and M. Schafer. 2007. Nerve growth factor governs the enhanced ability of opioids to suppress inflammatory pain. *Brain* 130:502-513.
32. Mousa, S. A., Q. Zhang, N. Sitte, R. Ji, and C. Stein. 2001. beta-Endorphin-containing memory-cells and mu-opioid receptors undergo transport to peripheral inflamed tissue. *J Neuroimmunol* 115:71-78.
33. Zhang, Q., M. Schaffer, R. Elde, and C. Stein. 1998. Effects of neurotoxins and hindpaw inflammation on opioid receptor immunoreactivities in dorsal root ganglia. *Neuroscience* 85:281-291.
34. Yamdeu, R. S., M. Shaqura, S. A. Mousa, M. Schafer, and J. Droese. p38 Mitogen-activated protein kinase activation by nerve growth factor in primary sensory neurons upregulates mu-opioid receptors to enhance opioid responsiveness toward better pain control. *Anesthesiology* 114:150-161.

35. Shaqura, M. A., C. Zollner, S. A. Mousa, C. Stein, and M. Schafer. 2004. Characterization of mu opioid receptor binding and G protein coupling in rat hypothalamus, spinal cord, and primary afferent neurons during inflammatory pain. *J Pharmacol Exp Ther* 308:712-718.
36. Zollner, C., M. A. Shaqura, C. P. Bopaiah, S. Mousa, C. Stein, and M. Schafer. 2003. Painful inflammation-induced increase in mu-opioid receptor binding and G-protein coupling in primary afferent neurons. *Mol Pharmacol* 64:202-210.
37. Inoue, N., and H. Hatanaka. 1982. Nerve growth factor induces specific enkephalin binding sites in a nerve cell line. *J Biol Chem* 257:9238-9241.
38. Chen, J. J., J. Dymshitz, and M. R. Vasko. 1997. Regulation of opioid receptors in rat sensory neurons in culture. *Mol Pharmacol* 51:666-673.
39. Molliver, D. C., J. Lindsay, K. M. Albers, and B. M. Davis. 2005. Overexpression of NGF or GDNF alters transcriptional plasticity evoked by inflammation. *Pain* 113:277-284.
40. Zwick, M., D. C. Molliver, J. Lindsay, C. A. Fairbanks, T. Sengoku, K. M. Albers, and B. M. Davis. 2003. Transgenic mice possessing increased numbers of nociceptors do not exhibit increased behavioral sensitivity in models of inflammatory and neuropathic pain. *Pain* 106:491-500.
41. McMahon, S. B., D. L. Bennett, J. V. Priestley, and D. L. Shelton. 1995. The biological effects of endogenous nerve growth factor on adult sensory neurons revealed by a trkA-IgG fusion molecule. *Nat Med* 1:774-780.
42. Donnerer, J., R. Schuligoi, and C. Stein. 1992. Increased content and transport of substance P and calcitonin gene-related peptide in sensory nerves innervating inflamed tissue: evidence for a regulatory function of nerve growth factor in vivo. *Neuroscience* 49:693-698.
43. Mamet, J., A. Baron, M. Lazdunski, and N. Voilley. 2002. Proinflammatory mediators, stimulators of sensory neuron excitability via the expression of acid-sensing ion channels. *J Neurosci* 22:10662-10670.
44. Nicol, G. D., and M. R. Vasko. 2007. Unraveling the story of NGF-mediated sensitization of nociceptive sensory neurons: ON or OFF the Trks? *Mol Interv* 7:26-41.
45. Averill, S., J. D. Delcroix, G. J. Michael, D. R. Tomlinson, P. Fernyhough, and J. V. Priestley. 2001. Nerve growth factor modulates the activation status and fast axonal transport of ERK 1/2 in adult nociceptive neurones. *Mol Cell Neurosci* 18:183-196.
46. Cunningham, M. E., and L. A. Greene. 1998. A function-structure model for NGF-activated TRK. *EMBO J* 17:7282-7293.
47. Widmann, C., S. Gibson, M. B. Jarpe, and G. L. Johnson. 1999. Mitogen-activated protein kinase: conservation of a three-kinase module from yeast to human. *Physiol Rev* 79:143-180.
48. Xing, J., J. M. Kornhauser, Z. Xia, E. A. Thiele, and M. E. Greenberg. 1998. Nerve growth factor activates extracellular signal-regulated kinase and p38 mitogen-activated protein kinase pathways to stimulate CREB serine 133 phosphorylation. *Mol Cell Biol* 18:1946-1955.
49. Kieffer, B. L. 1995. Recent advances in molecular recognition and signal transduction of active peptides: receptors for opioid peptides. *Cell Mol Neurobiol* 15:615-635.
50. Corbett, A. D., G. Henderson, A. T. McKnight, and S. J. Paterson. 2006. 75 years of opioid research: the exciting but vain quest for the Holy Grail. *Br J Pharmacol* 147 Suppl 1:S153-162.
51. Waldhoer, M., S. E. Bartlett, and J. L. Whistler. 2004. Opioid receptors. *Annu Rev Biochem* 73:953-990.

52. Massotte, D., and B. L. Kieffer. 2005. The second extracellular loop: a damper for G protein-coupled receptors? *Nat Struct Mol Biol* 12:287-288.
53. Surratt, C. K., P. S. Johnson, A. Moriwaki, B. K. Seidleck, C. J. Blaschak, J. B. Wang, and G. R. Uhl. 1994. -mu opiate receptor. Charged transmembrane domain amino acids are critical for agonist recognition and intrinsic activity. *J Biol Chem* 269:20548-20553.
54. Pogozheva, I. D., M. J. Przydzial, and H. I. Mosberg. 2005. Homology modeling of opioid receptor-ligand complexes using experimental constraints. *AAPS J* 7:E434-448.
55. Raynor, K., H. Kong, J. Hines, G. Kong, J. Benovic, K. Yasuda, G. I. Bell, and T. Reisine. 1994. Molecular mechanisms of agonist-induced desensitization of the cloned mouse kappa opioid receptor. *J Pharmacol Exp Ther* 270:1381-1386.
56. Doyle, G. A., X. Rebecca Sheng, S. S. Lin, D. M. Press, D. E. Grice, R. J. Buono, T. N. Ferraro, and W. H. Berrettini. 2007. Identification of three mouse mu-opioid receptor (MOR) gene (Oprm1) splice variants containing a newly identified alternatively spliced exon. *Gene* 388:135-147.
57. Doyle, G. A., X. R. Sheng, S. S. Lin, D. M. Press, D. E. Grice, R. J. Buono, T. N. Ferraro, and W. H. Berrettini. 2007. Identification of five mouse mu-opioid receptor (MOR) gene (Oprm1) splice variants containing a newly identified alternatively spliced exon. *Gene* 395:98-107.
58. Kraus, J., C. Borner, E. Giannini, and V. Hollt. 2003. The role of nuclear factor kappaB in tumor necrosis factor-regulated transcription of the human mu-opioid receptor gene. *Mol Pharmacol* 64:876-884.
59. Lee, P. W., and Y. M. Lee. 2003. Transcriptional regulation of mu opioid receptor gene by cAMP pathway. *Mol Pharmacol* 64:1410-1418.
60. Borner, C., M. Woltje, V. Hollt, and J. Kraus. 2004. STAT6 transcription factor binding sites with mismatches within the canonical 5'-TTC...GAA-3' motif involved in regulation of delta- and mu-opioid receptors. *J Neurochem* 91:1493-1500.
61. Kraus, J., C. Borner, E. Giannini, K. Hickfang, H. Braun, P. Mayer, M. R. Hoehe, A. Ambrosch, W. Konig, and V. Hollt. 2001. Regulation of mu-opioid receptor gene transcription by interleukin-4 and influence of an allelic variation within a STAT6 transcription factor binding site. *J Biol Chem* 276:43901-43908.
62. Lapalu, S., C. Moisand, H. Mazarguil, G. Cambois, C. Mollereau, and J. C. Meunier. 1997. Comparison of the structure-activity relationships of nociceptin and dynorphin A using chimeric peptides. *FEBS Lett* 417:333-336.
63. Lapalu, S., C. Moisand, J. L. Butour, C. Mollereau, and J. C. Meunier. 1998. Different domains of the ORL1 and kappa-opioid receptors are involved in recognition of nociceptin and dynorphin A. *FEBS Lett* 427:296-300.
64. Zadina, J. E., L. Hackler, L. J. Ge, and A. J. Kastin. 1997. A potent and selective endogenous agonist for the mu-opiate receptor. *Nature* 386:499-502.
65. Guillemin, R., T. Vargo, J. Rossier, S. Minick, N. Ling, C. Rivier, W. Vale, and F. Bloom. 1977. beta-Endorphin and adrenocorticotropin are selected concomitantly by the pituitary gland. *Science* 197:1367-1369.
66. Smith, A. I., and J. W. Funder. 1988. Proopiomelanocortin processing in the pituitary, central nervous system, and peripheral tissues. *Endocr Rev* 9:159-179.
67. Sibinga, N. E., and A. Goldstein. 1988. Opioid peptides and opioid receptors in cells of the immune system. *Annu Rev Immunol* 6:219-249.
68. Przewlocki, R., A. H. Hassan, W. Lason, C. Epplen, A. Herz, and C. Stein. 1992. Gene expression and localization of opioid peptides in immune cells of inflamed tissue: functional role in antinociception. *Neuroscience* 48:491-500.
69. Vindrola, O., M. R. Padros, A. Sterin-Prync, A. Ase, S. Finkielman, and V. Nahmod. 1990. Proenkephalin system in human polymorphonuclear cells. Production and

release of a novel 1.0-kD peptide derived from synenkephalin. *J Clin Invest* 86:531-537.

70. Rouille, Y., S. J. Duguay, K. Lund, M. Furuta, Q. Gong, G. Lipkind, A. A. Oliva, Jr., S. J. Chan, and D. F. Steiner. 1995. Proteolytic processing mechanisms in the biosynthesis of neuroendocrine peptides: the subtilisin-like proprotein convertases. *Front Neuroendocrinol* 16:322-361.
71. Taylor, N. A., W. J. Van De Ven, and J. W. Creemers. 2003. Curbing activation: proprotein convertases in homeostasis and pathology. *FASEB J* 17:1215-1227.
72. Bergeron, F., R. Leduc, and R. Day. 2000. Subtilase-like pro-protein convertases: from molecular specificity to therapeutic applications. *J Mol Endocrinol* 24:1-22.
73. Day, R., M. K. Schafer, M. W. Collard, E. Weihe, and H. Akil. 1993. Prodynorphin gene expression in the rat intermediate pituitary lobe: gender differences and postpartum regulation. *Endocrinology* 133:2652-2659.
74. Seidah, N. G., J. Hamelin, M. Mamarbachi, W. Dong, H. Tardos, M. Mbikay, M. Chretien, and R. Day. 1996. cDNA structure, tissue distribution, and chromosomal localization of rat PC7, a novel mammalian proprotein convertase closest to yeast kexin-like proteinases. *Proc Natl Acad Sci U S A* 93:3388-3393.
75. Lusson, J., D. Vieau, J. Hamelin, R. Day, M. Chretien, and N. G. Seidah. 1993. cDNA structure of the mouse and rat subtilisin/kexin-like PC5: a candidate proprotein convertase expressed in endocrine and nonendocrine cells. *Proc Natl Acad Sci U S A* 90:6691-6695.
76. Steiner, D. F. 1998. The proprotein convertases. *Curr Opin Chem Biol* 2:31-39.
77. Weigent, D. A., and J. E. Blalock. 1997. Production of peptide hormones and neurotransmitters by the immune system. *Chem Immunol* 69:1-30.
78. Seidah, N. G., and M. Chretien. 1994. Pro-protein convertases of subtilisin/kexin family. *Methods Enzymol* 244:175-188.
79. Benjannet, S., N. Rondeau, L. Paquet, A. Boudreault, C. Lazure, M. Chretien, and N. G. Seidah. 1993. Comparative biosynthesis, covalent post-translational modifications and efficiency of prosegment cleavage of the prohormone convertases PC1 and PC2: glycosylation, sulphation and identification of the intracellular site of prosegment cleavage of PC1 and PC2. *Biochem J* 294 (Pt 3):735-743.
80. Zhou, Y., and I. Lindberg. 1993. Purification and characterization of the prohormone convertase PC1(PC3). *J Biol Chem* 268:5615-5623.
81. Autelitano, D. J., M. Blum, and J. L. Roberts. 1989. Changes in rat pituitary nuclear and cytoplasmic pro-opiomelanocortin RNAs associated with adrenalectomy and glucocorticoid replacement. *Mol Cell Endocrinol* 66:171-180.
82. Galin, F. S., R. D. LeBoeuf, and J. E. Blalock. 1991. Corticotropin-releasing factor upregulates expression of two truncated pro-opiomelanocortin transcripts in murine lymphocytes. *J Neuroimmunol* 31:51-58.
83. Panerai, A. E., and P. Sacerdote. 1997. Beta-endorphin in the immune system: a role at last? *Immunol Today* 18:317-319.
84. Sharp, B., and T. Yaksh. 1997. Pain killers of the immune system. *Nat Med* 3:831-832.
85. Lacaze-Masmonteil, T., Y. de Keyzer, J. P. Luton, A. Kahn, and X. Bertagna. 1987. Characterization of proopiomelanocortin transcripts in human nonpituitary tissues. *Proc Natl Acad Sci U S A* 84:7261-7265.
86. Lyons, P. D., and J. E. Blalock. 1997. Pro-opiomelanocortin gene expression and protein processing in rat mononuclear leukocytes. *J Neuroimmunol* 78:47-56.
87. Sitte, N., M. Busch, S. A. Mousa, D. Labuz, H. Rittner, C. Gore, H. Krause, C. Stein, and M. Schafer. 2007. Lymphocytes upregulate signal sequence-encoding

proopiomelanocortin mRNA and beta-endorphin during painful inflammation in vivo. *J Neuroimmunol* 183:133-145.
88. Eipper, B. A., and R. E. Mains. 1980. Structure and biosynthesis of pro-adrenocorticotropin/endorphin and related peptides. *Endocr Rev* 1:1-27.
89. Johanning, K., M. A. Juliano, L. Juliano, C. Lazure, N. S. Lamango, D. F. Steiner, and I. Lindberg. 1998. Specificity of prohormone convertase 2 on proenkephalin and proenkephalin-related substrates. *J Biol Chem* 273:22672-22680.
90. Berman, Y., N. Mzhavia, A. Polonskaia, M. Furuta, D. F. Steiner, J. E. Pintar, and L. A. Devi. 2000. Defective prodynorphin processing in mice lacking prohormone convertase PC2. *J Neurochem* 75:1763-1770.
91. Schafer, M., S. A. Mousa, and C. Stein. 1997. Corticotropin-releasing factor in antinociception and inflammation. *Eur J Pharmacol* 323:1-10.
92. Pina-Oviedo, S., and C. Ortiz-Hidalgo. 2008. The normal and neoplastic perineurium: a review. *Adv Anat Pathol* 15:147-164.
93. Cravioto, H. 1966. The perineurium as a diffusion barrier. Ultrastructural correlates. *Bull Los Angeles Neurol Soc* 31:196-208.
94. Klemm, H. 1970. [The perineurium: a diffusion barrier for peroxidase in epineurial and endoneurial application]. *Z Zellforsch Mikrosk Anat* 108:431-445.
95. Kristensson, K., and Y. Olsson. 1971. The perineurium as a diffusion barrier to protein tracers. Differences between mature and immature animals. *Acta Neuropathol* 17:127-138.
96. Antonijevic, I., S. A. Mousa, M. Schafer, and C. Stein. 1995. Perineurial defect and peripheral opioid analgesia in inflammation. *J Neurosci* 15:165-172.
97. Rechthand, E., and S. I. Rapoport. 1987. Regulation of the microenvironment of peripheral nerve: role of the blood-nerve barrier. *Prog Neurobiol* 28:303-343.
98. Bockman, D. E., M. Buchler, P. Malfertheiner, and H. G. Beger. 1988. Analysis of nerves in chronic pancreatitis. *Gastroenterology* 94:1459-1469.
99. Mizisin, A. P., M. W. Kalichman, R. R. Myers, and H. C. Powell. 1990. Role of the blood-nerve barrier in experimental nerve edema. *Toxicol Pathol* 18:170-185.
100. Olsson, Y. 1990. Microenvironment of the peripheral nervous system under normal and pathological conditions. *Crit Rev Neurobiol* 5:265-311.
101. Rittner, H. L., D. Hackel, R. S. Yamdeu, S. A. Mousa, C. Stein, M. Schafer, and A. Brack. 2009. Antinociception by neutrophil-derived opioid peptides in noninflamed tissue--role of hypertonicity and the perineurium. *Brain Behav Immun* 23:548-557.
102. Wenk, H. N., J. D. Brederson, and C. N. Honda. 2006. Morphine directly inhibits nociceptors in inflamed skin. *J Neurophysiol* 95:2083-2097.
103. Rittner, H. L., D. Hackel, P. Voigt, S. Mousa, A. Stolz, D. Labuz, M. Schafer, M. Schaefer, C. Stein, and A. Brack. 2009. Mycobacteria attenuate nociceptive responses by formyl peptide receptor triggered opioid peptide release from neutrophils. *PLoS Pathog* 5:e1000362.
104. Ji, R. R., K. Befort, G. J. Brenner, and C. J. Woolf. 2002. ERK MAP kinase activation in superficial spinal cord neurons induces prodynorphin and NK-1 up-regulation and contributes to persistent inflammatory pain hypersensitivity. *J Neurosci* 22:478-485.
105. Ji, R. R., H. Baba, G. J. Brenner, and C. J. Woolf. 1999. Nociceptive-specific activation of ERK in spinal neurons contributes to pain hypersensitivity. *Nat Neurosci* 2:1114-1119.
106. Ji, R. R., and F. Rupp. 1997. Phosphorylation of transcription factor CREB in rat spinal cord after formalin-induced hyperalgesia: relationship to c-fos induction. *J Neurosci* 17:1776-1785.

107. Frank, A. J., and M. J. Tilby. 2003. Quantification of DNA adducts in individual cells by immunofluorescence: effects of variation in DNA conformation. *Exp Cell Res* 283:127-134.
108. Wu, Q., M. Chen, M. Buchwald, and R. A. Phillips. 1995. A simple, rapid method for isolation of high quality genomic DNA from animal tissues. *Nucleic Acids Res* 23:5087-5088.
109. Furuta, M., H. Yano, A. Zhou, Y. Rouille, J. J. Holst, R. Carroll, M. Ravazzola, L. Orci, H. Furuta, and D. F. Steiner. 1997. Defective prohormone processing and altered pancreatic islet morphology in mice lacking active SPC2. *Proc Natl Acad Sci U S A* 94:6646-6651.
110. Rittner, H. L., D. Labuz, M. Schaefer, S. A. Mousa, S. Schulz, M. Schafer, C. Stein, and A. Brack. 2006. Pain control by CXCR2 ligands through Ca2+-regulated release of opioid peptides from polymorphonuclear cells. *FASEB J* 20:2627-2629.
111. Stein, C., C. Gramsch, and A. Herz. 1990. Intrinsic mechanisms of antinociception in inflammation: local opioid receptors and beta-endorphin. *J Neurosci* 10:1292-1298.
112. Chandler, D. E., J. P. Bennett, and B. Gomperts. 1983. Freeze-fracture studies of chemotactic peptide-induced exocytosis in neutrophils: evidence for two patterns of secretory granule fusion. *J Ultrastruct Res* 82:221-232.
113. Hernandez, L., A. Romero, P. Almela, P. Garcia-Nogales, M. L. Laorden, and M. M. Puig. 2009. Tolerance to the antinociceptive effects of peripherally administered opioids. Expression of beta-arrestins. *Brain Res* 1248:31-39.
114. Safieh-Garabedian, B., S. Poole, A. Allchorne, J. Winter, and C. J. Woolf. 1995. Contribution of interleukin-1 beta to the inflammation-induced increase in nerve growth factor levels and inflammatory hyperalgesia. *Br J Pharmacol* 115:1265-1275.
115. Yassen, A., E. Olofsen, R. Romberg, E. Sarton, M. Danhof, and A. Dahan. 2006. Mechanism-based pharmacokinetic-pharmacodynamic modeling of the antinociceptive effect of buprenorphine in healthy volunteers. *Anesthesiology* 104:1232-1242.
116. Silbert, S. C., D. W. Beacham, and E. W. McCleskey. 2003. Quantitative single-cell differences in mu-opioid receptor mRNA distinguish myelinated and unmyelinated nociceptors. *J Neurosci* 23:34-42.
117. Suzuki, S., T. Miyagi, T. K. Chuang, L. F. Chuang, R. H. Doi, and R. Y. Chuang. 2000. Morphine upregulates mu opioid receptors of human and monkey lymphocytes. *Biochem Biophys Res Commun* 279:621-628.
118. Endres-Becker, J., P. A. Heppenstall, S. A. Mousa, D. Labuz, A. Oksche, M. Schafer, C. Stein, and C. Zollner. 2007. Mu-opioid receptor activation modulates transient receptor potential vanilloid 1 (TRPV1) currents in sensory neurons in a model of inflammatory pain. *Mol Pharmacol* 71:12-18.
119. Yu, V. C., and W. Sadee. 1988. Efficacy and tolerance of narcotic analgesics at the mu opioid receptor in differentiated human neuroblastoma cells. *J Pharmacol Exp Ther* 245:350-355.
120. Delcroix, J. D., J. S. Valletta, C. Wu, S. J. Hunt, A. S. Kowal, and W. C. Mobley. 2003. NGF signaling in sensory neurons: evidence that early endosomes carry NGF retrograde signals. *Neuron* 39:69-84.
121. Ji, R. R., R. W. t. Gereau, M. Malcangio, and G. R. Strichartz. 2009. MAP kinase and pain. *Brain Res Rev* 60:135-148.
122. Ohmichi, M., S. J. Decker, and A. R. Saltiel. 1992. Nerve growth factor stimulates the tyrosine phosphorylation of a 38-kDa protein that specifically associates with the src homology domain of phospholipase C-gamma 1. *J Biol Chem* 267:21601-21606.

123. Ji, R. R., T. A. Samad, S. X. Jin, R. Schmoll, and C. J. Woolf. 2002. p38 MAPK activation by NGF in primary sensory neurons after inflammation increases TRPV1 levels and maintains heat hyperalgesia. *Neuron* 36:57-68.
124. Zhong, H., T. J. Murphy, and K. P. Minneman. 2000. Activation of signal transducers and activators of transcription by alpha(1A)-adrenergic receptor stimulation in PC12 cells. *Mol Pharmacol* 57:961-967.
125. Wendel, B., and M. R. Hoehe. 1998. The human mu opioid receptor gene: 5' regulatory and intronic sequences. *J Mol Med* 76:525-532.
126. Tamura, S., Y. Morikawa, and E. Senba. 2005. Up-regulated phosphorylation of signal transducer and activator of transcription 3 and cyclic AMP-responsive element binding protein by peripheral inflammation in primary afferent neurons possibly through oncostatin M receptor. *Neuroscience* 133:797-806.
127. Hassan, A. H., A. Ableitner, C. Stein, and A. Herz. 1993. Inflammation of the rat paw enhances axonal transport of opioid receptors in the sciatic nerve and increases their density in the inflamed tissue. *Neuroscience* 55:185-195.
128. Ji, R. R., and M. R. Suter. 2007. p38 MAPK, microglial signaling, and neuropathic pain. *Mol Pain* 3:33.
129. Zheng, M., R. D. Streck, R. E. Scott, N. G. Seidah, and J. E. Pintar. 1994. The developmental expression in rat of proteases furin, PC1, PC2, and carboxypeptidase E: implications for early maturation of proteolytic processing capacity. *J Neurosci* 14:4656-4673.
130. Nakashima, M., Y. Nie, Q. L. Li, and T. C. Friedman. 2001. Up-regulation of splenic prohormone convertases PC1 and PC2 in diabetic rats. *Regul Pept* 102:135-145.
131. Laurent, V., L. Jaubert-Miazza, R. Desjardins, R. Day, and I. Lindberg. 2004. Biosynthesis of proopiomelanocortin-derived peptides in prohormone convertase 2 and 7B2 null mice. *Endocrinology* 145:519-528.
132. Breslin, M. B., I. Lindberg, S. Benjannet, J. P. Mathis, C. Lazure, and N. G. Seidah. 1993. Differential processing of proenkephalin by prohormone convertases 1(3) and 2 and furin. *J Biol Chem* 268:27084-27093.
133. Allen, R. G., B. Peng, M. J. Pellegrino, E. D. Miller, D. K. Grandy, J. R. Lundblad, C. L. Washburn, and J. E. Pintar. 2001. Altered processing of pro-orphanin FQ/nociceptin and pro-opiomelanocortin-derived peptides in the brains of mice expressing defective prohormone convertase 2. *J Neurosci* 21:5864-5870.
134. Miller, R., T. Toneff, D. Vishnuvardhan, M. Beinfeld, and V. Y. Hook. 2003. Selective roles for the PC2 processing enzyme in the regulation of peptide neurotransmitter levels in brain and peripheral neuroendocrine tissues of PC2 deficient mice. *Neuropeptides* 37:140-148.
135. Rittner, H., D. Hackel, R. S. Yamdeu, S. A. Mousa, M. Schaefer, C. Stein, and A. Brack. 2009. Antinociception by neutrophil-derived opioid peptides in noninflamed tissue - role of hypertonicity and the perineurium. *Brain Behav Immun* 23:548-557.
136. Dalpiaz, A., S. Spisani, C. Biondi, E. Fabbri, M. Nalli, and M. E. Ferretti. 2003. Studies on human neutrophil biological functions by means of formyl-peptide receptor agonists and antagonists. *Curr Drug Targets Immune Endocr Metabol Disord* 3:33-42.
137. Anton, P., J. O'Connell, D. O'Connell, L. Whitaker, G. C. O'Sullivan, J. K. Collins, and F. Shanahan. 1998. Mucosal subepithelial binding sites for the bacterial chemotactic peptide, formyl-methionyl-leucyl-phenylalanine (FMLP). *Gut* 42:374-379.
138. Rittner, H. L., A. Brack, H. Machelska, S. A. Mousa, M. Bauer, M. Schafer, and C. Stein. 2001. Opioid peptide-expressing leukocytes: identification, recruitment, and simultaneously increasing inhibition of inflammatory pain. *Anesthesiology* 95:500-508.

139. Cool, D. R., and Y. P. Loh. 1994. Identification of a sorting signal for the regulated secretory pathway at the N-terminus of pro-opiomelanocortin. *Biochimie* 76:265-270.
140. Cabot, P. J., L. Carter, C. Gaiddon, Q. Zhang, M. Schafer, J. P. Loeffler, and C. Stein. 1997. Immune cell-derived beta-endorphin. Production, release, and control of inflammatory pain in rats. *J Clin Invest* 100:142-148.
141. Stein, C., M. J. Millan, and A. Herz. 1988. Unilateral inflammation of the hindpaw in rats as a model of prolonged noxious stimulation: alterations in behavior and nociceptive thresholds. *Pharmacol Biochem Behav* 31:445-451.
142. Taguchi, R., T. Taguchi, and H. Kitakoji. Involvement of peripheral opioid receptors in electroacupuncture analgesia for carrageenan-induced hyperalgesia. *Brain Res* 1355:97-103.
143. Stein, C., and A. Yassouridis. 1997. Peripheral morphine analgesia. *Pain* 71:119-121.
144. Brack, A., D. Labuz, A. Schiltz, H. L. Rittner, H. Machelska, M. Schafer, R. Reszka, and C. Stein. 2004. Tissue monocytes/macrophages in inflammation: hyperalgesia versus opioid-mediated peripheral antinociception. *Anesthesiology* 101:204-211.
145. Kajimura, M., M. E. O'Donnell, and F. E. Curry. 1997. Effect of cell shrinkage on permeability of cultured bovine aortic endothelia and frog mesenteric capillaries. *J Physiol* 503 (Pt 2):413-425.
146. Rapoport, S. I., W. R. Fredericks, K. Ohno, and K. D. Pettigrew. 1980. Quantitative aspects of reversible osmotic opening of the blood-brain barrier. *Am J Physiol* 238:R421-431.
147. Weerasuriya, A., S. I. Rapoport, and R. E. Taylor. 1979. Modification of permeability of frog perineurium to [14C]-sucrose by stretch and hypertonicity. *Brain Res* 173:503-512.
148. Piccolo, M. T., Y. Wang, S. Verbrugge, R. L. Warner, P. Sannomiya, N. S. Piccolo, M. S. Piccolo, T. E. Hugli, P. A. Ward, and G. O. Till. 1999. Role of chemotactic factors in neutrophil activation after thermal injury in rats. *Inflammation* 23:371-385.
149. Moore, T. A., M. W. Newstead, R. M. Strieter, B. Mehrad, B. L. Beaman, and T. J. Standiford. 2000. Bacterial clearance and survival are dependent on CXC chemokine receptor-2 ligands in a murine model of pulmonary Nocardia asteroides infection. *J Immunol* 164:908-915.

7 Acknowledgements

I am indebted to many people for their long-lasting support and encouragement which was invaluable for the successful completion of this research work. In the following lines some of them are gratefully acknowledged. However, I am aware of the fact that there are many more and these words cannot express the gratitude and respect I feel for all of those.

I owe my most sincerely thanks to my supervisor, Professor Michael Schäfer for introducing me to pain research. It was his inspiration, help, encouragement, support, enthusiastic and constructive discussion of the manuscript and patience that have guided me through this great journey. I further want to express my gratitude to Dr. Shaaban Mousa for his professional expertise, encouragement and advice and for the great help he gave me in any kind of way. Sincere thank also to Prof. Dr. med. Christoph Stein for his support. I would like to show my gratitude to Prof. Süßmuth for the care he has taken in examining this thesis. Many thanks to Dr. Rittner and Dr. Shaqura for their help in Flow cytometry and binding experiments, respectively. A special thank to Cecile Cayla for her friendship, help, advice, and lunch as well as proof-reading of this manuscript and a lot of thanks to all my colleagues in Prof. Schäfer's research group, a team working in a good atmosphere for their availability and good mood in the lab.

I would like to thank especially my husband for believing, encouraging and supporting me during this period, making research possible. I am particularly indebted to my parents and brothers, Firmin and Gaston for their never-ending encouragement, confidence, patience, love, and constant support. Without their support and love, I could never have reached this point. I would thank especially my Son, Tagne Sepngang Christian Nelson the ultimate source of my courage. Last but not least, many thanks to Octavie and Hermine who took time for a chat, thereby finding words of deep sense, not always related to science but to life in general.

8 Publications

8.1 Papers

1. Yamdeu RS, Shaqura M, Mousa SA, Schäfer M, Droese J. p38 Mitogen-activated protein kinase activation by nerve growth factor in primary sensory neurons upregulates μ-opioid receptors to enhance opioid responsiveness toward better pain control. Anesthesiology 2011; 114(1):150-61.

2. Rittner HL, Hackel D, Yamdeu RS, Mousa SA, Stein C, Schäfer M, Brack A. Antinociception by neutrophil-derived opioid peptides in noninflamed tissue-role of hypertonicity and the perineurium. Brain Behav Immun. 2009; 23(4):548-57. Epub 2009 Feb 20.

3. Mousa SA, Bopaiah CP, Richter JF, Yamdeu RS, Schäfer M. Inhibition of inflammatory pain by CRF at peripheral, spinal and supraspinal sites: involvement of areas co expressing CRF receptors and opioid peptides. Neuropsychopharmacology 2007; 32(12):2530-42. Epub 2007 Mar 21.

4. H. L. Rittner , R. Moshourab , S. Amasheh , V. Spahn , D. Hackel , R.-S. Yamdeu , M. Fromm , C. Zöllner , C. Stein , A. Brack. Regulation of exogenous peripheral opioid antinociception in non-inflamed tissue. (submitted)

8.2 Abstracts

1. R.S Yamdeu, M. Shakibaei, M. Schäfer, C. Stein, S.A. Mousa. The Society for Neuroscience (SfN) Conference. Chicago, 2008. Defective proopiomelanocortin, proenkephalin and prodynorphin processing within immunocytes of mice lacking prohormone convertase 2 and carboxypeptidase E.

2. R.S. Yamdeu, J. Dröse, M. Shaqura, M.Schäfer. The International Narcotics Research Conference (INRC) Berlin, 2007.Involvement of the p38 MAPK but not ERK pathway in the NGF-dependent up-regulation of sensory neuron opioid receptor Expression

3. Reine S. Yamdeu, Michael Schäfer, Christoph Stein and Shaaban A. Mousa. Berlin Brain Day (BBD), 2006. Subcellular pathways of Met-enkephalin synthesis, processing, and release from immunocytes in inflammatory pain.

4. Yumo HA, Ndembi N, Yamdeu R, Makamdeu F, Ngansop C, Kemogne P, Kamdem D, Watsop D, Meli J, Mbanya D, Kaptue LN. The 2nd International Aids Society (IAS) Conference on HIV Pathogenesis and Treatment. Paris, 2003. A comparative study of HIV/AIDS risk factors and of syphylis and HIV infection prevalence among a pygmy population and its neighbouring Bantus of Southern Cameroon. Antivir Ther. 2003; 8 (Suppl.1): abstract no. 1114. Departement of Immuno-Hematology, Faculty of Medicine and Biomedical Sciences, University of Yaounde I, Cameroon.